



APOLLO SPACECRAFT FLIGHT HISTORY

| <u>Mission</u> | <u>Spacecraft</u> | <u>Description</u>  | <u>Launch date</u> | <u>Launch site</u>                       |
|----------------|-------------------|---|--------------------|--|
| PA-1           | BP-6              | First pad abort   | Nov. 7, 1963       | White Sands<br>Missile Range,<br>N. Mex. |
| A-001          | BP-12             | Transonic abort   | May 13, 1964       | White Sands<br>Missile Range,<br>N. Mex. |
| AS-101         | BP-13             | Nominal launch and<br>exit environment  | May 28, 1964       | Cape Kennedy,<br>Fla.                    |
| AS-102         | BP-15             | Nominal launch and<br>exit environment  | Sept. 18, 1964     | Cape Kennedy,<br>Fla.                    |
| A-002          | BP-23             | Maximum dynamic<br>pressure abort   | Dec. 8, 1964       | White Sands<br>Missile Range,<br>N. Mex. |
| AS-103         | BP-16             | Micrometeoroid<br>experiment  | Feb. 16, 1965      | Cape Kennedy,<br>Fla.                    |
| A-003          | BP-22             | Low-altitude abort<br>(planned high-<br>altitude abort)                         | May 19, 1965       | White Sands<br>Missile Range,<br>N. Mex. |
| AS-104         | BP-26             | Micrometeoroid<br>experiment and<br>service module<br>RCS launch<br>environment | May 25, 1965       | Cape Kennedy,<br>Fla.                    |
| PA-2           | BP-23A            | Second pad abort  | June 29, 1965      | White Sands<br>Missile Range,<br>N. Mex. |
| AS-105         | BP-9A             | Micrometeoroid<br>experiment and<br>service module<br>RCS launch<br>environment | July 30, 1965      | Cape Kennedy,<br>Fla.                    |
| A-004          | SC-002            | Power-on tumbling<br>boundary abort   | Jan. 20, 1966      | White Sands<br>Missile Range,<br>N. Mex. |
| AS-201         | SC-009            | Supercircular<br>entry with high<br>heat rate                                   | Feb. 26, 1966      | Cape Kennedy,<br>Fla.                    |
| AS-202         | SC-011            | Supercircular<br>entry with high<br>heat load                                   | Aug. 25, 1966      | Cape Kennedy,<br>Fla.                    |

(Continued inside back cover)

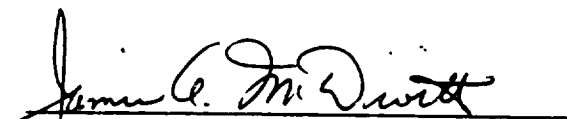


APOLLO 12 MISSION REPORT

PREPARED BY

Mission Evaluation Team

APPROVED BY



---

James A. McDivitt  
Colonel, USAF  
Manager, Apollo Spacecraft Program

NATIONAL AERONAUTICS AND SPACE ADMINISTRATION  
MANNED SPACECRAFT CENTER  
HOUSTON, TEXAS  
March 1970

U U U E E E E E E E E E E E E E E E E



















M M M M M M E E E E E E E E E E E E E E E E



### 3.0 LUNAR SURFACE EXPLORATION

This section contains a discussion of the formal experiments conducted for Apollo 12 and presents a preliminary laboratory assessment of returned samples. The experiments discussed includes those associated with the Apollo lunar surface experiments package and the solar wind composition, lunar geology, lunar surface photography, and multispectral photography experiments. The evaluations in this section are based on the data received during the first lunar day. All final experiment results will be published in a separate science report when the detailed analyses are complete (appendix E).

Lunar surface scientific activities were performed essentially as planned within the allotted time periods. Three hours after landing, the crew began preparations for egress and the first traverse of the lunar surface. During the first extravehicular activity period, which lasted 4 hours, the crew accomplished the following:

- a. Deployed the modularized equipment stowage assembly, which permitted transmission of color television pictures of the Commander descending the lunar module ladder
- b. Transferred a contingency surface sample to the lunar module
- c. Erected the solar wind composition foil
- d. Collected a core-tube soil specimen and additional surface samples
- e. Deployed the Apollo lunar surface experiments package for an extended collection of lunar scientific data via a radio link.

The experiments package included a cold cathode gage, a lunar surface magnetometer, a passive seismometer, a solar wind spectrometer, a dust detector, and a suprathreshold ion detector. A brief description of the experiment equipment is presented in appendix A. Certain difficulties in deploying the equipment are mentioned in this section and are discussed in greater detail in section 14.3. Anomalies in the operation of the equipment since activation are also mentioned, but the nature and cause of each experiment anomaly will be summarized in a later science report (appendix E).

Following a 7-hour rest period, the second extravehicular activity period began with preparations for the geology traverse. The duration of the second extravehicular activity was 3-3/4 hours, during which the crew accomplished the following:

U U U E E E E E E E E U U U U U U U U U U U U U U U U



NASA-S-70-525

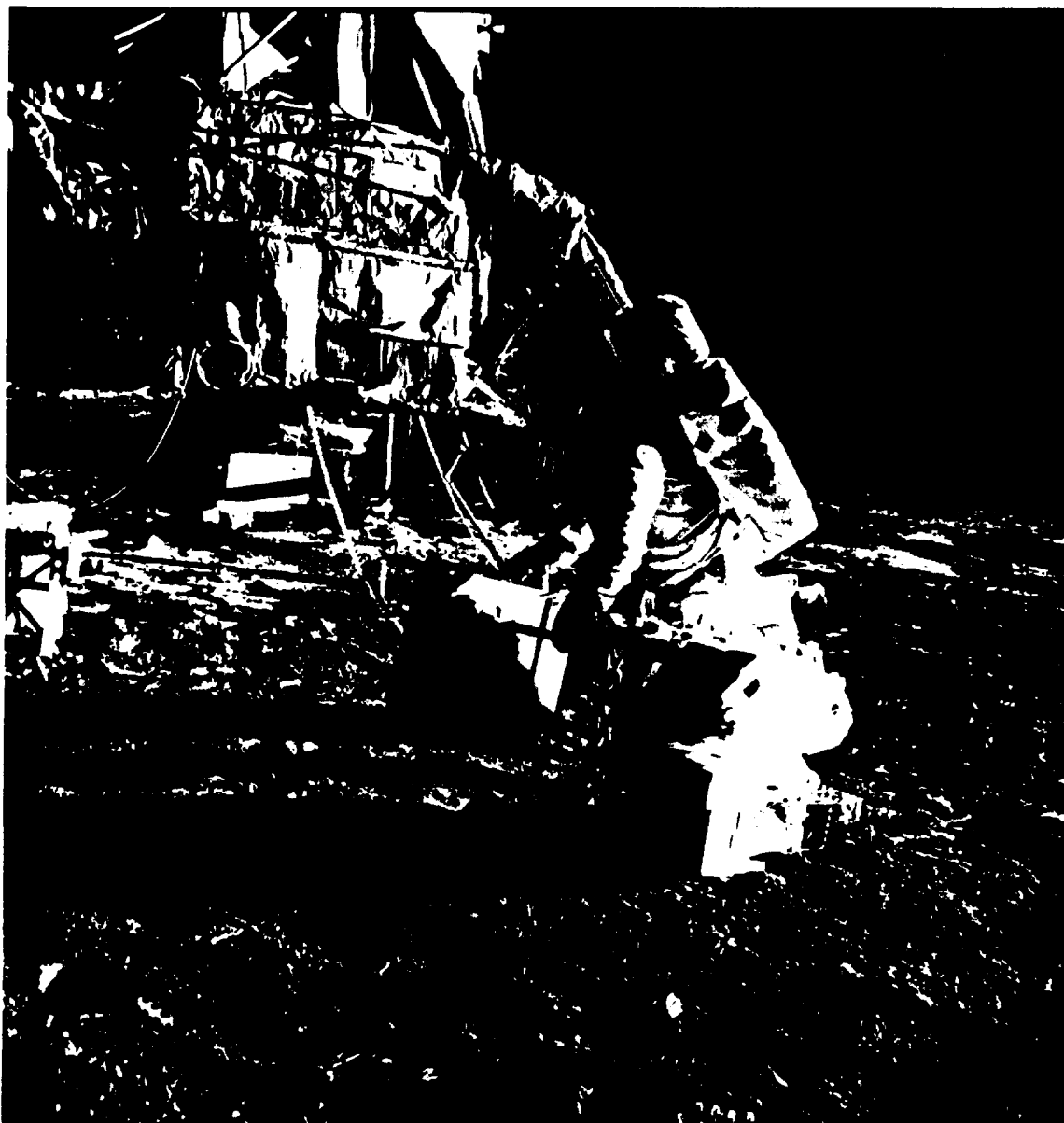


Figure 3-1.- Lunar Module Pilot lifting Apollo lunar surface experiments package prior to deployment traverse.

M M M E E E E E E E E E E E E E E E E









NASA-S-70-530

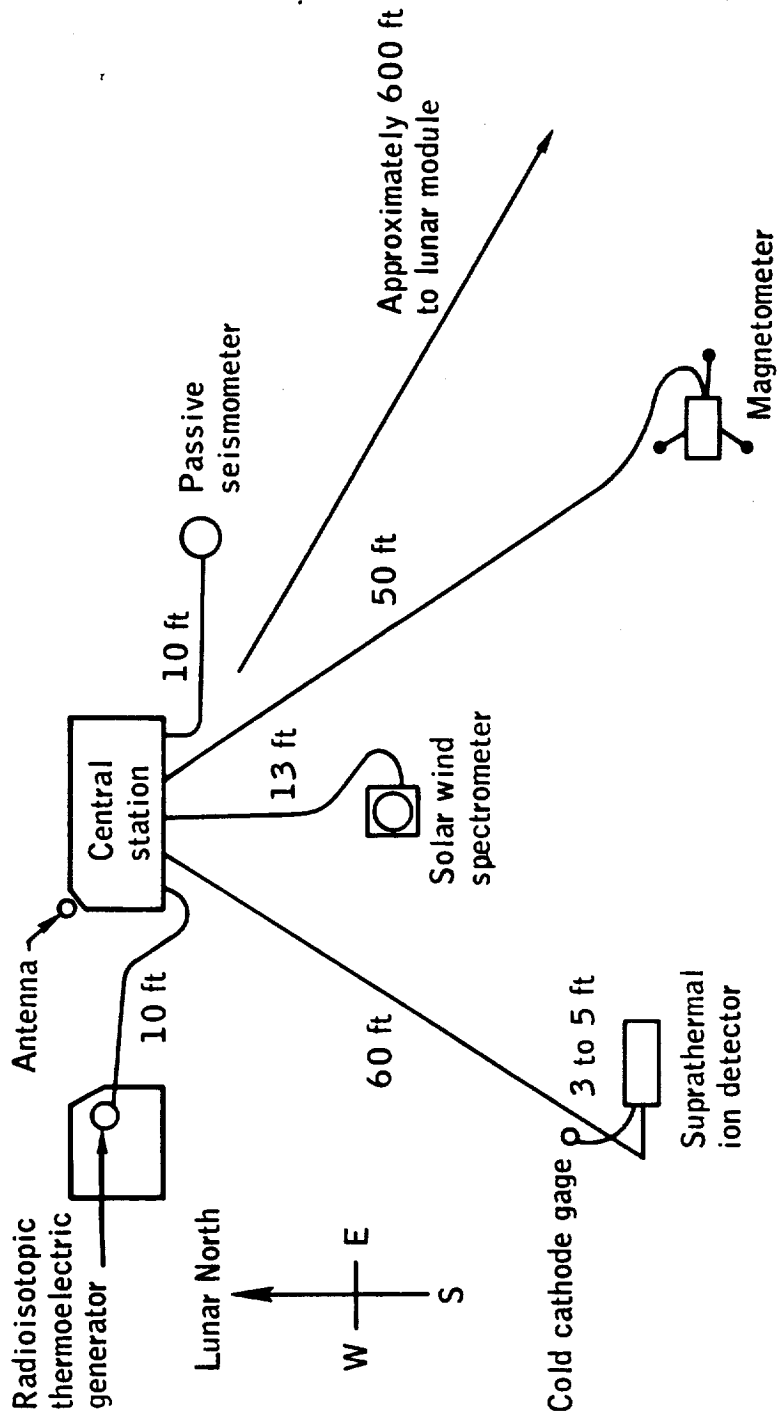


Figure 3-6.- Deployment configuration of the Apollo lunar surface experiments package.













NASA-S-70-534



Figure 3-10.- Lunar surface magnetometer deployed.

M M

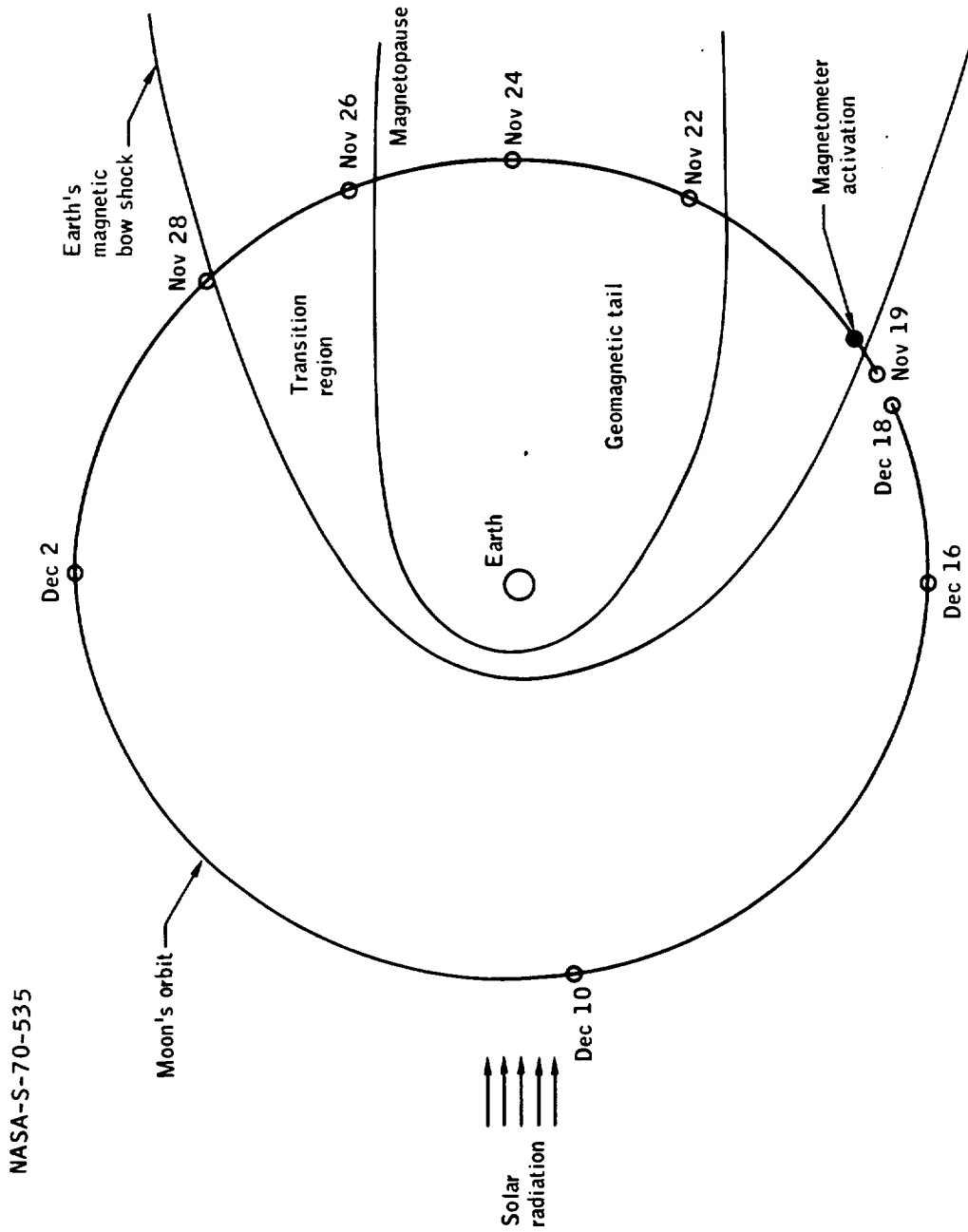
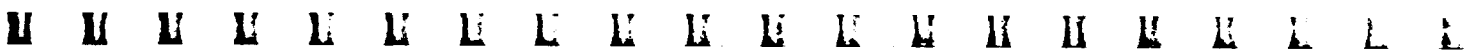


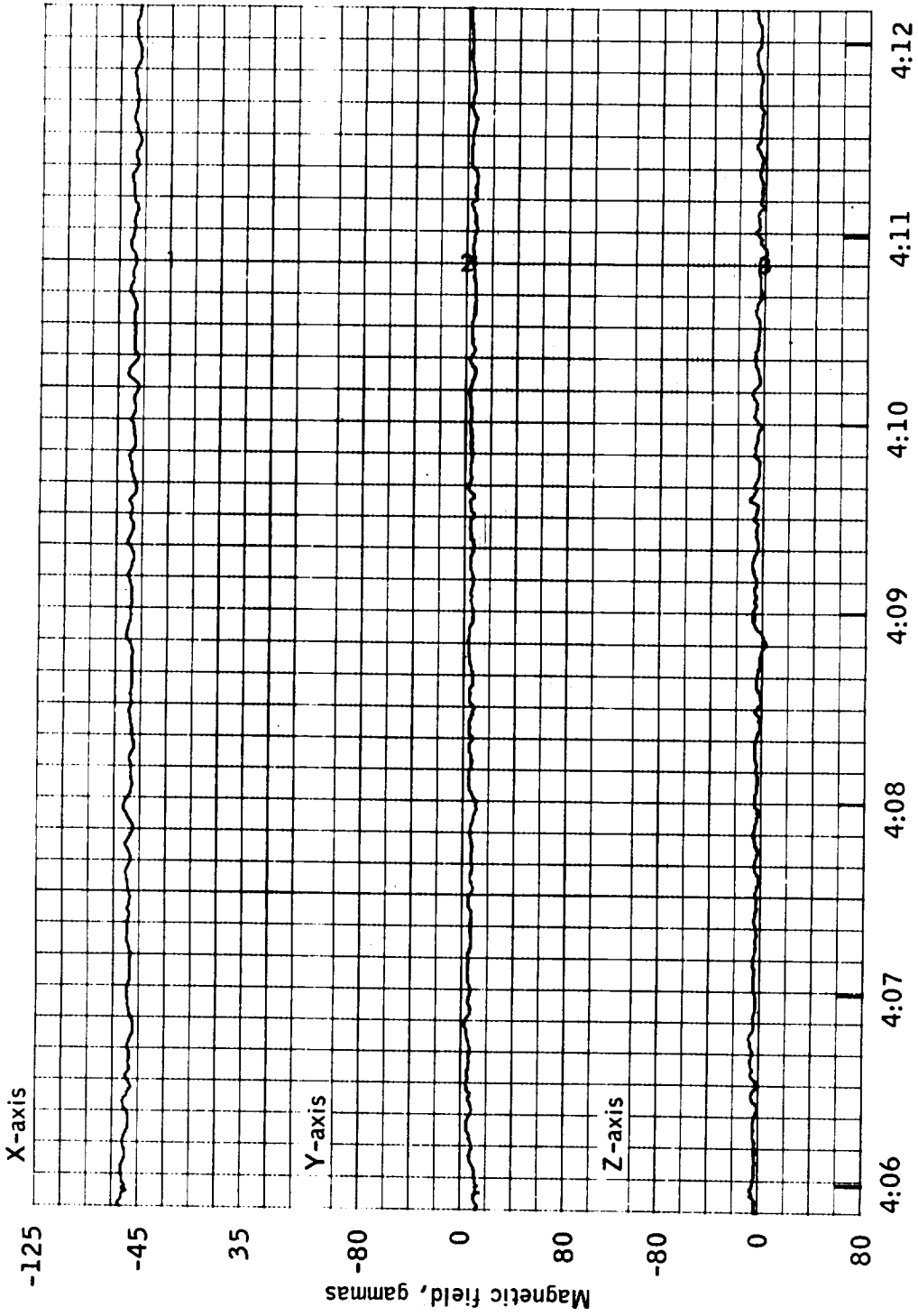
Figure 3-11.- Geometry of the earth's magnetic field regions in the solar plasma.







NASA-S-70-536



G.m.t., hr:min  
November 28, 1969

Figure 3-12.- Interplanetary field region on the lunar surface in sunlight.

NASA-S-70-537

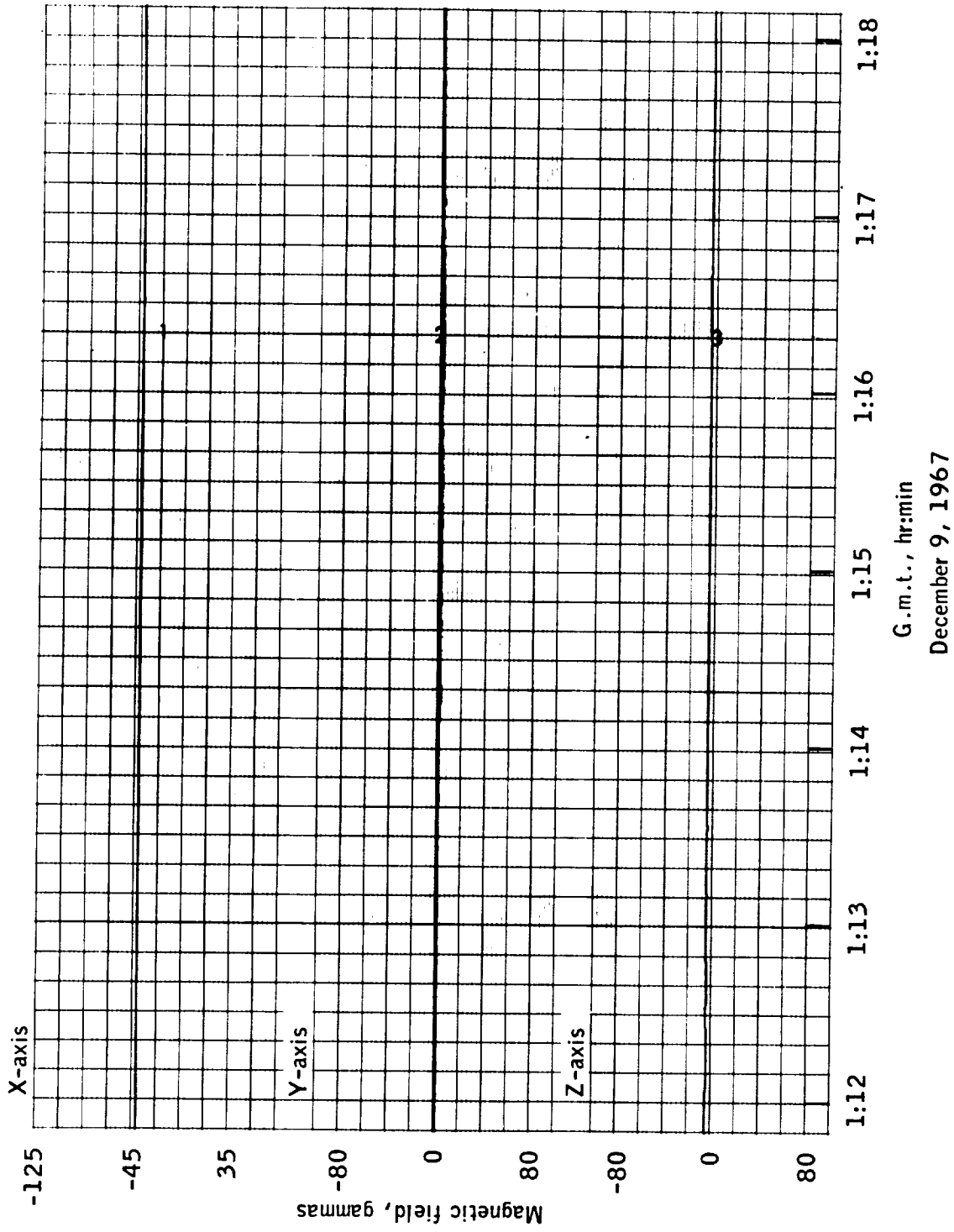


Figure 3-13. - Interplanetary field region on the lunar surface in darkness.



NASA-S-70-539

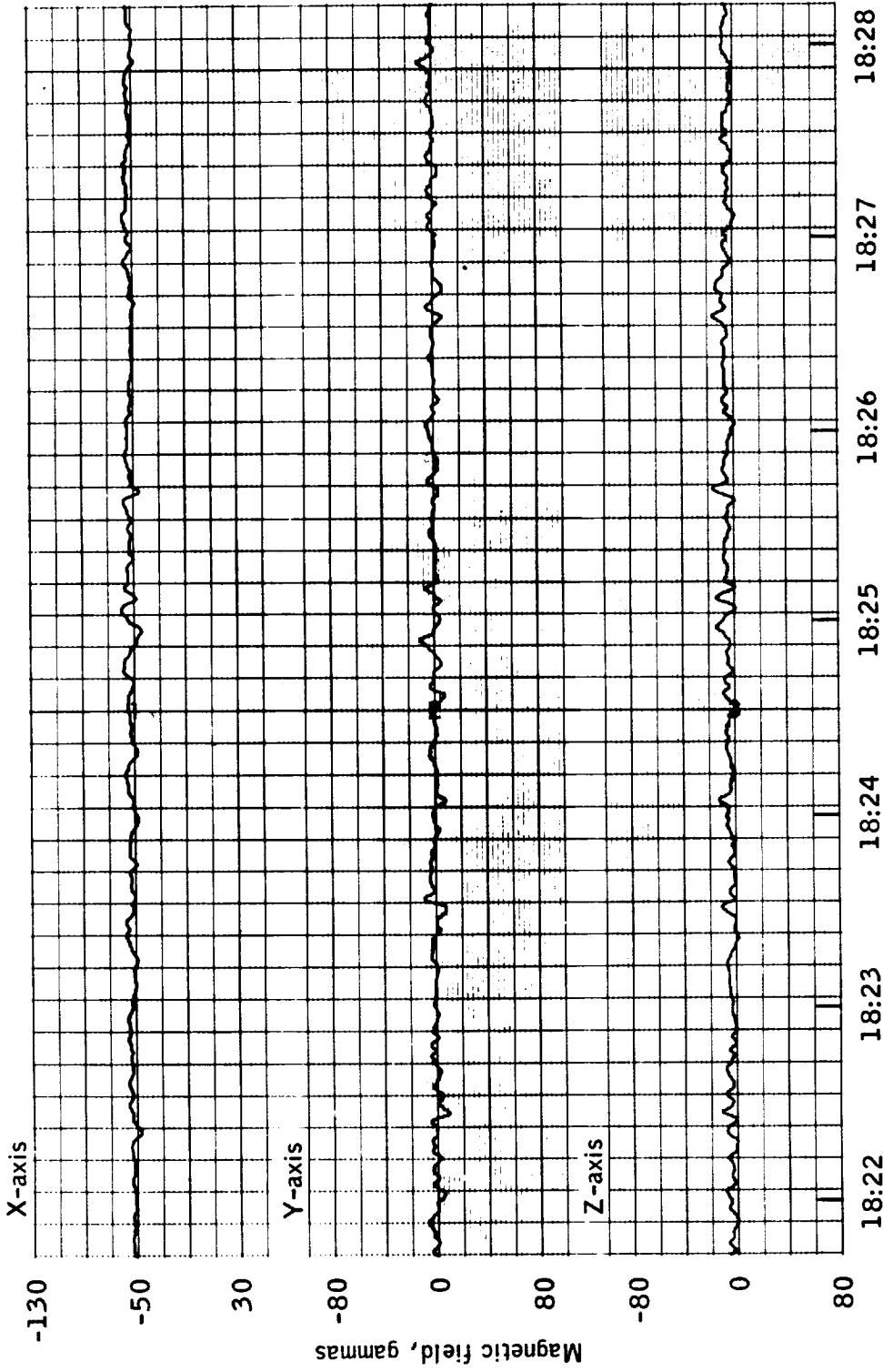


Figure 3-15.- Instrument passage through the transition region between the magnetopause and the earth's bow shock.













NASA-S-70-541

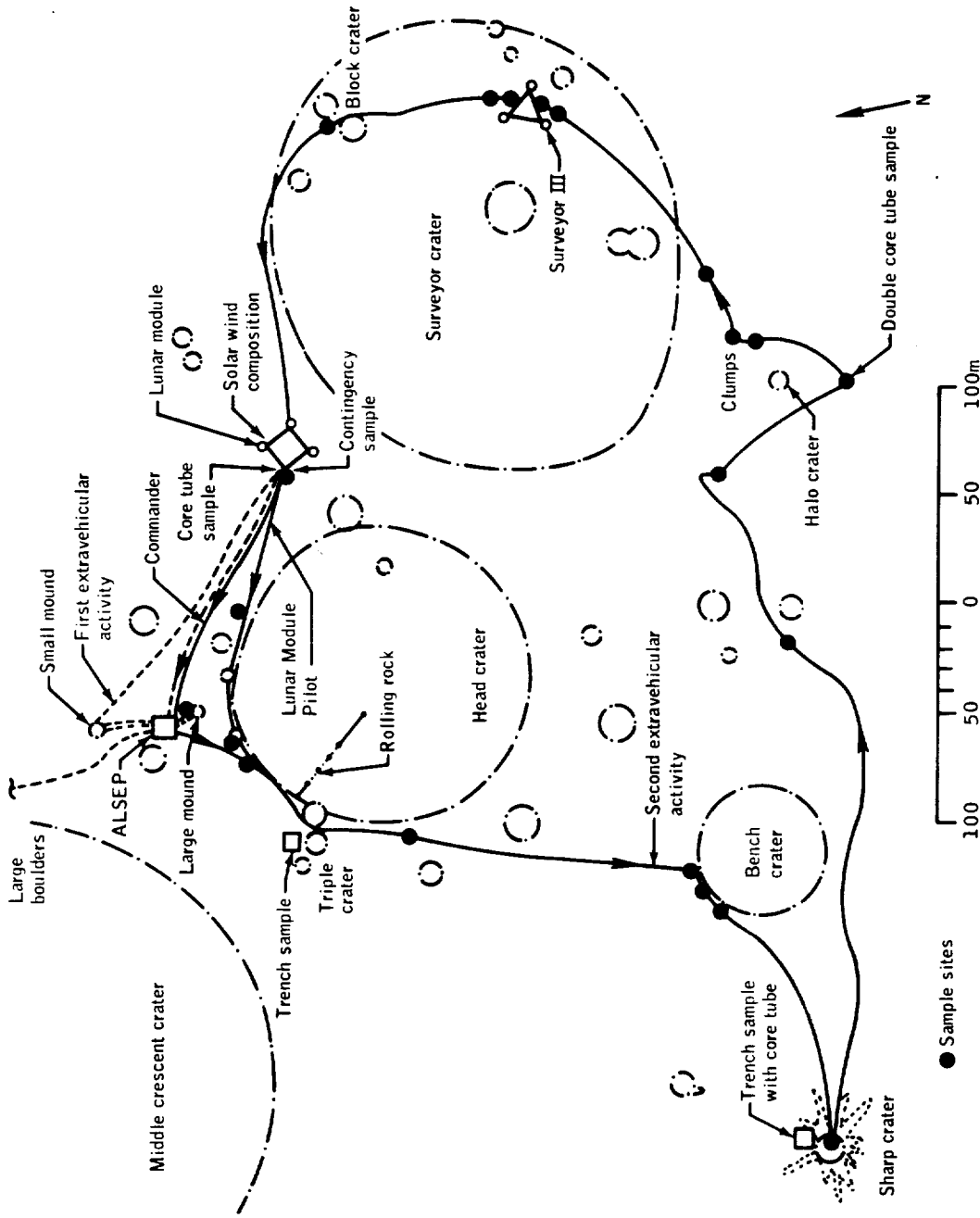


Figure 3-17.- Traverse map.







NASA-S-70-542



Figure 3-18.- Blocky ejecta near a small crater photographed during the first extravehicular activity period.

U M U E E U E U E E E E H H H H R L L A

NASA-S-70-543



Figure 3-19.- Photograph of Bench crater showing probable bedrock.

M M M E E E L L E E L L M M M E E L L











NASA-S-70-546

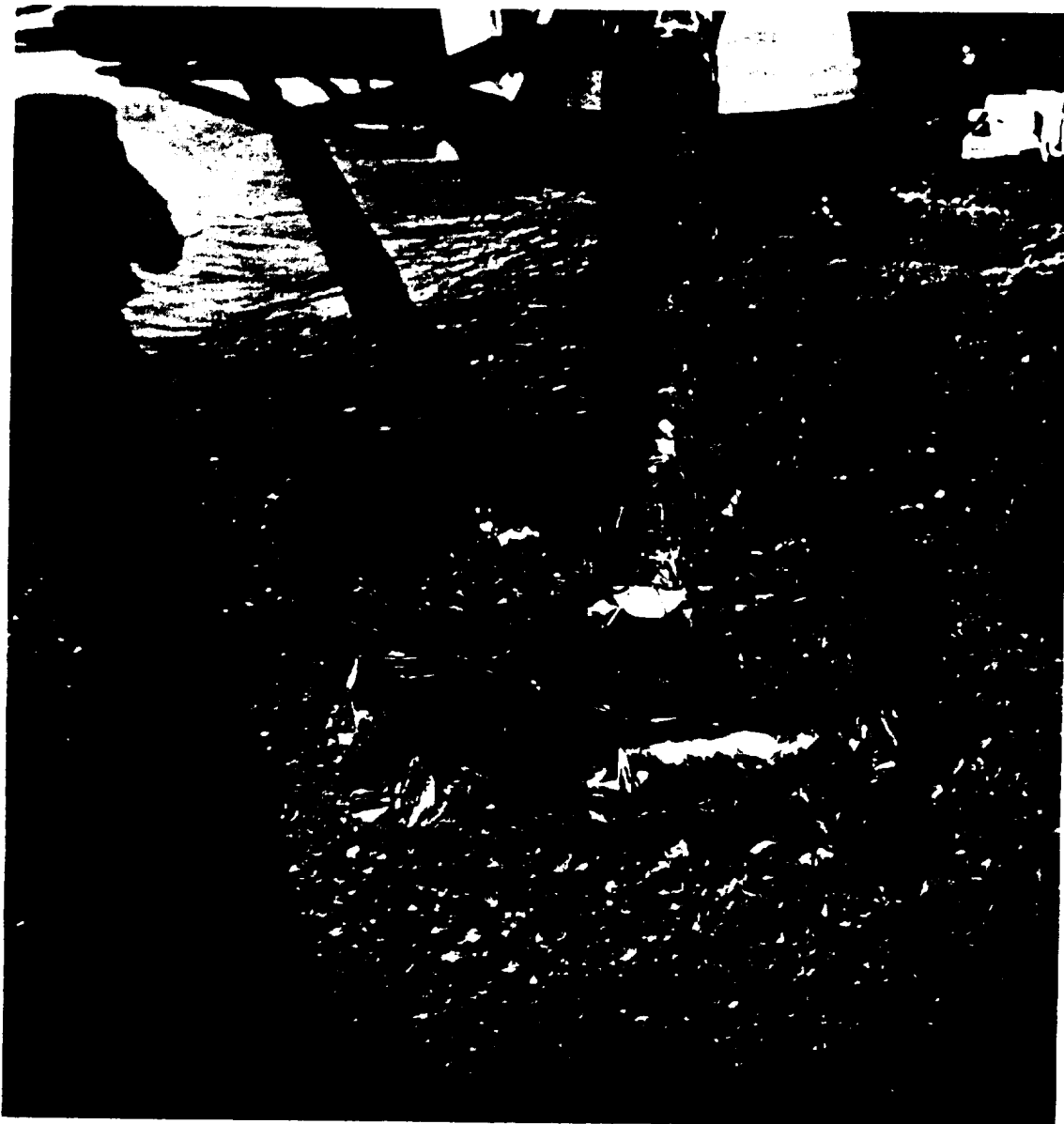


Figure 3-22.- Detail of lunar module minus Z footpad showing disturbance of fine-grained material as viewed from the east.

U U





NASA-S-70-548

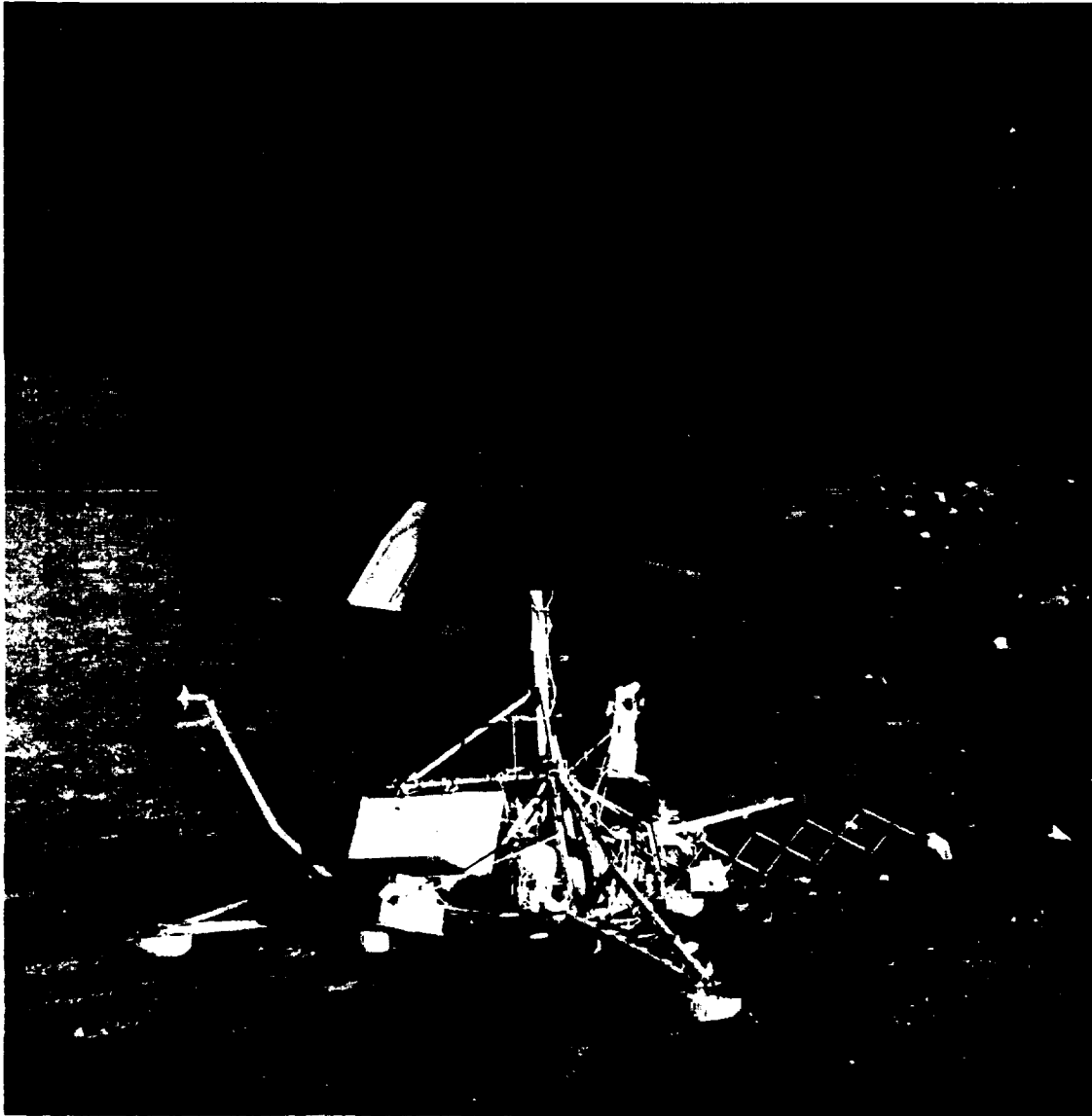


Figure 3-24.- Surveyor III with the lunar module in the background.

U U

















M M M M M K E E E K E E E M K H M K E E E

## 4.0 LUNAR DESCENT AND LANDING

The factors influencing the selection of the Apollo 12 landing site, the actual landing operation, and the final determination of the landing site coordinates are discussed. A more detailed discussion of the landing site selection process will be published in a supplemental report (see appendix E).

### 4.1 LANDING SITE SELECTION

Two major considerations influence the selection of lunar landing sites: (1) operational and scientific objectives, and (2) launch window factors, which are related to both spacecraft performance and operational constraints. This section discusses those aspects of landing site selection significant to Apollo 11 and 12 mission planning.

#### 4.1.1 Site Selection Criteria

Landing site selection for any lunar mission involves the consideration of various operational constraints, crew training requirements, terrain analyses, constraints on the preparation of support products (such as maps and models), and mission objectives. Because of the lead-time necessary to meet several of these requirements, the Apollo 12 site had to be chosen prior to the Apollo 11 launch. The site chosen had to be such that it could take advantage of an Apollo 11 success and thereby represent the next reasonable step in the lunar exploration program; at the same time provisions had to be made to land at a less ambitious site in the event Apollo 11 was not successful. The discussion of this selection process and its evolution will be presented in detail in a supplement to the mission report (appendix E).

Because of a lead time of 5 months prior to launch, the initiation time for launch-vehicle targeting corresponding to an Apollo 12 November launch occurred before Apollo 11 lift-off. After the Apollo 11 success, site selection for Apollo 12 was greatly simplified. Of the four candidates (sites 2, 3, 5, and 7), site 5 was the most desirable backup site for Apollo 12. Site 7 was selected based on satisfying all the selection criteria, including bootstrap photography of a leading landing-site candidate for Apollo 13 (Fra Mauro) and an opportunity to land next to a previously landed spacecraft (Surveyor III).

The Surveyor III site was located in a fairly distinct pattern of surface features which are necessary to the crew's ability to recognize and redesignate to the target. Figure 3-24 illustrates how effectively the goal of landing near the Surveyor was achieved.

U U



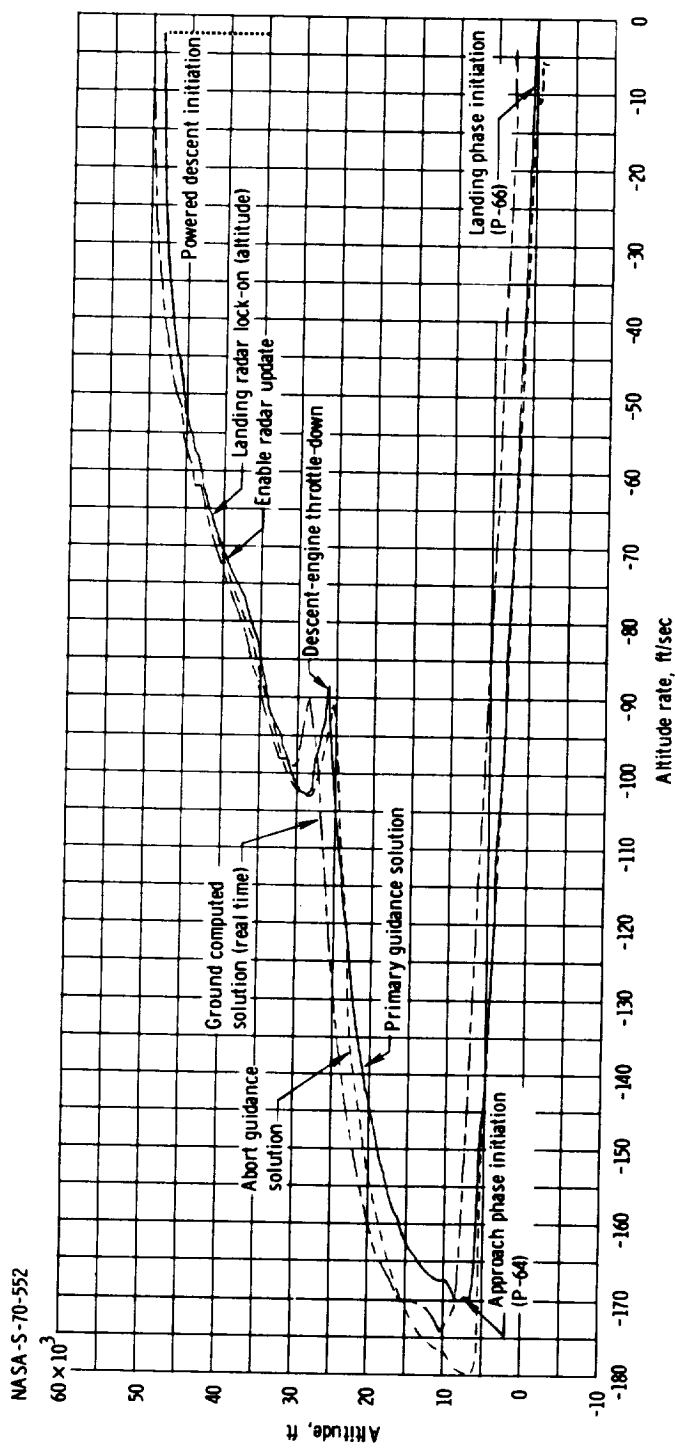












(a) Descent phase.

Figure 4-2. - Comparison of altitude and altitude rate.



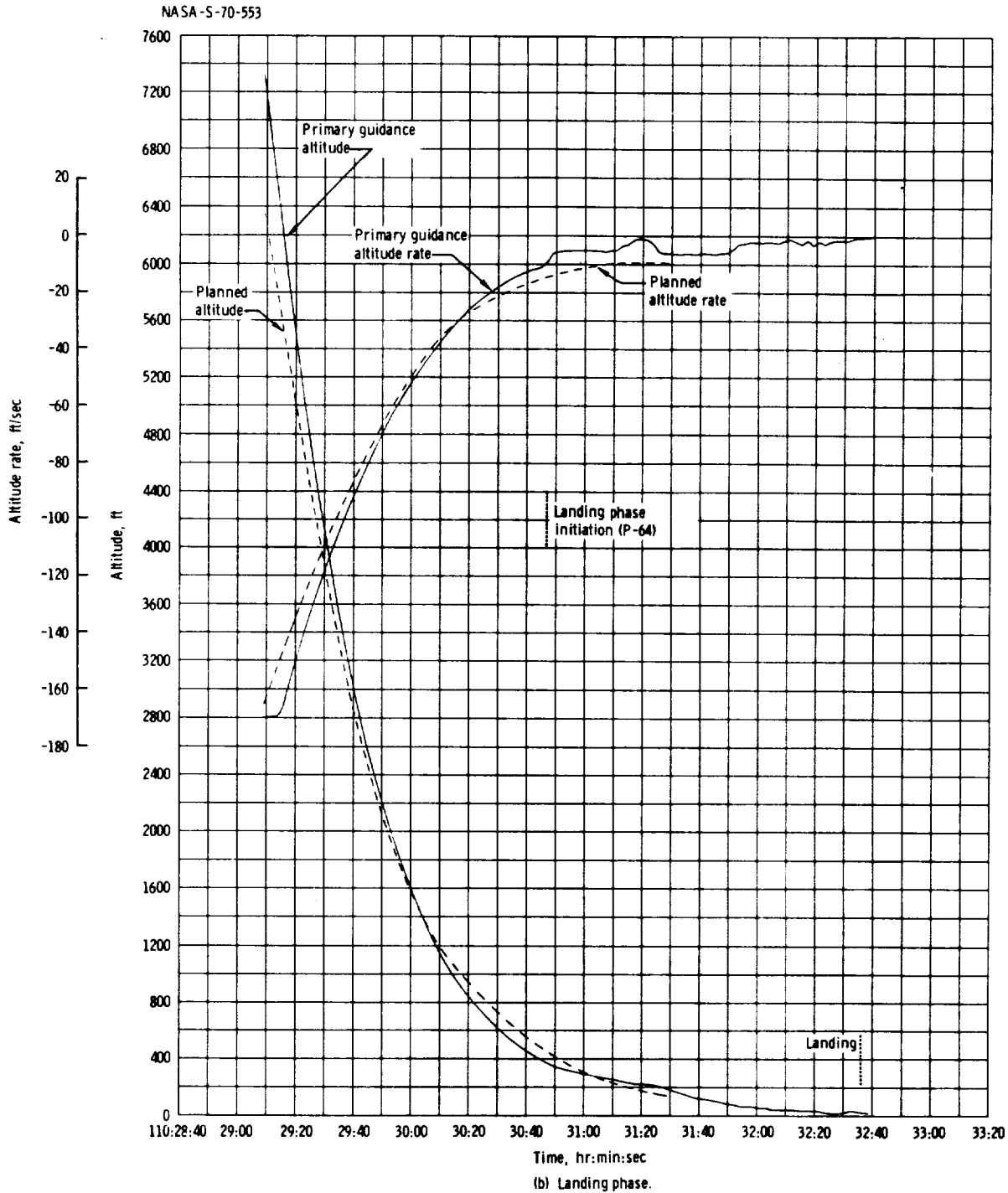
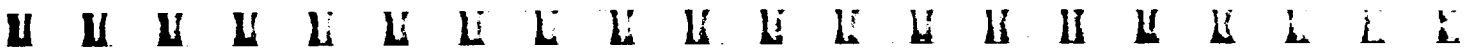


Figure 4-2. - Concluded.





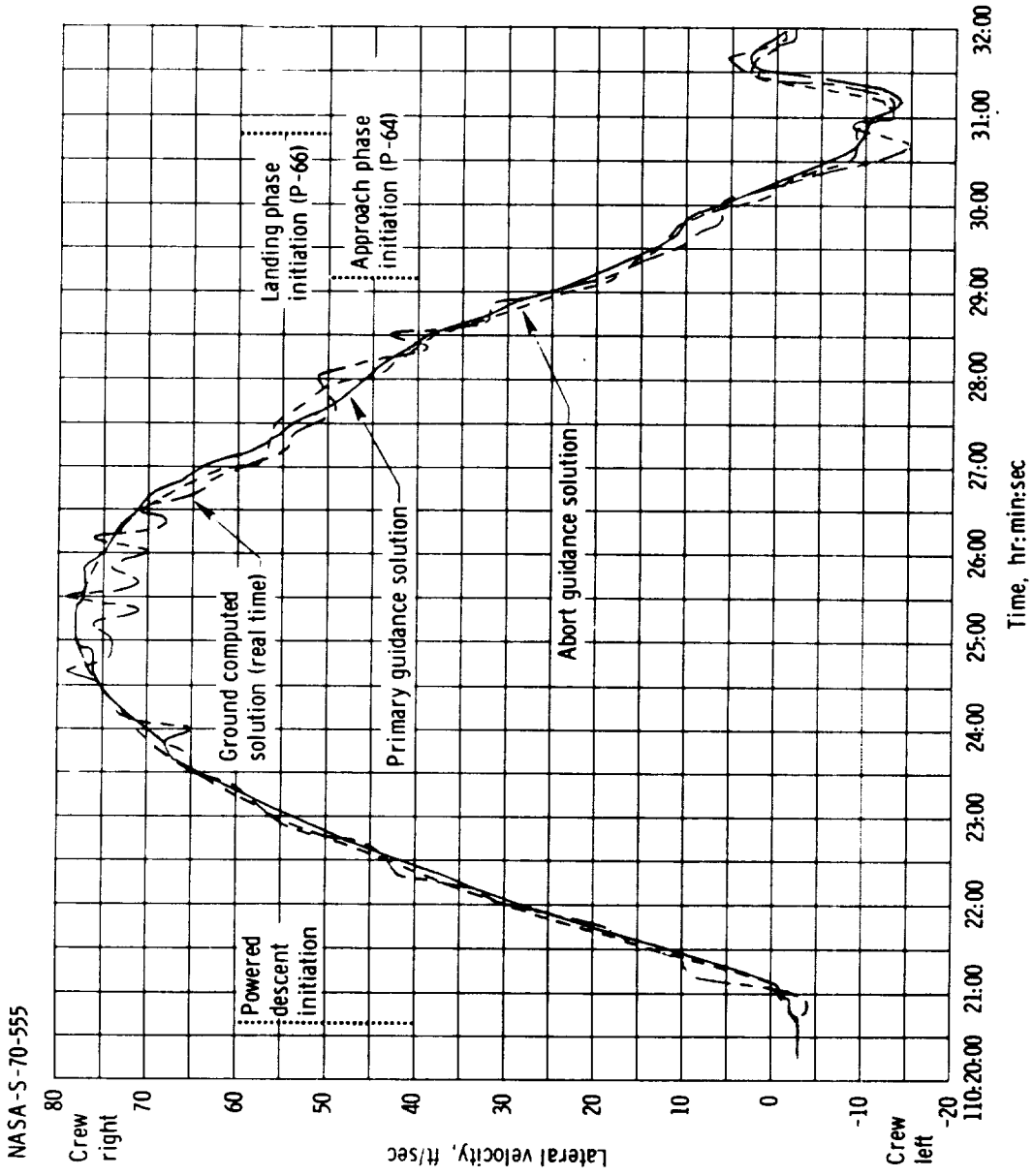


Figure 4-4. - Lateral velocity during descent.



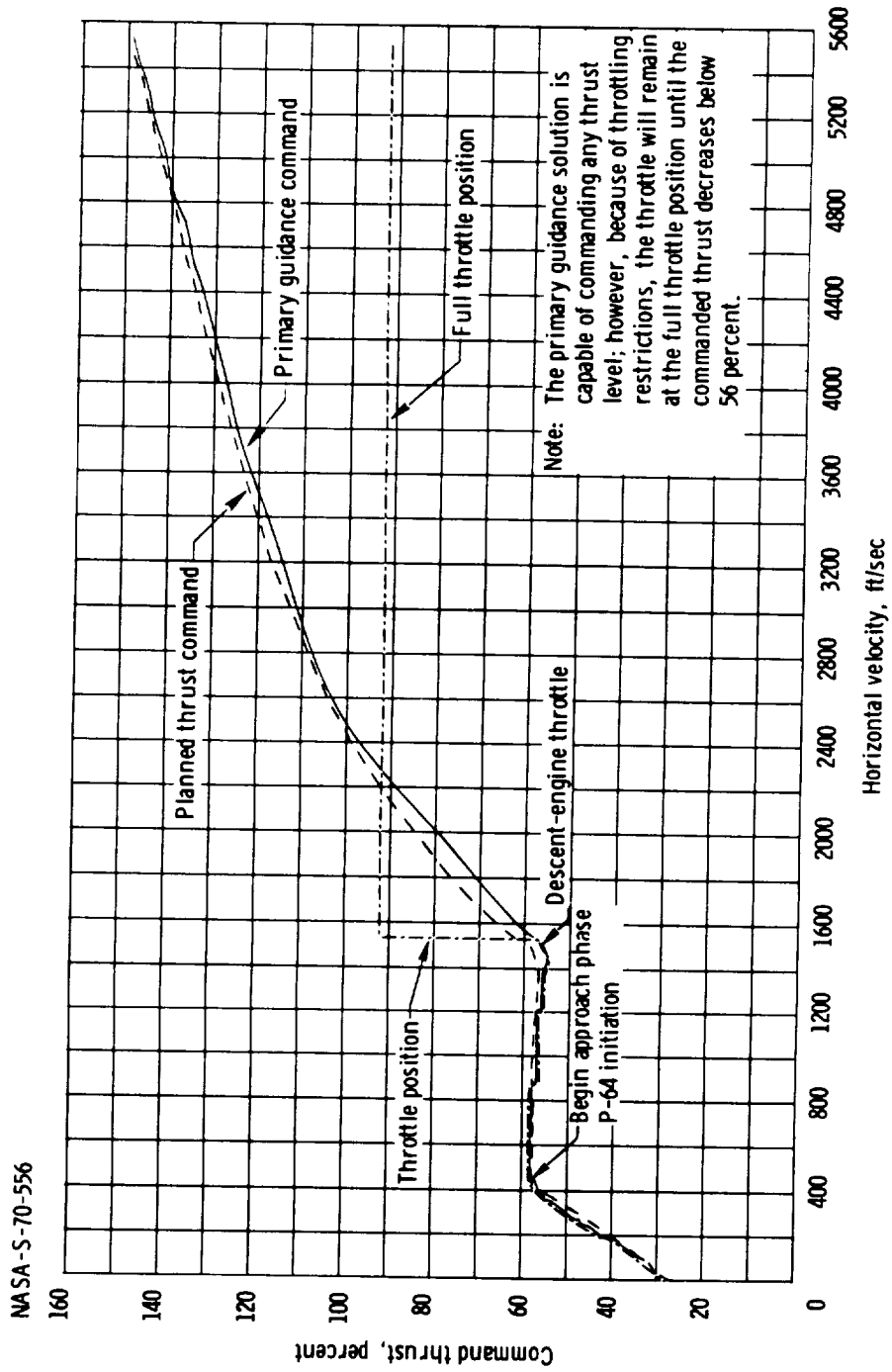


Figure 4-5. - Comparison of percent commanded thrust and horizontal velocity.









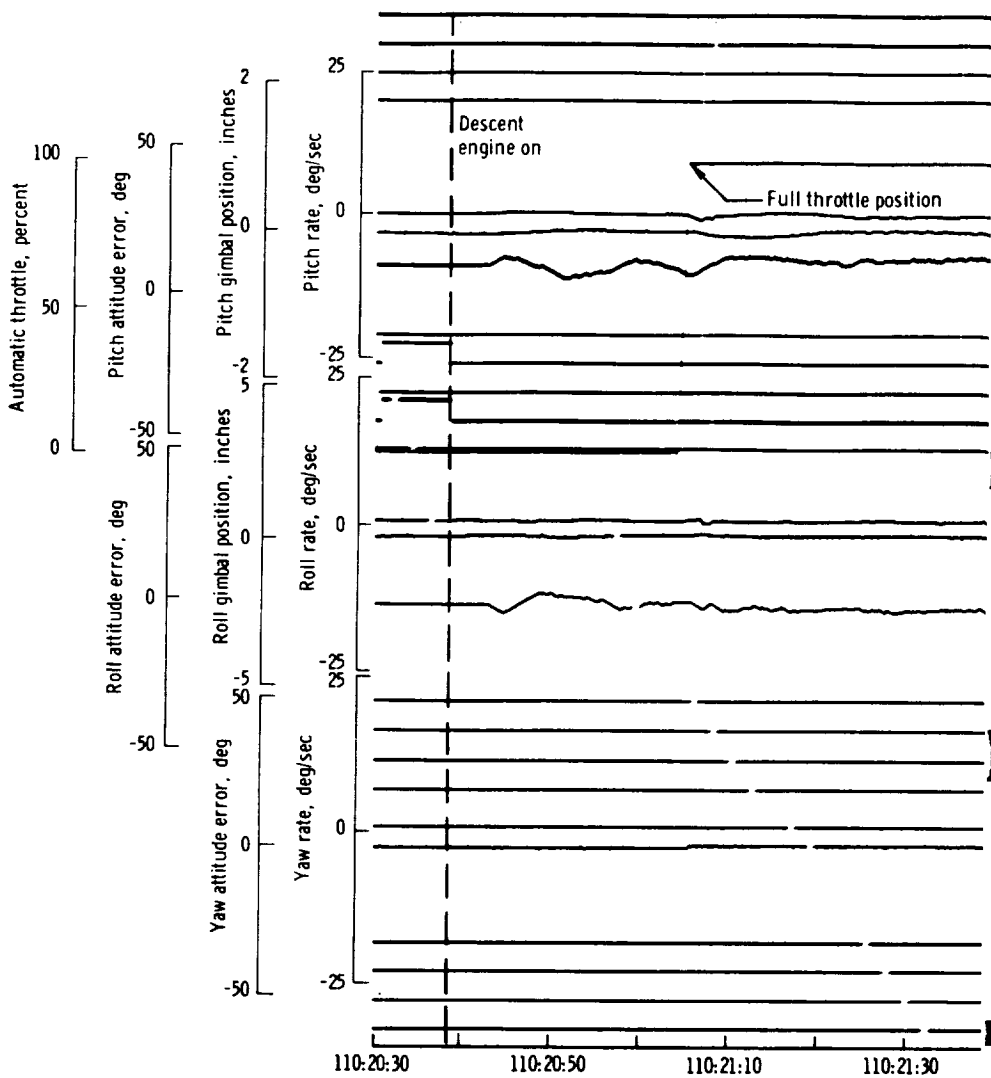
NASA-S-70-558

4U On  
 3U On  
 2U On  
 1U On

4D On  
 3D On  
 2D On  
 1D On  
 Hand controller out of detent On

4F On  
 3A On  
 2A On  
 1F On

4R On  
 3R On  
 2L On  
 1L On



(a) 110:20:30 to 110:26:40.

Figure 4-7. - Spacecraft dynamics during powered descent.

















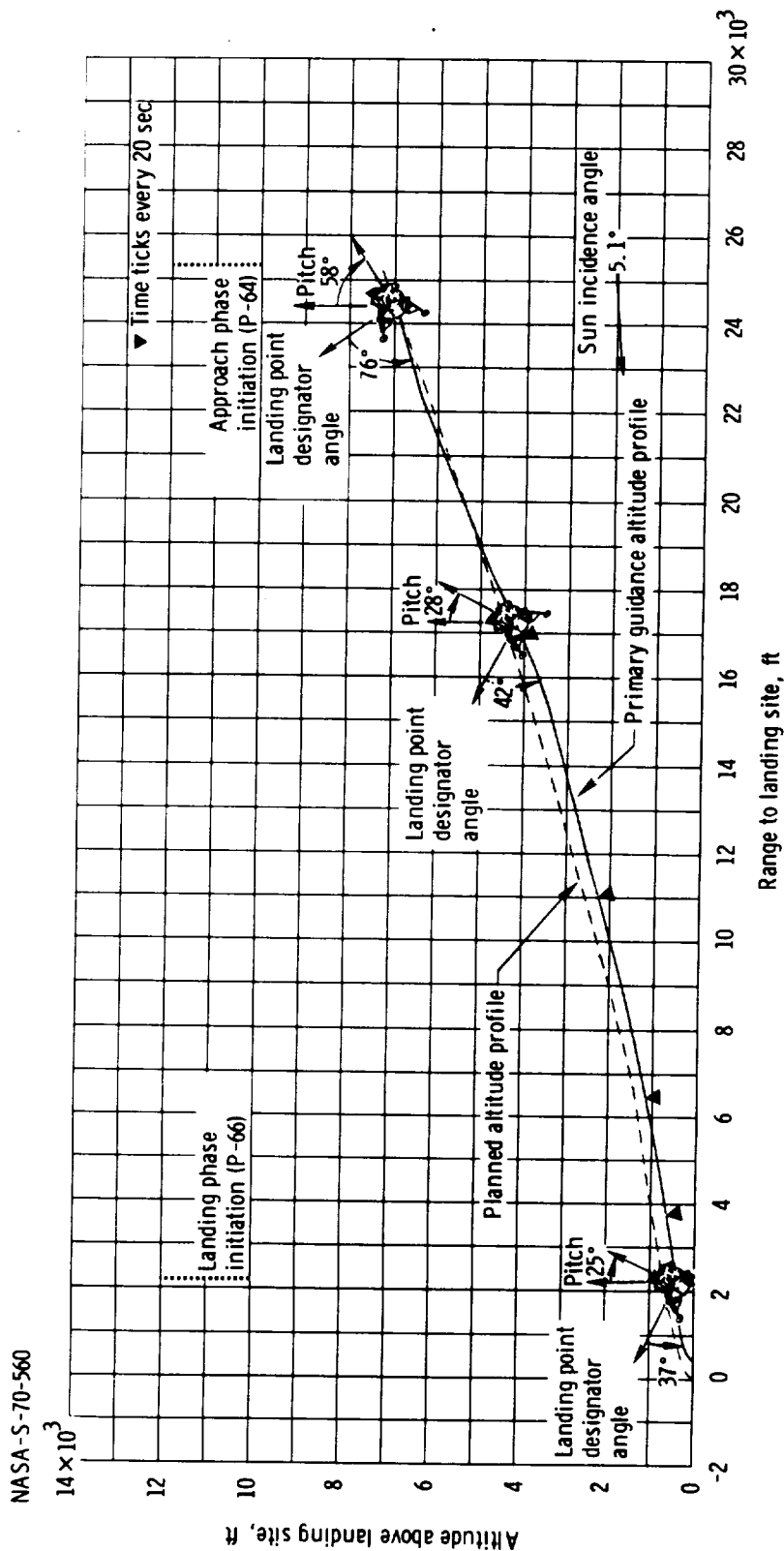












(a) 26 000 feet to landing.

Figure 4-8.- Comparison of altitude and range from the landing site.

M M





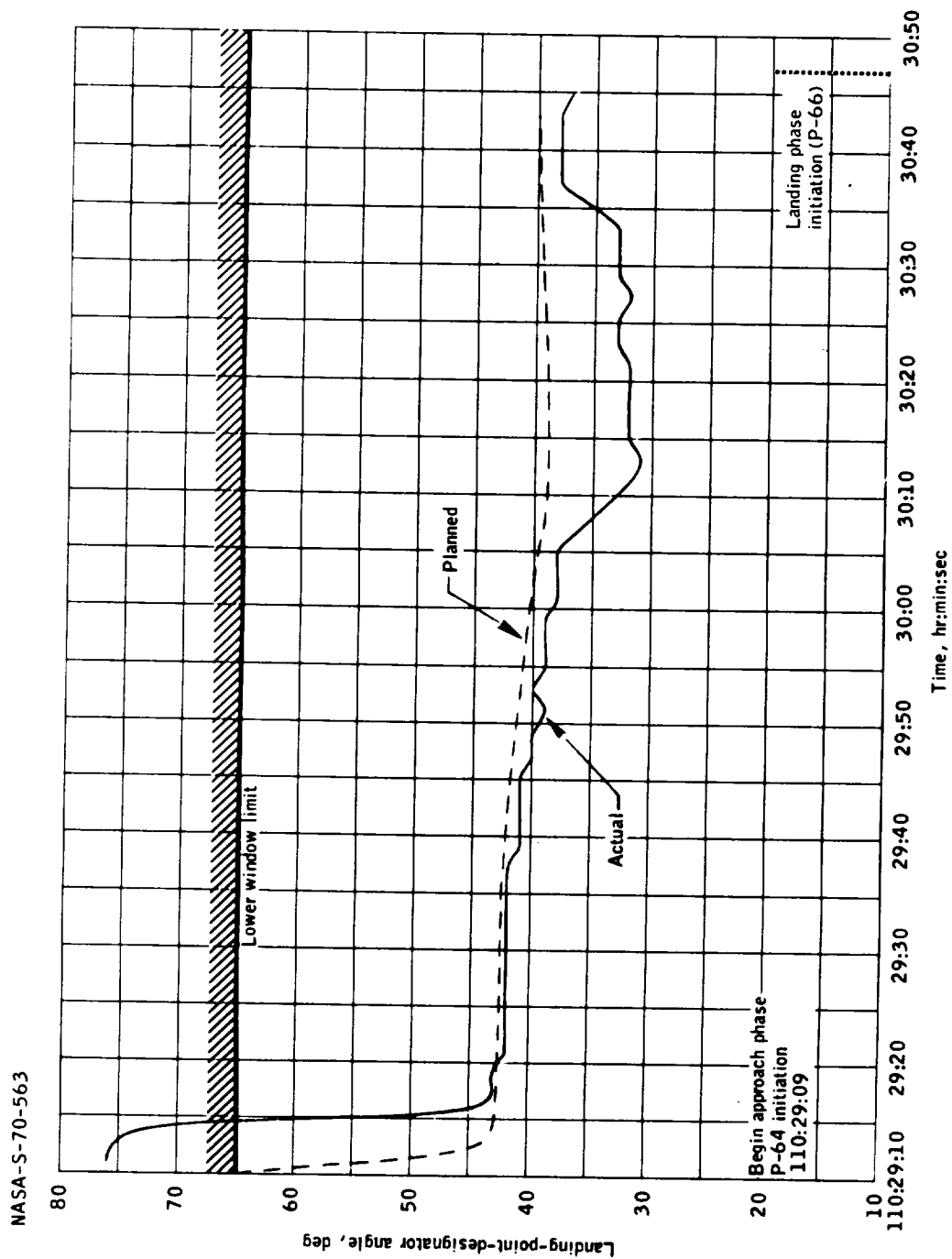
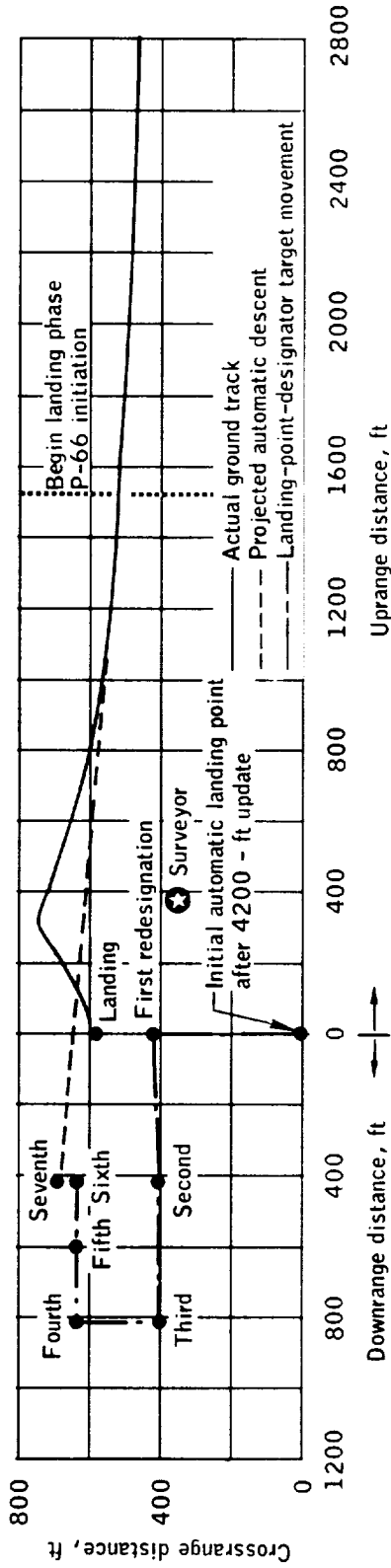
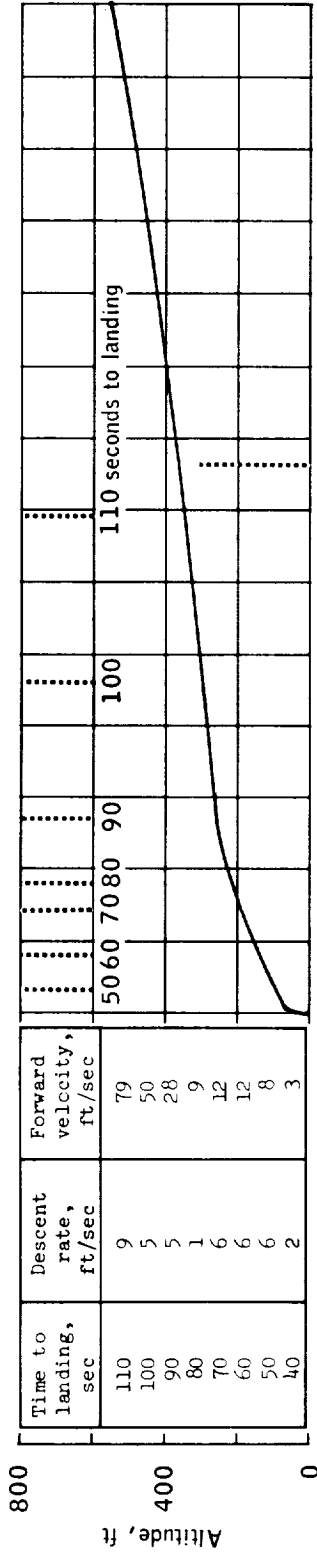


Figure 4-10.- Comparison of landing point designator angle and time during the approach phase.

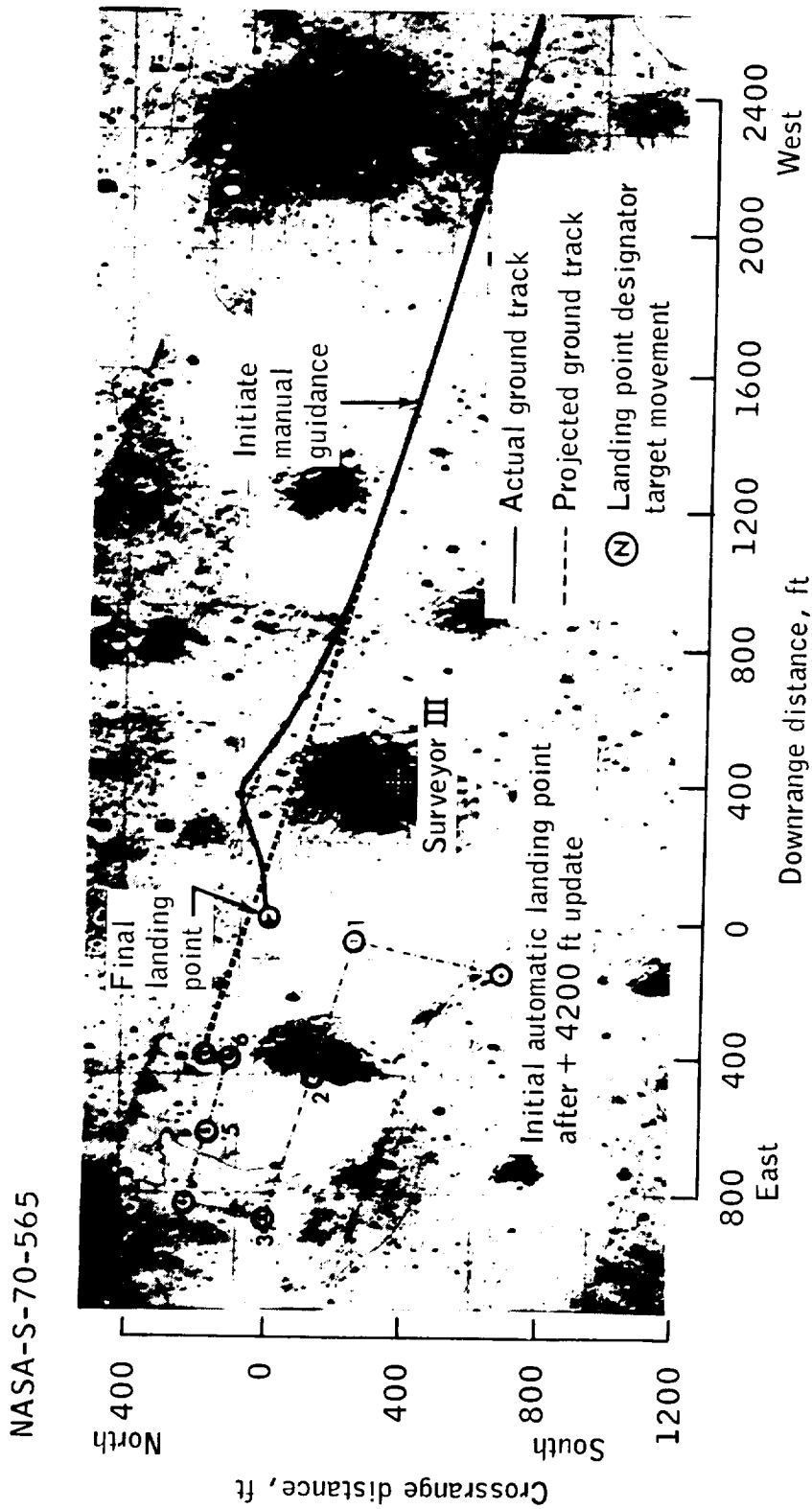
NASA-S-70-563

NASA-S-70-564



(a) Altitude and range from landing site.

Figure 4-11.- Landing phase altitude and range histories.



(b) Ground track map.

Figure 4-11.- Concluded.

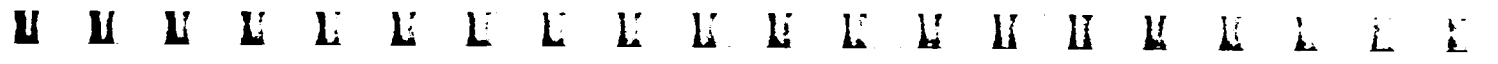






























TABLE 5-IV.- TRANSLUNAR MANEUVER SUMMARY

| Maneuver   | System                               | Ignition time,<br>hr:min:sec | Firing time,<br>sec | Velocity<br>change,<br>ft/sec | Resultant pericynthion conditions |                     |                  |                   |                             |
|--|--------------------------------------|------------------------------|---------------------|-------------------------------|-----------------------------------|---------------------|------------------|-------------------|-----------------------------|
|  |                                      |                              |                     |                               | Altitude,<br>miles                | Velocity,<br>ft/sec | Latitude,<br>deg | Longitude,<br>deg | Arrival time,<br>hr:min:sec |
| Translunar injection                             | S-IVB                                | 2:47:22.7                    | 341.3               | 10 515.0                      | 280.2                             | 7595                | 29.732S          | 169.111E          | 83:44:04.4                  |
| Command and service mod-<br>ule/S-IVB separation | Reaction control                     | 3:18:04.9                    |                     |                               |                                   |                     |                  |                   |                             |
| Spacecraft/S-IVB<br>separation                   | S-IVB auxiliary<br>propulsion system | 4:26:41.1                    | 80.0                |                               |                                   |                     |                  |                   |                             |
| First midcourse correc-<br>tion                  | Service propulsion                   | 30:52:44.4                   | 9.2                 | 61.8                          | 65.1                              | 8234                | 0.7N             | 161.968E          | 83:28:38.8                  |





TABLE 5-VI.- LUNAR ORBIT MANEUVER SUMMARY

| Maneuver                               | System                          | Ignition time,<br>hr:min:sec | Firing time,<br>sec | Velocity<br>change,<br>ft/sec | Resultant orbit       |                        |
|--|---------------------------------|------------------------------|---------------------|-------------------------------|-----------------------|------------------------|
|  |                                 |                              |                     |                               | Apocynthion,<br>miles | Pericynthion,<br>miles |
| Lunar orbit insertion                  | Service propulsion              | 83:25:23.4                   | 352.3               | 2889.5                        | 168.8                 | 62.6                   |
| Lunar orbit circularization            | Service propulsion              | 87:48:48.1                   | 16.9                | 165.2                         | 66.1                  | 54.3                   |
| Command module/lunar module separation | Command module reaction control | 108:24:36.8                  | 14.4                | 2.4                           | 63.5                  | 56.3                   |
| Descent orbit insertion                | Descent propulsion              | 109:23:39.9                  | 29.0                | 72.4                          | 60.6                  | 8.1                    |
| Powered descent initiation             | Descent propulsion              | 110:20:38.1                  | 717.0               | --                            | --                    | --                     |
| First lunar orbit plane change         | Service propulsion              | 119:47:13.2                  | 18.2                | 349.9                         | 62.5                  | 57.6                   |
| Lunar orbit insertion                  | Ascent propulsion               | 142:10:59.9                  | 423.2               | 6057.0                        | 46.3                  | 8.8                    |
| Coelliptic sequence initiation         | Lunar module reaction control   | 143:01:51                    | 41.1                | 45.0                          | 51.0                  | 41.5                   |
| Constant differential height           | Lunar module reaction control   | 144:00:02.6                  | 13.0                | 13.8                          | 44.4                  | 40.4                   |
| Terminal phase initiation              | Lunar module reaction control   | 144:36:26                    | 26.0                | 29.0                          | 60.2                  | 43.8                   |
| Terminal phase finalization            | Lunar module reaction control   | 145:19:29.3                  | 38.0                | 40.0                          | 62.3                  | 58.3                   |
| Final separation                       | Service module reaction control | 148:04:30.9                  | 5.4                 | 1.0                           | 62.0                  | 57.5                   |
| Lunar module deorbit                   | Lunar module reaction control   | 149:55:16.4                  | 82.1                | 196.3                         | --                    | --                     |
| Second lunar orbit plane change        | Service propulsion              | 159:04:45.5                  | 19.2                | 381.8                         | 64.7                  | 56.8                   |

TABLE 5-VII.- RENDEZVOUS MANEUVER SOLUTIONS

| Maneuver                       | Lunar module     |   |                  |   |                  |   | Real-time nominal                         |                  | Command module guidance <sup>a</sup>      |                  | Actual                                    |                  |
|--------------------------------|------------------|---|------------------|---|------------------|---|---|------------------|---|------------------|---|------------------|
|                                | Primary guidance |   |                  | Abort guidance                            |                  |   | Time, hr:min:sec                          | Velocity, ft/sec | Time, hr:min:sec                          | Velocity, ft/sec | Time, hr:min:sec                          | Velocity, ft/sec |
|                                | Time, hr:min:sec | Velocity, ft/sec                          | Time, hr:min:sec | Velocity, ft/sec                          | Time, hr:min:sec | Velocity, ft/sec                          |   |                  |   |                  |   |                  |
| Coelliptic sequence initiation | 143:01:51        | 45.3 posi-grade                           | 143:01:51        | 46.1 posi-grade                           | 143:01:51        | 49.0 posi-grade                           | 44.9 posi-grade                           | 143:01:51        | 44.9 posi-grade                           | 143:01:51        | 51.6 posi-grade<br>0.1 south<br>0.3 down  |                  |
| Constant differential height   | 144:00:02        | 10.2 retro-grade<br>9.3 down              | 144:00:02        | 9.4 retro-grade<br>13.5 down              | 143:59:53        | 2.3 down                                  | 10.3 retro-grade<br>0.4 south<br>7.8 down | 144:00:02        | 10.3 retro-grade<br>0.4 south<br>7.8 down | 144:00:02        | 10.1 retro-grade<br>9.1 down              |                  |
| Terminal phase initiation      | 144:36:29        | 25.9 posi-grade<br>1.5 south<br>11.9 down | 144:33:33        | 28.2 posi-grade<br>1.7 south<br>10.9 down | 144:38:00        | 22.2 posi-grade<br>0.1 south<br>10.9 down | 25.5 posi-grade<br>1.7 south<br>10.9 down | 144:36:57        | 25.5 posi-grade<br>1.7 south<br>10.9 down | 144:36:39        | 25.8 posi-grade<br>1.4 south<br>11.1 down |                  |
| First midcourse correction     | 144:51:29        | 0.5 retro-grade<br>2.0 up                 | 144:51:29        | 3.8 retro-grade<br>0.3 north<br>4.6 down  | (c)              | 0.0                                       | 1.6 retro-grade<br>0.1 north<br>5.3 down  | 144:51:29        | 1.6 retro-grade<br>0.1 north<br>5.3 down  | 144:51:29        | (b)                                       |                  |
| Second midcourse correction    | 145:06:29        | 0.9 retro-grade<br>0.3 south<br>0.7 down  | (c)              | (c)                                       | (c)              | 0.0                                       | 6.1 retro-grade<br>0.3 north<br>1.6 up    | 145:06:29        | 6.1 retro-grade<br>0.3 north<br>1.6 up    | 145:06:29        | (b)                                       |                  |

<sup>a</sup>For lunar module execution; midcourse solutions obtained from VIF ranging data only (tracking light failed).

<sup>b</sup>Data not available because of moon occultation.

<sup>c</sup>Solution not obtained.















in the right-hand lunar module window. On Apollo 12 this camera was operated at 12 frames/sec. Additional photographic data on erosion are obtained from 70-mm still photographs taken in the vicinity of the lunar module during extravehicular activity. Finally, an accurate reconstruction of the trajectory from tracking and telemetry data is necessary to correlate position and time with the varying visibility conditions observed by the crew and recorded on the photographs. There is no assurance that the sequence film records the same impressions as stated by the crew for the following reasons:

- a. The camera has a relatively narrow field of view compared to the crewman
- b. The camera line-of-sight is more depressed toward the vertical than the crewman's normal line-of-sight; hence, the two data sources normally view different scenes
- c. The range of optical response for the film is less than that of the crewman's eye
- d. The environment under which the crewman made his observations is considerably different from that in which the film is viewed after the flight.

The first time that dust is detected from the photographic observations occurs 52 seconds before touchdown. This time corresponds to an altitude of about 100 feet. There is no commentary in the voice transcription relative to dust at this point, but postflight debriefings indicate the crew noticed the movement of dust particles on the surface from a relatively higher altitude. At 180 feet altitude the Lunar Module Pilot made the comment that they could expect to get some dust before long. However, the initial effect of the dust, as first observed in the film or by the crew, indicates that there was no degradation in visibility prior to about 100 feet in altitude. However, the crew stated that dust was first observed at an altitude of about 175 feet (section 9.0). Dust continued to appear in the sequence camera photographs for the next 10 or 12 seconds as the lunar module descended to about 60 to 70 feet in altitude. Visibility is seen to have degraded, but not markedly. Beyond this point, the film shows the dust becoming more dense. Although surface features are still visible through the dust, impairment of visibility is beginning. Degradation of visibility continues until the surface is completely obscured and conditions are blind. The point at which this total obscuration occurs is somewhat subjective. At 25 seconds before touchdown, the dust cloud is quite dense, although observations of the film show some visibility of the surface. From the pilot's point of view, however, visibility is seen to be essentially zero at this time, which corresponds to an altitude of about 40 feet. Therefore, the pilot's assessment that total

U U U E E U U E E E E U U U U U E L L L























TABLE 7.6-1.- PLATFORM ALIGNMENT SUMMARY

| Time,<br>hr:min | Program<br>option* | Star used                  | Gyro torquing angle,<br>deg |        |         | Star angle<br>difference,<br>deg | Gyro drift, mFRU |      |       | Comments                |
|-----------------|--------------------|----------------------------|-----------------------------|--------|---------|----------------------------------|------------------|------|-------|-------------------------|
|                 |                    |                            | X                           | Y      | Z       |                                  | X                | Y    | Z     |                         |
| 00:24           |                    |                            |                             |        |         |                                  |                  |      |       |                         |
| 00:52           | 1                  | 14 Canopus, 15 Sirius      | +0.755                      | +0.941 | -0.366  | 0.01                             | --               | --   |       | Program 51              |
| 02:20           | 3                  | 01 Alpheratz, 45 Fomalhaut | -0.014                      | -0.028 | +0.018  | 0.01                             | +0.8             | +1.7 | +1.1  |                         |
| 05:53           | 1                  | 14 Canopus, 16 Procyon     | +0.764                      | +0.576 | -1.187  | 0.01                             | --               | --   | --    |                         |
| 14:57           | 3                  | 16 Procyon, 12 Rigel       | +0.127                      | -0.171 | -0.281  | 0.00                             | -0.9             | +1.3 | -2.1  |                         |
| 29:48           | 3                  | 24 Gienah, 27 Alkaid       | +0.250                      | -0.246 | +0.125  | 0.01                             | -1.1             | +1.1 | +0.6  | Check star 22 Regulus   |
| 55:02           | 3                  | 03 Navi, 13 Capella        | +0.515                      | -0.492 | +0.289  | 0.01                             | -1.4             | +1.3 | +0.8  | Check star 20 Dnoes     |
| 78:21           | 3                  | 03 Navi, 13 Capella        | +0.400                      | -0.462 | +0.263  | 0.02                             | -1.1             | +1.3 | +0.8  |                         |
| 81:06           | 1                  | 01 Alpheratz, 10 Mirfak    | +0.180                      | +0.259 | +0.658  | 0.02                             | --               | --   | --    |                         |
| 86:45           | 3                  | 7 Menkar, 13 Capella       | +0.078                      | -0.111 | +0.090  | 0.02                             | -0.9             | +1.3 | +1.05 | Check star 11 Aldebaran |
| 88:55           | 3                  | 16 Procyon, 20 Dnoes       | +0.013                      | -0.029 | +0.069  | 0.02                             | -0.4             | +0.9 | +2.1  | Check star 22 Regulus   |
| 102:50          | 1                  | 20 Dnoes, 27 Alkaid        | +0.238                      | -0.294 | +0.061  | 0.01                             | --               | --   | --    |                         |
| 108:49          | 3                  | 11 Aldebaran, 10 Mirfak    | +0.135                      | -0.061 | +0.000  | 0.01                             | -1.5             | +0.7 | 0.0   |                         |
| 110:44          | 3                  | 21 Alpheratz, 26 Spica     | -0.035                      | -0.056 | +0.44   | 0.01                             | +1.2             | +1.9 | +1.5  |                         |
| 118:32          | 1                  | 03 Navi, 20 Dnoes          | +0.562                      | +0.000 | +0.670  | 0.02                             | --               | --   | --    |                         |
| 120:35          | 1                  | 12 Rigel, 21 Alpherat      | -0.708                      | -0.961 | -0.392  | 0.02                             | --               | --   | --    |                         |
| 132:45          | 3                  | 12 Rigel, 21 Alpherat      | +0.255                      | -0.228 | +0.141  | --                               | -1.4             | +1.3 | +0.8  |                         |
| 138:20          | 3                  | 22 Regulus, 26 Spica       | +0.088                      | -0.160 | +0.102  | 0.02                             | -1.0             | +1.8 | +1.2  |                         |
| 140:17          | 3                  | 11 Aldebaran, 20 Dnoes     | +0.022                      | -0.021 | -0.043  | 0.01                             | -0.8             | +0.7 | -1.5  |                         |
| 142:19          | 3                  | 23 Denebola, 26 Spica      | +0.028                      | -0.014 | +0.019  | 0.00                             | -0.9             | +1.5 | +0.6  |                         |
| 158:17          | 1                  | 22 Regulus, 27 Alkaid      | -0.382                      | -0.048 | +0.331  | --                               | --               | --   | --    |                         |
| 159:16          | 1                  |                            | -84.79                      |        | -49.479 | --                               | --               | --   | --    | Pulse torqued to orient |
| 159:54          | 3                  | 16 Procyon, 23 Denebola    | +0.065                      | -0.037 | -0.098  | 0.01                             | --               | --   | --    |                         |
| 164:06          | 3                  | 21 Alpherat, 26 Spica      | +0.095                      | -0.088 | -0.003  | 0.03                             | -1.5             | +1.4 | -0.1  |                         |
| 165:52          | 3                  | 20 Dnoes, 21 Alpherat      | +0.023                      | -0.003 | +0.073  | --                               | --               | --   | --    |                         |
| 167:57          | 3                  | 16 Procyon, 20 Dnoes       | +0.053                      | -0.032 | +0.003  | 0.02                             | -1.7             | +1.0 | +0.1  |                         |
| 173:33          | 1                  |                            |                             |        |         |                                  |                  |      |       |                         |
| 173:52          | 3                  | 04 Achernar, 22 Regulus    | -0.216                      | -0.004 | +0.149  | 0.01                             | --               | --   | --    | Pulse torqued to orient |
| 187:55          | 3                  | 06 Achernar, 45 Fomalhaut  | +0.288                      | -0.211 | +0.211  | 0.01                             | -1.4             | +1.4 | +1.0  |                         |
| 210:09          | 3                  | 34 Atria, 30 Menkent       | +0.414                      | -0.396 | +0.240  | 0.02                             | -1.2             | +1.2 | +0.7  | Check star 25 Acrux     |
| 211:30          | 3                  | 15 Sirius, 12 Rigel        | +0.034                      | -0.053 | -0.002  | 0.04                             | --               | --   | --    | No torque               |
| 211:37          | 3                  | 45 Fomalhaut, 34 Atria     | +0.061                      | -0.009 | -0.004  | 0.02                             | --               | --   | --    | No torque               |
| 221:39          | 3                  | 25 Acrux, 17 Regor         | +0.191                      | -0.199 | +0.149  | --                               | -1.1             | +1.2 | +0.8  |                         |
| 240:08          | 1                  | 35 Rasalhague, 41 Dabih    | +0.195                      | -0.544 | -0.641  | 0.00                             | --               | --   | --    | Check star 37 Munki     |
| 243:01          | 3                  | 23 Denebola, 30 Menkent    | +0.053                      | -0.069 | +0.015  | 0.01                             | -1.2             | +1.6 | +0.4  |                         |

\*1 - Preferred; 2 - Nominal; 3 - REFSMUT; 4 - Landing site.

TABLE 7.6-11.- ENTRY MONITOR SYSTEM PERFORMANCE

|  | Maneuver                   |                       |                 |                    |                     |                       |                             | System test <sup>a</sup> |
|--|----------------------------|-----------------------|-----------------|--------------------|---------------------|-----------------------|-----------------------------|--------------------------|
|  | First midcourse correction | Lunar orbit insertion | Circularization | First plane change | Second plane change | Trans-earth injection | Second midcourse correction |                          |
| Total velocity change, ft/sec                            | +61.7                      | +2889.3               | +165.5          | +349.7             | +381.3              | +3042.3               | +2.0                        |                          |
| Velocity change set into counter, ft/sec                 | +57.2                      | +2882.4               | +159.4          | +337.1             | +368.2              | +3021.1               | +2.0                        | 0                        |
| Estimated time of counter operation, sec                 | 39                         | 368                   | 47              | 48                 | 49                  | 160                   | 38                          | 100                      |
| Planned residual, ft/sec                                 | -4.2                       | +1.0                  | -4.4            | -8.4               | -11.3               | -14.4                 | +1.8                        | n/a                      |
| Actual counter residual, ft/sec (corrected) <sup>b</sup> | -4.4                       | -6.8                  | -5.6            | -12.6              | -13.5               | -21.0                 | +0.2                        | n/a                      |
| Entry monitor system error, ft/sec                       | -0.2                       | -7.8                  | -1.2            | -4.2               | -2.2                | -6.6                  | -1.6                        | -2.2                     |
| Estimated bias <sup>c</sup> , ft/sec/sec                 | -.005                      | -.020                 | -.025           | -.055              | -.045               | -.045                 | -.042                       | -0.022                   |

<sup>a</sup> Performed at 238 hours.

<sup>b</sup> A value of 0.2 ft/sec and the observed command module computer X-axis residual were added to determine the corrected error.

<sup>c</sup> Corrected error divided by estimated counter operating time, i.e. firing time plus 30 seconds.



TABLE 7.6-III.- GUIDANCE AND CONTROL MANEUVER SUMMARY

| Parameter   | Maneuver                   |                       |                             |                    |                     |                   | Transearth Injection |
|---|----------------------------|-----------------------|-----------------------------|--------------------|---------------------|-------------------|----------------------|
|   | First midcourse correction | Lunar orbit insertion | Lunar orbit circularization | First plane change | Second plane change |                   |                      |
| Time  |                            |                       |                             |                    |                     |                   |                      |
| Ignition, hr:min:sec                                    | 30:52:44.36                | 83:25:23.36           | 87:48:48.08                 | 119:47:13.23       | 159:04:45.47        | 172:27:16.81      |                      |
| Cutoff, hr:min:sec                                      | 30:52:53.55                | 83:31:15.61           | 87:49:04.99                 | 119:47:31.46       | 159:05:04.72        | 172:29:27.13      |                      |
| Duration, min:sec                                       | 0:09:19                    | 5:52:25               | 0:16:91                     | 0:18:23            | 0:19:25             | 2:10:32           |                      |
| Velocity gained, ft/sec*<br>(desired/actual)            |                            |                       |                             |                    |                     |                   |                      |
| X   | +19.60/+19.70              | -1401.93/-1401.93     | -159.86/-159.59             | +44.05/+44.11      | +23.23/+23.06       | -1772.09/-1771.92 |                      |
| Y   | +41.10/+41.60              | -1224.43/-1224.74     | -13.60/-13.70               | +197.26/+197.72    | +214.51/+215.06     | +2244.91/+2245.22 |                      |
| Z   | -41.61/-42.54              | -2209.88/-2210.05     | -40.59/-40.55               | -285.36/-285.27    | -314.30/-314.31     | +1036.97/+1036.24 |                      |
| Velocity residual, ft/sec<br>(spacecraft coordinates)** |                            |                       |                             |                    |                     |                   |                      |
| X   | -0.1                       | -0.2                  | +0.3                        | -0.3               | -0.7                | -0.1              |                      |
| Y   | -0.3                       | 0.0                   | 0.0                         | +0.1               | +0.3                | +0.6              |                      |
| Z   | 0.0                        | +0.1                  | +0.4                        | +0.4               | +0.6                | +0.1              |                      |
| Entry monitor system                                    | -0.2                       | -7.8                  | -1.2                        | -4.2               | -2.2                | -6.6              |                      |
| Engine gimbal position, deg                             |                            |                       |                             |                    |                     |                   |                      |
| Initial   |                            |                       |                             |                    |                     |                   |                      |
| Pitch   | +0.99                      | +0.94                 | +1.51                       | -0.65              | -0.70               | -0.57             |                      |
| Yaw   | -0.18                      | -0.10                 | -0.54                       | +0.54              | +0.33               | +0.28             |                      |
| Maximum excursion                                       |                            |                       |                             |                    |                     |                   |                      |
| Pitch   | +0.39                      | +0.35                 | +0.31                       | -1.98              | -2.10               | -2.06             |                      |
| Yaw   | -0.38                      | -0.34                 | -0.24                       | +1.53              | +2.04               | +1.78             |                      |
| Steady-state  |                            |                       |                             |                    |                     |                   |                      |
| Pitch   | +1.21                      | +1.08                 | +1.78                       | -0.31              | -0.18               | -0.31             |                      |
| Yaw   | +0.20                      | +0.07                 | -0.35                       | +0.71              | +0.75               | +0.45             |                      |
| Cutoff  |                            |                       |                             |                    |                     |                   |                      |
| Pitch   | +1.21                      | +1.68                 | +1.58                       | -0.44              | -0.35               | -0.48             |                      |
| Yaw   | -0.01                      | -0.31                 | -0.42                       | +0.54              | +0.45               | -1.20             |                      |
| Maximum rate excursion, deg/sec                         |                            |                       |                             |                    |                     |                   |                      |
| Pitch   | +0.04                      | -0.04                 | -0.04                       | +1.27              | +1.67               | +1.39             |                      |
| Yaw   | +0.08                      | +0.12                 | +0.20                       | -0.60              | -0.68               | -0.51             |                      |
| Roll  | -0.04                      | -0.04                 | -0.45                       | -0.85              | +1.01               | -0.89             |                      |
| Maximum attitude error, deg                             |                            |                       |                             |                    |                     |                   |                      |
| Pitch   | -0.08                      | +0.19                 | +0.24                       | +0.08              | +0.37               | -0.24             |                      |
| Yaw   | +0.20                      | -0.08                 | -0.10                       | -0.28              | +0.32               | -0.28             |                      |
| Roll  | -0.13                      | -5.00***              | -2.40                       | -4.28              | +0.42               | -5.00***          |                      |

\*Velocity residuals in spacecraft coordinates after trimming has been completed.

\*\*Velocity gained in earth- or moon-centered inertial coordinates.

\*\*\*Telemetry signal saturated.

7-11 A

7-11 B

7-11-C

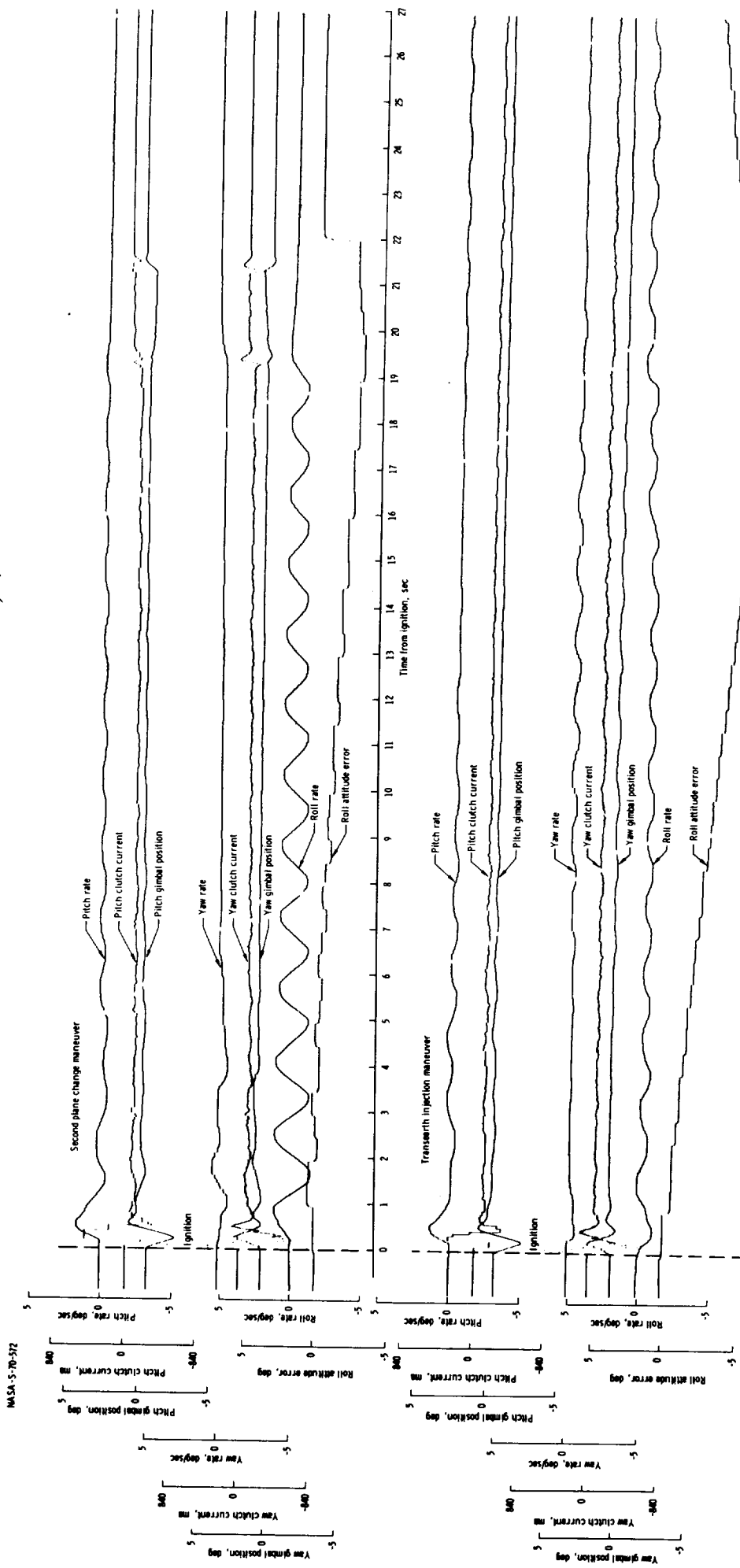


Figure 7.6-1.- Comparison of spacecraft dynamics during second plane change and transverse injection maneuvers.

NASA-S-70-572









TABLE 7.6-IV.- INERTIAL COMPONENT PREFLIGHT HISTORY - COMMAND MODULE

| Error:  | Sample mean | Standard deviation | No. of samples | Countdown value | Flight load | Flight performance |
|---|-------------|--------------------|----------------|-----------------|-------------|--------------------|
| Accelerometers  |             |                    |                |                 |             |                    |
| X - Scale factor error, ppm . . . . .                     | -173        | 40                 | 7              | -202            | -220        | --                 |
| Bias, cm/sec <sup>2</sup> . . . . .                       | -0.01       | 0.13               | 7              | -0.09           | -0.09       | 0.0                |
| Y - Scale factor error, ppm . . . . .                     | -243        | 65                 | 9              | -330            | -350        | --                 |
| Bias, cm/sec <sup>2</sup> . . . . .                       | -0.13       | 0.05               | 9              | -0.08           | -0.09       | -0.15              |
| Z - Scale factor error, ppm . . . . .                     | -306        | 59                 | 7              | -419            | -370        | --                 |
| Bias, cm/sec <sup>2</sup> . . . . .                       | -0.19       | 0.03               | 7              | -0.13           | -0.16       | -0.16              |
| Gyroscopes  |             |                    |                |                 |             |                    |
| X - Null bias drift, mERU . . . . .                       | -1.5        | 1.8                | 9              | -1.3            | -0.1        | -0.9               |
| Acceleration drift, spin reference axis, mERU/g . . . . . | -1.4        | 5.3                | 7              | -3.5            | -4.0        | --                 |
| Acceleration drift, input axis, mERU/g . . . . .          | 6.7         | 6.7                | 7              | 18.2            | 13.0        | --                 |
| Y - Null bias drift, mERU . . . . .                       | -0.6        | 0.8                | 9              | 0.2             | -0.1        | 1.3                |
| Acceleration drift, spin reference axis, mERU/g . . . . . | -3.3        | 0.4                | 7              | -3.3            | -4.0        | --                 |
| Acceleration drift, input axis, mERU/g . . . . .          | 0.7         | 0                  | 7              | 1.7             | 0.0         | --                 |
| Z - Null bias drift, mERU . . . . .                       | -2.8        | 1.3                | 9              | -1.4            | 40.1        | +0.5               |
| Acceleration drift, spin reference axis, mERU/g . . . . . | -3.5        | 4.2                | 7              | -4.6            | -6.0        | --                 |
| Acceleration drift, input axis, mERU/g . . . . .          | -0.1        | 2.3                | 7              | 0.1             | -1.0        | --                 |





Engine transient performance during all starts and shutdowns was satisfactory. During the initial firing, minor oscillations in the measured chamber pressure were observed beginning approximately 1.8 seconds after ignition. The magnitude of the oscillations was less than 30 psi peak-to-peak, and by approximately 2.1 seconds after ignition, the chamber pressure data were indicating normal steady-state operation. Similar oscillations observed during the first firing for Apollo 11 were attributed to a small amount of helium which was probably trapped in the heat exchanger after completion of bleed procedures during propellant loading.

The propellant utilization and gaging system operated satisfactorily throughout the mission. During Apollo 9, 10, and 11, the engine mixture ratio was less than expected, based on engine ground test data. Although the cause of the observed negative mixture ratio shifts have not been completely determined, the predicted flight mixture ratio for this mission was biased, based on previous flight experience, to account more closely for the expected flight mixture ratio. This biased prediction involved conducting the entire mission with the propellant utilization valve in the increase position to achieve a final propellant unbalance close to zero. Soon after ignition for the first firing, the crew moved this valve to the increase position, where it remained throughout the entire flight. The final propellant unbalance was approximately 50 pounds of oxidizer greater than the optimum quantity distribution.

## 7.9 ENVIRONMENTAL CONTROL SYSTEM

The environmental control system performed satisfactorily and provided a comfortable environment for the crew and adequate thermal control of the spacecraft equipment. The only anomalies noted were associated with instrumentation (see section 7.5) and clogging of both urine filters.

### 7.9.1 Oxygen Distribution

The oxygen distribution system operated normally and maintained cabin pressure at 5.0 to 5.1 psia. The overall environmental control oxygen usage rate was approximately 0.45 lb/hr, which is higher than on previous missions but is still within acceptable limits. This higher consumption is attributed to the increased purging requirements of the redesigned urine receptacle assembly and to excessive cabin leakage, which required a waiver prior to launch. However, the total indicated cryogenic oxygen usage was greater than the sum of the calculated fuel cell and environmental control usage by about 27 pounds. This discrepancy is discussed in section 14.1.7.

U U























TABLE 8.6-1.- INFLIGHT AND LUNAR SURFACE ALIGNMENT DATA

| Time,<br>hr:min | Type<br>alignment | Alignment mode      |                        | Telescope<br>detent <sup>c</sup> /star<br>used | Star angle<br>difference,<br>deg | Gyro torquing angle, deg |        |        | Gyro drift, mERU |                  |                  |
|-----------------|-------------------|---------------------|------------------------|--|----------------------------------|--------------------------|--------|--------|------------------|------------------|------------------|
|                 |                   | Option <sup>a</sup> | Technique <sup>b</sup> |  |                                  | X                        | Y      | Z      | X                | Y                | Z                |
| 104:52          |                   |                     | Docked alignment       |  |                                  | -0.250                   | -0.360 | +0.050 | --               | --               | --               |
| 108:11          |                   |                     | Docked alignment       |  |                                  | -0.045                   | -0.035 | -0.092 | <sup>d</sup> 0.9 | <sup>d</sup> 0.7 | <sup>d</sup> 1.8 |
| 108:48          | P52               | 3                   | NA                     | 2/13; 2/12                                     | 0.02                             | +0.018                   | -0.002 | -0.069 | 0.3              | 0.0              | 1.2              |
| 110:46          | P57               | 3                   | 1                      | NA   | 0.07                             | -0.011                   | +0.064 | -0.054 | 0.4              | 2.2              | 1.8              |
| 110:54          | P57               | 3                   | 2                      | 1/15; 2/00                                     | 0.01                             | +0.027                   | -0.017 | -0.045 | --               | --               | --               |
| 111:22          | P57               | 3                   | 2                      | 1/16; 6/17                                     | 0.02                             | +0.034                   | +0.036 | +0.019 | --               | --               | --               |
| 139:26          | P57               | 4                   | 3                      | 1/16; -/-                                      | 0.04                             | +0.001                   | +0.057 | +0.033 | --               | --               | --               |
| 141:29          | P57               | 4                   | 3                      | 1/16; -/-                                      | 0.04                             | -0.023                   | +0.004 | +0.015 | 0.7              | 0.1              | 0.5              |
| 142:23          | P52               | 3                   | NA                     | 2/12; 2/13                                     | 0.01                             | +0.008                   | +0.010 | -0.046 |                  |                  |                  |

<sup>a</sup>1 - Preferred; 2 - Nominal; 3 - REFSMMAT; 4 - Landing site.

<sup>b</sup>0 - Anytime; 1 - REFSMMAT plus g; 2 - Two bodies; 3 - One body plus g.

<sup>c</sup>1 - Left front; 2 - Front; 3 - Right front; 4 - Right rear; 5 - Rear; 6 - Left rear.

<sup>d</sup>Not torqued.

Star names:

- 13 Capella
- 12 Rigel
- 15 Sirius
- 00 Pollux
- 16 Procyon
- 17 Regor

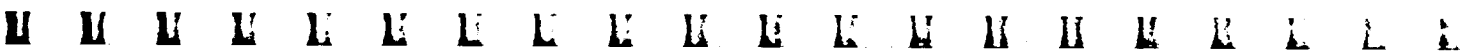












TABLE 8.6-IV.- MECHANICAL COMPONENT FREQUENCY RESPONSE - LOUIS M. 1014F

(a) Accelerometers

| Error                                 | Sample mean | Standard deviation | Number of samples | Countdown value | Flight load | Inflight performance |                 |                       |                              |                 |                      |
|---------------------------------------|-------------|--------------------|-------------------|-----------------|-------------|----------------------|-----------------|-----------------------|------------------------------|-----------------|----------------------|
|                                       |             |                    |                   |                 |             | Power-up to 106:43   | Update (106:43) | Landing to power-down | Surface power-up to lift-off | Update (143:45) | 143:45 to rendezvous |
| X - Scale factor error, ppm . . . . . | -649        | 18                 | 4                 | -640            | -660        | --                   | --              | --                    | --                           | --              | --                   |
| Bias, cm/sec <sup>2</sup> . . . . .   | -0.39       | 0.02               | 4                 | -0.37           | -0.38       | -0.33                | -0.33           | -0.40                 | -0.10                        | -0.15           | -0.17                |
| Y - Scale factor error, ppm . . . . . | -681        | 72                 | 4                 | -727            | -720        | --                   | --              | --                    | --                           | --              | --                   |
| Bias, cm/sec <sup>2</sup> . . . . .   | 0.03        | 0.01               | 4                 | 0.03            | 0.02        | 0.01                 | --              | 0.05                  | 0.20                         | 0.20            | 0.18                 |
| Z - Scale factor error, ppm . . . . . | -885        | 42                 | 4                 | -943            | -890        | --                   | --              | --                    | --                           | --              | --                   |
| Bias, cm/sec <sup>2</sup> . . . . .   | 0.60        | 0.05               | 4                 | 0.63            | 0.62        | 0.68                 | 0.68            | 0.73                  | 0.34                         | 0.39            | 0.42                 |

(b) Gyroscopes

| Error   | Sample mean | Standard deviation | Number of samples | Countdown value | Flight load | Inflight performance |
|---|-------------|--------------------|-------------------|-----------------|-------------|----------------------|
| X - Null bias drift, mERU . . . . .                       | -1.0        | 0.3                | 5                 | -1.3            | 0.1         | 0.6                  |
| Acceleration drift, spin reference axis, mERU/g . . . . . | -1.3        | 1.4                | 4                 | -0.4            | -2.0        | --                   |
| Acceleration drift, input axis, mERU/g . . . . .          | 10.6        | 6.5                | 4                 | 14.0            | 7.0         | --                   |
| Y - Null bias drift, mERU . . . . .                       | 0.7         | 1.0                | 5                 | -0.2            | 0.8         | 0.8                  |
| Acceleration drift, spin reference axis, mERU/g . . . . . | 4.1         | 1.4                | 4                 | 5.3             | +4.0        | --                   |
| Acceleration drift, input axis, mERU/g . . . . .          | -16.0       | 6.8                | 4                 | -23.3           | -15.0       | --                   |
| Z - Null bias drift, mERU . . . . .                       | 2.8         | 0.9                | 5                 | 3.3             | 3.0         | 1.3                  |
| Acceleration drift, spin reference axis, mERU/g . . . . . | -0.3        | 4.2                | 4                 | -2.6            | -2.0        | --                   |
| Acceleration drift, input axis, mERU/g . . . . .          | 10.8        | 4.8                | 4                 | 12.8            | 13.0        | --                   |



TABLE 8.6-VI.- ABORT GUIDANCE SYSTEM GYRO CALIBRATION DATA

|                                   | X,<br>deg/hr | Y,<br>deg/hr | Z,<br>deg/hr |
|-----------------------------------|--------------|--------------|--------------|
| Preinstallation calibration       | +0.06        | -0.16        | -0.07        |
| Final earth prelaunch calibration | -0.27        | -0.31        | -0.06        |
| Inflight calibration              | -0.04        | -0.19        | 0            |
| First lunar surface calibration   | -0.19        | -0.28        | +0.11        |
| Third lunar surface calibration   | -0.20        | -0.31        | +0.05        |

### 8.7 REACTION CONTROL

Reaction control system performance was normal in all respects. On-board measurement of propellant consumption through ascent stage jettison was 315 pounds, compared with the predicted value of 305 pounds. Reaction control system interconnect operation was satisfactory during the ascent maneuver; however, the indicator for the system A main shutoff valve remained in the valve-closed position after the valves had been initially commanded open. This indicator operated normally when the valves were recycled (section 8.11.1 has a more complete discussion).

The thrust-chamber pressure switch on the quad 4 side-firing engine failed in the closed position for about 2 minutes during powered descent. This switch, which also failed closed several times during ascent, was slow in opening on all firings after undocking. However, engine performance was nominal at these times. This type of failure, noted on all previous manned lunar modules, is attributed to particulate contamination of the switch. The only consequence of such a failure is that a failed-off engine cannot be detected from instrumentation sources.

### 8.8 DESCENT PROPULSION

Descent propulsion system operation, including engine starts and throttle response, was normal.

U U









TABLE 8.9-I.- STEADY-STATE PERFORMANCE

| Parameter                                   | 10 seconds after ignition |                       | 400 seconds after ignition |                       |
|---|---------------------------|-----------------------|----------------------------|-----------------------|
|   | Predicted <sup>a</sup>    | Measured <sup>b</sup> | Predicted <sup>a</sup>     | Measured <sup>b</sup> |
| Regulator outlet pressure, psia . . . . .   | 184                       | 184 <sup>c</sup>      | 184                        | 184 <sup>c</sup>      |
| Oxidizer bulk temperature, °F . . . . .     | 69.9                      | 68.5                  | 69.0                       | 67.8                  |
| Fuel bulk temperature, °F . . . . .         | 69.7                      | 68.5                  | 69.5                       | 68.5                  |
| Oxidizer interface pressure, psia . . . . . | 171.1                     | 168.0                 | 170.2                      | 167.5                 |
| Fuel interface pressure, psia . . . . .     | 170.6                     | 167.5                 | 169.8                      | 166.7                 |
| Engine chamber pressure, psia . . . . .     | 123.0                     | 120.0                 | 122.7                      | 119.5                 |
| Mixture ratio . . . . .                     | 1.611                     | ---                   | 1.602                      | ---                   |
| Thrust, lb . . . . .                        | 3495                      | ---                   | 3460                       | ---                   |
| Specific impulse, sec . . . . .             | 309.5                     | ---                   | 309.2                      | ---                   |

<sup>a</sup>Preflight prediction based on acceptance test data and assuming nominal system performance.

<sup>b</sup>Actual flight data with known biases removed.

<sup>c</sup>These values are approximate due to oscillations noted in text.

## 8.10 ENVIRONMENTAL CONTROL SYSTEM

The environmental control system satisfactorily supported all lunar module operations throughout the mission. Although water in the suit loop and an erratic carbon dioxide sensor have been identified as anomalies, overall performance was nominal and lunar module operations were not compromised.

On the lunar surface, the cabin was depressurized through the forward dump valve without a cabin-gas bacteria filter installed as modified for this mission. Cabin pressure decreased rapidly, as predicted, and the crew was able to open the hatch 3 minutes after actuation.

Prior to the first extravehicular activity, the crew reported free water in the suit inlet umbilicals. After the mission, the umbilical assemblies were tested under flight conditions, and no condensation was observed. During postflight tests, condensate was observed to bypass the water separators because the separator rotational velocity was excessive as a result of the suit-circuit flow being higher than the specification value. For Apollo 13 and thereafter, an orifice will be placed in the suit circuit to reduce the flow and should decrease the separator velocity to within expected ranges. Further details are given in section 14.2.2.

The Apollo 11 crew had reported that sleep was difficult because of a cold environment. This condition was remedied for Apollo 12 through the use of hammocks and through procedural changes which eliminated prechilling of the crew prior to the beginning of their sleep period. Although the crew reported they were comfortable during the sleep period on the lunar surface, they were awakened on occasion by an apparent change in the sound pitch produced from the water/glycol pump installation. This pump package is mounted on a bulkhead in the aft cabin floor area which is not generally subjected to significant variations in cabin temperature or pressure. All pump performance data, including temperature, line pressure, and input voltage, appear normal during the sleep period, indicating the pump frequency could not have varied perceptibly. Cabin temperature and pressure were also essentially constant during this period. The only explanation for the change in pitch, while unlikely, is that the fluid lines and supporting structure near and downstream from the pump experienced physical changes which altered the vibrational harmonics sufficient to produce, on occasion, detectable changes in pitch frequency. Because all pump parameters indicated normal operation, no system modifications are required. However, reports on past flights of an annoying noise level in the cabin has prompted a modification to the plumbing for future flights which significantly reduces noise and which will probably eliminate any pitch variations from surrounding structure.

U U U E U U E U E E E U U U U U U U U















8.13.3 Reaction Control System Propellant

The preflight planned usage includes 105 pounds for a landing site redesignation maneuver of 60 ft/sec and 2 minutes flying time from 500 feet altitude. The reaction control propellant consumption was calculated from telemetered helium tank pressure histories using the relationships between pressure, volume, and temperature.

| Condition                        | Actual value, lb |          |       | Predicted value, lb |
|----------------------------------|------------------|----------|-------|---------------------|
|                                  | Fuel             | Oxidizer | Total |                     |
| Loaded                           |                  |          |       |                     |
| System A                         | 108              | 209      |       |                     |
| System B                         | 108              | 209      |       |                     |
| Total                            | 216              | 418      | 634   | 633                 |
| Consumed to:                     |                  |          |       |                     |
| Docking                          |                  |          | 315   | 305                 |
| Impact <sup>a</sup>              |                  |          | 433   | 424                 |
| Remaining at lunar module impact |                  |          | 201   | 209                 |

<sup>a</sup>Essentially includes that consumed in the deorbit maneuver.























### 9.5.2 Translunar Coast

Activities during translunar coast were similar to those of previous lunar missions and were conducted as planned. The only change from nominal procedures was an early entry into the lunar module to verify that the systems had suffered no damage as a result of the potential discharges during launch. Navigation sightings using the earth limb showed a significant variation in the height of the atmosphere. Future crews should use the apparent visible horizon, instead of the airglow layer, for consistently accurate sightings. Attitude stability was excellent during passive thermal control, which was initiated as planned.

### 9.5.3 Midcourse Correction

The only midcourse correction required was performed at the second option point with the service propulsion system. This maneuver, the only major change from Apollo 11 during this phase, placed the spacecraft on a "hybrid" non-free-return trajectory (section 5.0). Longitudinal velocity residuals were trimmed to within 0.1 ft/sec.

## 9.6 LUNAR ORBIT INSERTION

The lunar orbit insertion and circularization maneuvers were conducted in accordance with established procedures using the service propulsion system and primary guidance. Residuals were within 0.1 ft/sec about all axes. The computer indicated that the spacecraft was inserted into a 170.0- by 61.8-mile orbit. The planned firing time calculated from ground tracking was 5 minutes 58 seconds, whereas the firing time as observed onboard, was 5 minutes 52 seconds. The circularization maneuver two revolutions later inserted the spacecraft into a 66.3- by 54.7-mile orbit, which included a planned navigation bias as was used in Apollo 11.

## 9.7 LUNAR MODULE CHECKOUT

Activities after circularization were generally routine in nature and closely followed the flight plan. The Commander and the Lunar Module Pilot entered the lunar module for inspection, cleanup, and stowage. During this time, a scheduled landmark tracking of a crater (designated H-1) in the vicinity of Fra Mauro was normal in all respects and established procedures were used without difficulty.

M M M U E E E E E E E E E H H H E L L L























on an automobile that has been driven through several mud puddles and allowed to dry. While the dust was on all sides of the Surveyor, it was not uniform around each specific item. Generally, the dust was thickest on the areas that were most easily viewed when walking around the spacecraft. For example, the side of a tube or strut that faced the interior of the Surveyor was relatively clean when compared to a side facing outward.

Retrieving the television camera was not difficult using the cutting tool. The tubes appeared to sever in a more brittle manner than the new tubes of the same material used in preflight exercises. The electrical cable insulation had aged and appeared to have the texture of old asbestos. The mirrors on the surface of the electronic packages were generally in good condition. A few cracks were seen but no large pittings. The only mirrors that had become unbonded and separated were those on the flight control electronics package. As a bonus, the Surveyor scoop was removed. Although the steel tape was thin enough to bend in the shears and could not be cut, the end attached to the scoop became debonded when the tape was twisted with the cutter. Several rock samples were collected in the field of view of the Surveyor television camera for comparison with original photographs. On the return traverse, the added weight of the Surveyor components and samples on the crewman's back did not appear to affect either stability or mobility.

#### 9.10.7 Lunar Surface Tools

The handtool carrier was light but was still troublesome to carry about. When a number of samples had been accumulated, it was tiring to hold the carrier at arm's length so that rapid movement was possible. If a means could be found to attach the carrier to the back of the portable life support system during the traverse from one geology site to another, the total geology operation could be carried out more efficiently. It was generally necessary to set the carrier down with great care to prevent it from tipping over. The practicality of a pushed or towed vehicle for transporting equipment, tools, and samples over the surface could not be resolved from the work performed in this mission. However, certain constraints, such as the dust which would be set in motion by any wheels, must be considered in the design of such a vehicle. Also, under the light gravity, objects carried on such a conveyance would have to be positively restrained.

The hammer proved to be an effective tool. Since arm motion is inaccurate in the pressurized suit, the front end of the hammer was generally not used when driving a core tube because its striking area was too small, and the side of the hammer was more useful. The pick portion of

U U U E E E E E E E E E E E E E E E E





NASA-S-70-591



Figure 9-4.- Lunar sample collection using tongs.

U U







### 9.10.9 Activity in the Spacecraft on the Surface

Cabin repressurization after each extravehicular period was positive and rapid. Once inside the spacecraft, the dust on the suits became a significant problem. Considerable dirt had adhered to the boots and gloves and to the lower portions of the suits. There were fillets of dirt around the interior angles of the oxygen hose connectors on the suit. The suit material just beneath the top of the lunar boots chafed sufficiently to wear through the outer suit layer in several spots. The dust and dirt resulted in a very pronounced increase in the operating force necessary to open and close the wrist rings and the oxygen hose connectors. The Commander's suit had no leakage, either prior to launch or prior to the first extravehicular activity. Just before his second egress, the leak rate was 0.15 psi/min and, prior to cabin depressurization for equipment jettison, was 0.25 psi/min. If the suit zippers had been operated for any reason, suit leakage might have exceeded the 0.30 psi/min limit of the integrity check. (Editor's note: See section 8.12)

After ascent orbit insertion, when the spacecraft was again subject to a zero-g environment, a great quantity of dust and small particles floated free within the cabin. This dust made breathing without the helmet difficult and hazardous, and enough dust and particles were present in the cabin atmosphere to affect vision (section 6.2). Some type of throwaway overgarment for use on the lunar surface may be necessary. During the transearth coast phase, it was noticed that much of the dust which had adhered to equipment (such as the camera magazines) while on the lunar surface had floated free in the zero-g condition, leaving the equipment relatively clean. This fact was also true of the suits, since they were not as dusty after flight as they were on the surface after final ingress.

The sleeping hammocks were particularly good under the reduced gravity conditions. The noise within the lunar module was loud, but not enough to prevent adequate sleep, and the earplugs were not used. The only noise problem was caused by the coolant pump changing frequency several times during the night. Temperature control was satisfactory during the sleep period, and the liquid cooling garment pump was not used. The suit hoses were generally disconnected from the suit, with the suit isolation valves open. The hoses were connected to the suit only a few times, as necessary to cool the feet and lower legs.

When the Commander connected his suit hoses after the first extravehicular activity, he felt free water in his suit. Upon removing the inlet hose, two or three 1/2-inch globules of water were blown from the system. Although both fans and both water separators were operated in an attempt to eliminate the problem, the presence of free water in the Commander's suit loop occurred subsequent to each cabin repressurization and provided a mildly uncomfortable environment. The Lunar Module Pilot's hoses provided adequately dry air at all times.





Although the midcourse corrections were small, both solutions were executed. It was not necessary to make any line-of-sight corrections in the lunar module until at a range of approximately 1000 feet from the command module, and these corrections were very small. The velocity limits for all braking gates were met, with the first gate at 6000 feet range requiring a velocity reduction from 38 to 30 ft/sec. The passive rendezvous procedures for the command module were normal in all respects. The ground uplinked the lunar module state vector immediately after insertion, and a platform alignment was conducted according to the checklist. This procedure was completed ahead of the nominal timeline and permitted orbital navigation to be commenced early. The VHF ranging system broke lock twice in the subsequent tracking timeline. For the out-of-plane solution, nine VHF ranging and 14 optics marks were obtained. The only procedural discrepancy noted was the initial few state-vector solutions did not converge as rapidly as expected; however, a solution for coelliptic sequence initiation of 38.8 ft/sec was eventually obtained. The command module navigation operation was continued, with the final computation completed on time after 14 VHF and 21 optics marks had been obtained. The final command module solutions for coelliptic sequence initiation and the constant differential height maneuver were comparable to those of the lunar module. The rendezvous timeline through the constant differential height maneuver was nominal in all respects.

Although sun shafting was evident in the sextant, eight optics marks were obtained before darkness. When the lunar module went into darkness, the Command Module Pilot observed that the lunar module tracking light was inoperative. All checks on board the lunar module indicated that switches were in the proper configuration, and it was assumed that the tracking light failed subsequent to coelliptic sequence initiation. Therefore, the remainder of the command module rendezvous operations were conducted using VHF ranging only. The solutions for terminal phase initiation in both vehicles were again comparable. As was known prior to flight, both midcourse correction solutions in the command module would be inaccurate when only VHF ranging was used.

### 9.11.3 Docking

The command module digital autopilot was set to narrow deadband and used to perform the pitch and yaw maneuver for the docking operation. At capture latch engagement, the command and service module control mode was then changed to free, while the lunar module remained in attitude-hold, narrow deadband. There were no noticeable docking transients or lunar module reaction control thruster firings. A slight attitude adjustment was made with the command and service module, and the probe was then retracted for a hard dock. Closing rates at contact are estimated to have been about 0.2 or 0.3 ft/sec.

U U U U U U U L L L L L L L L L L L L L L L L L L







#### 9.12.4 Bootstrap Photography

An additional day in lunar orbit had been planned following ascent stage deorbit to permit completion of bootstrap photography, which is so named because stereo-strip and high-resolution coverage of surface areas planned for future landings was involved. The stereostrip photography was conducted with the spacecraft longitudinal axis pointed down the lunar radius vector (local vertical) using orbit-rate torquing from the guidance system. The sextant was used for through-the-optics photography with the shaft angle set to zero and the trunnion angle to 45 degrees. In addition, the 70-mm camera, with the 80-mm lens and black-and-white film, was mounted in the right-hand rendezvous window. The strip photography was conducted using procedures outlined in the flight plan.

At the completion of the rest period at 102-1/2 hours, target-of-opportunity photographs were first taken of Fra Mauro out the right-hand window. These pictures were planned to support Apollo 13 and were taken with black-and-white film and the 80-mm lens.

High-resolution photography was obtained by using the 500-mm long-range lens and the 70-mm camera mounted on a special bracket in the right-hand rendezvous window. The crew optical sight was used for aligning the 500-mm lens. Ground-supplied gimbal angles and camera operating times were again used for this photography and subsequent landmark tracking. The high resolution photography was conducted on the areas near the craters Descartes, Fra Mauro, and Lalande, and as an additional bonus the Hershel crater area also was photographed.

Two revolutions of landmark tracking were conducted following the bootstrap photography. The telescope was used to track the target while the camera, mounted on the sextant, was used for photographic purposes. On each revolution four specified landmarks associated with future sites were tracked without difficulty.

#### 9.13 TRANSEARTH INJECTION

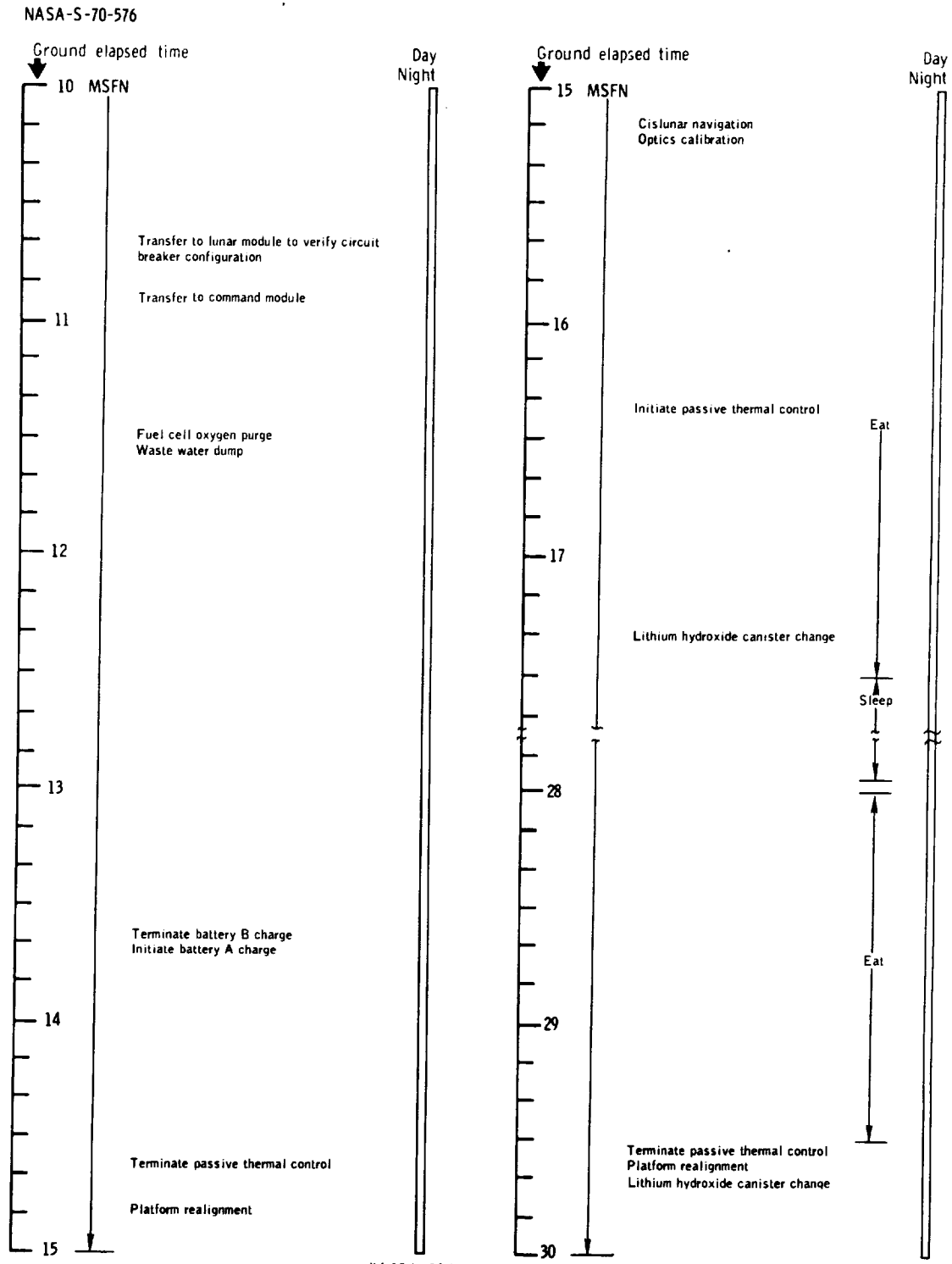
Following a day of photography and landmark sightings, described earlier, preparation was begun for transearth injection to be conducted at the end of the 45th lunar orbit revolution. This maneuver was performed nominally using the service propulsion system. The firing duration was 2 minutes 11 seconds and residuals were trimmed to within 0.2 ft/sec.

U U U E E E E E K K K H H H R R R L L L









(b) 10 to 30 hours.  
Figure 9-1. - Continued.









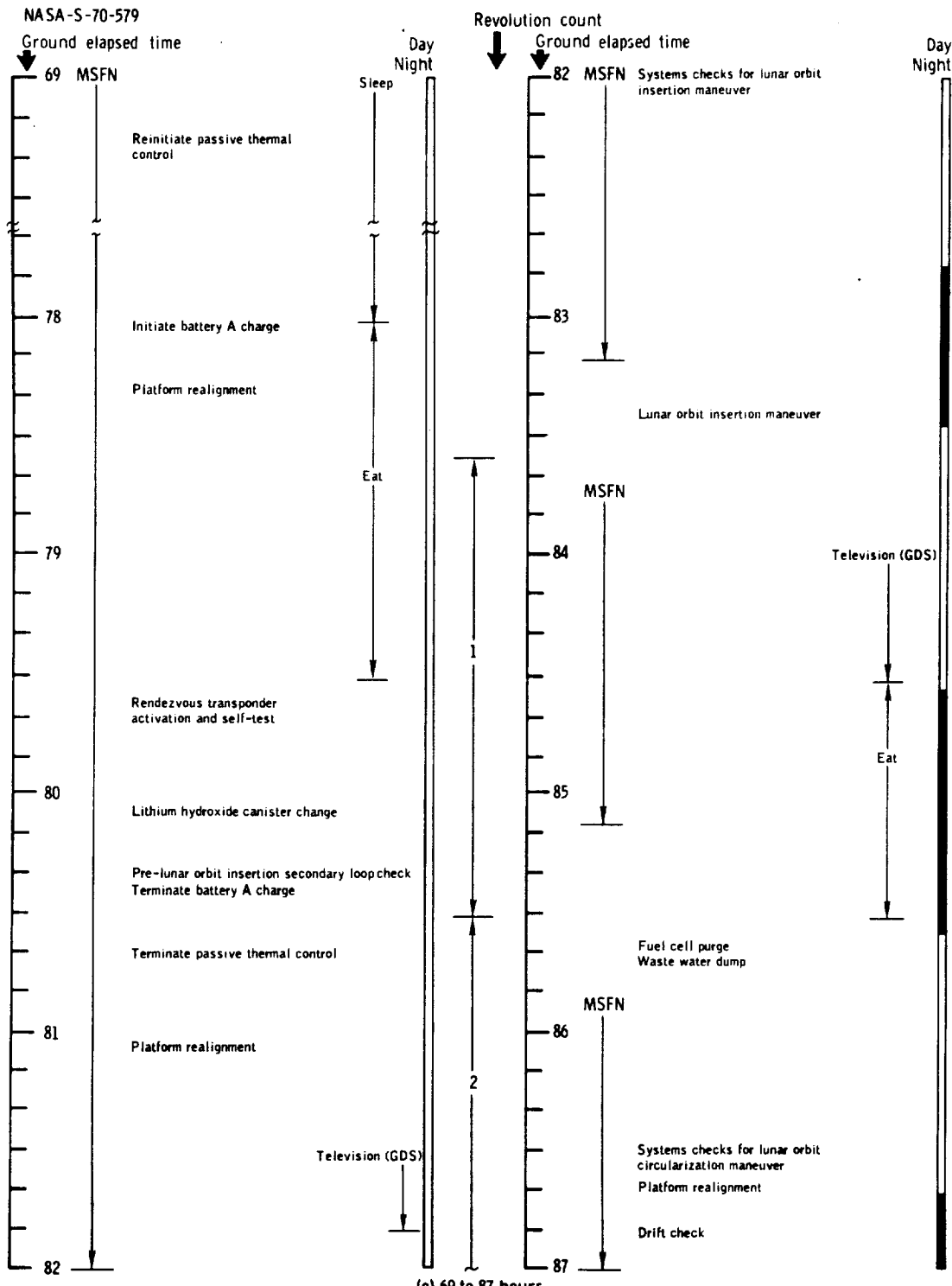


Figure 9-1. - Continued.



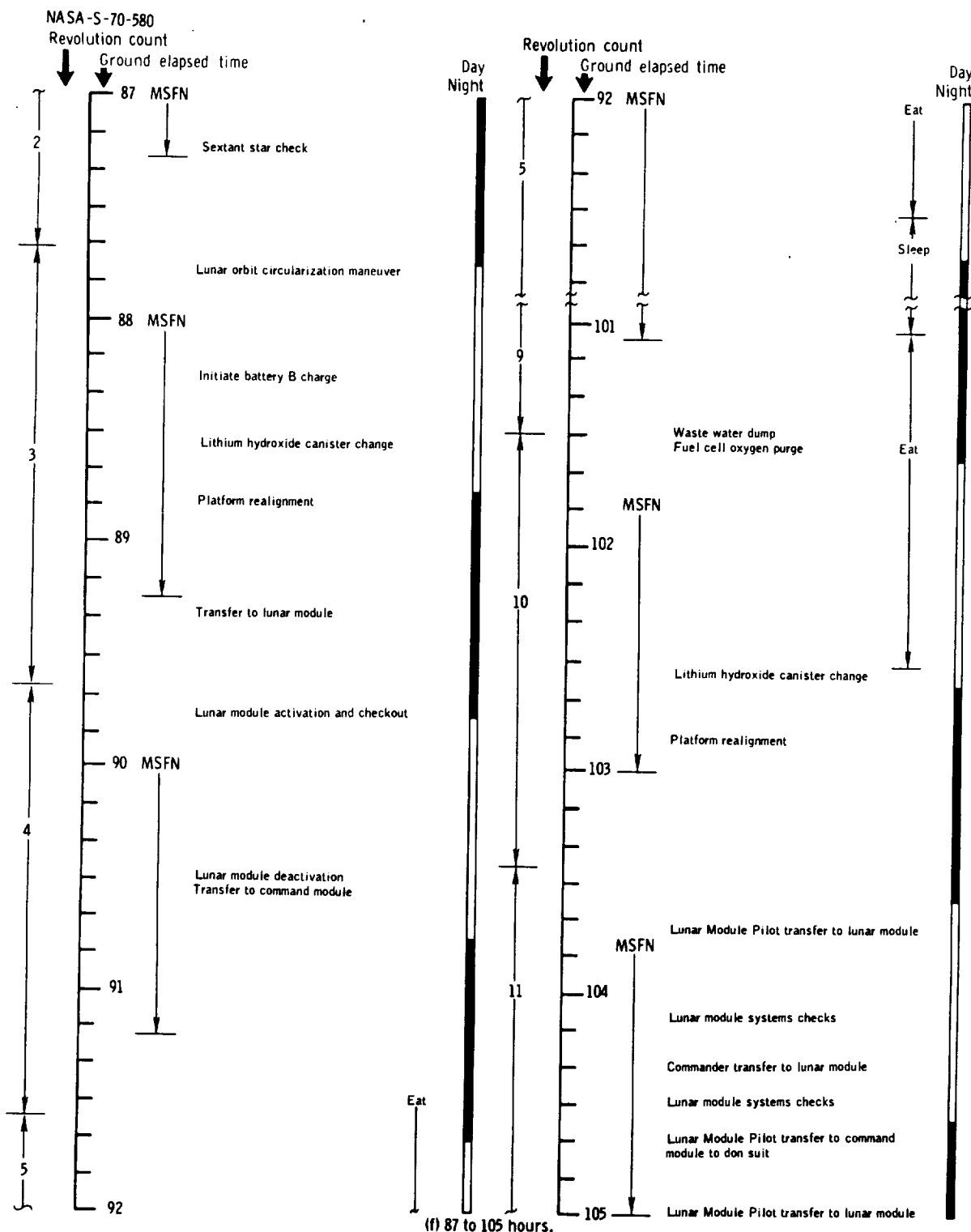


Figure 9-1. - Continued.



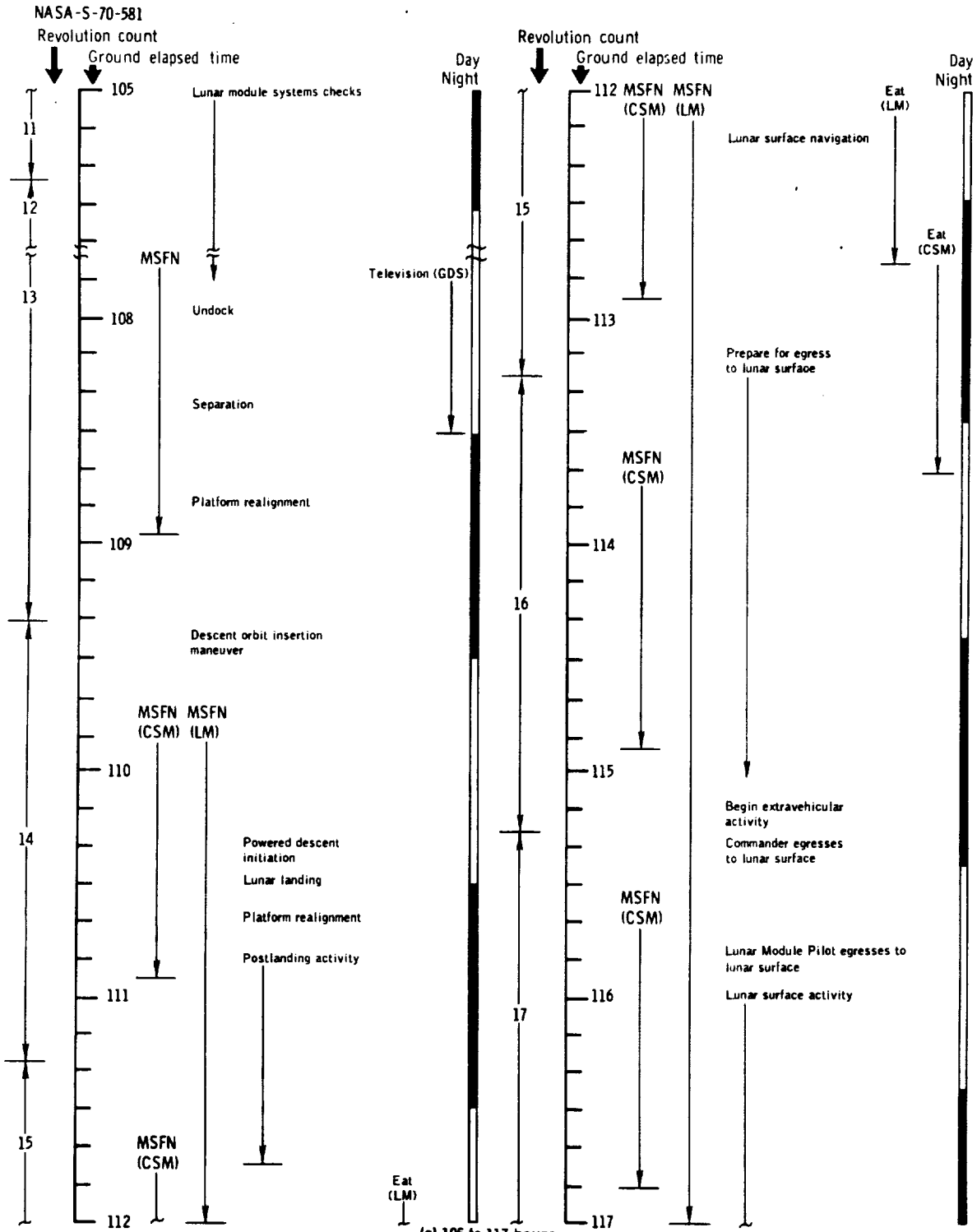


Figure 9-1. - Continued.





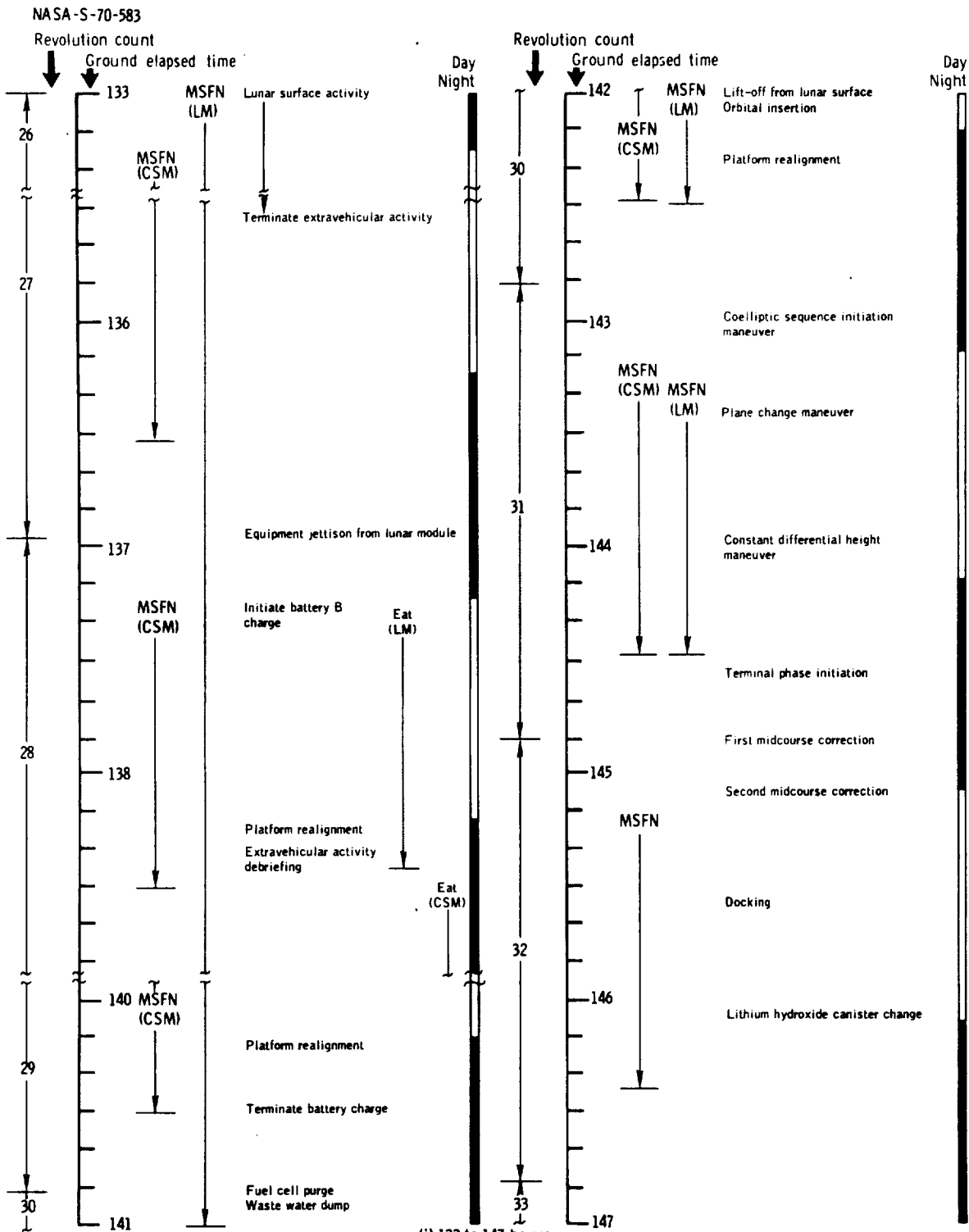


Figure 9-1. - Continued.



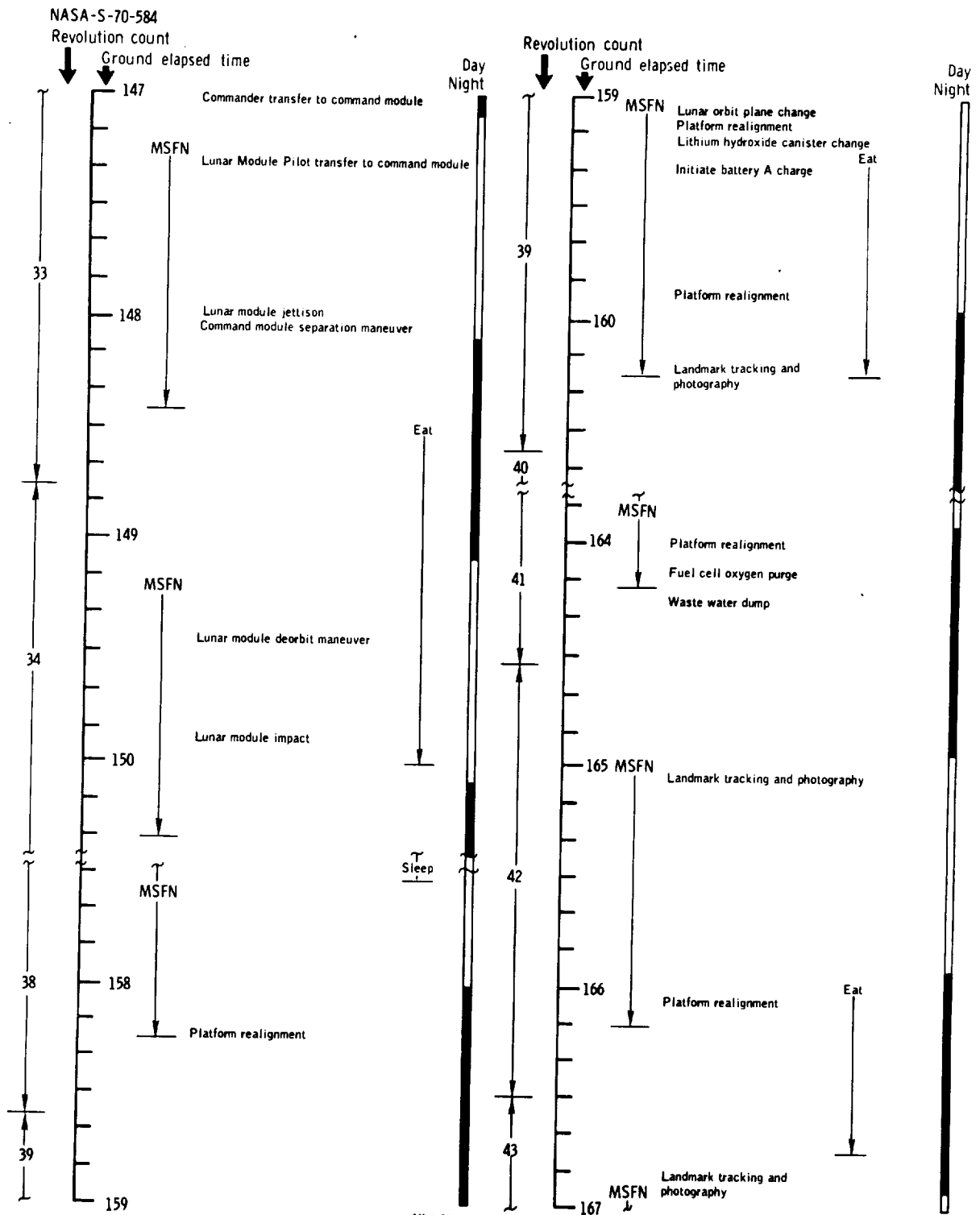
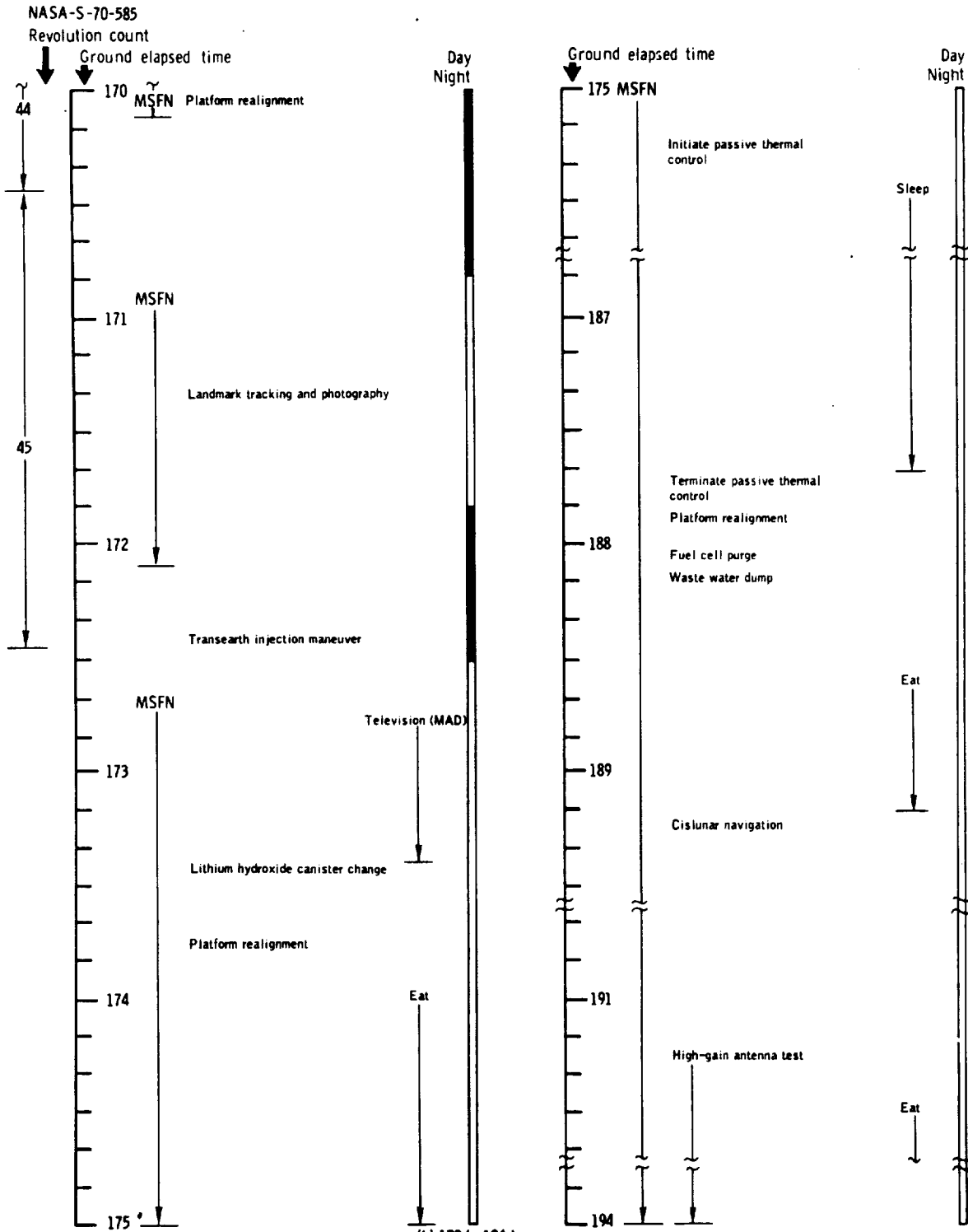
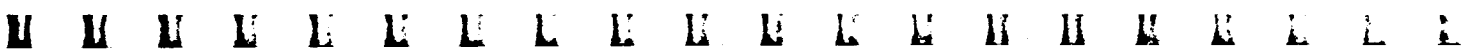


Figure 9-1. - Continued.





(k) 170 to 194 hours.  
Figure 9-1. - Continued.





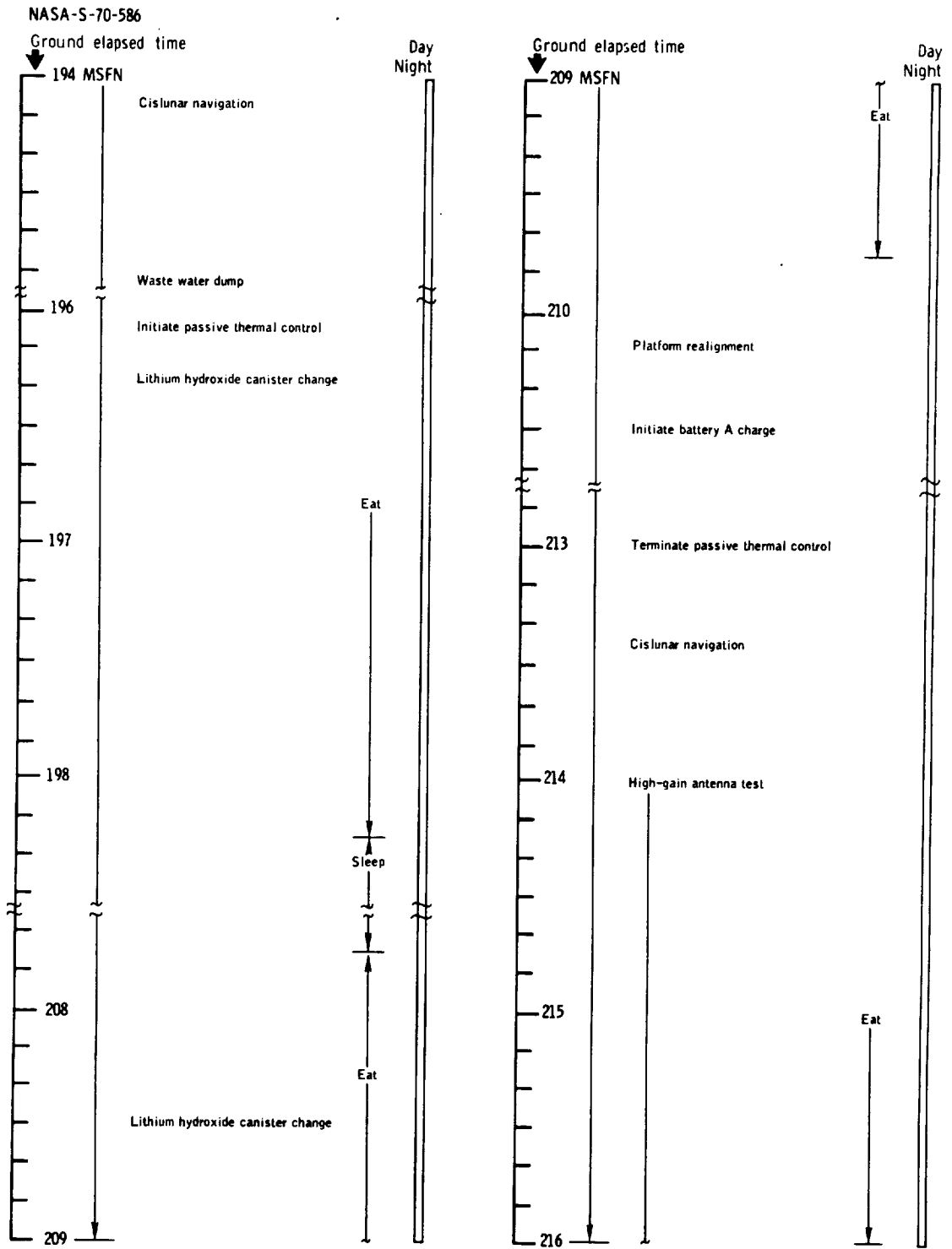
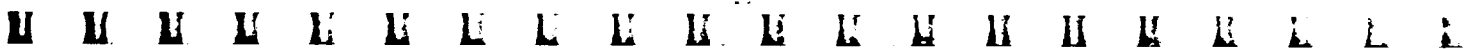


Figure 9-1. - Continued.



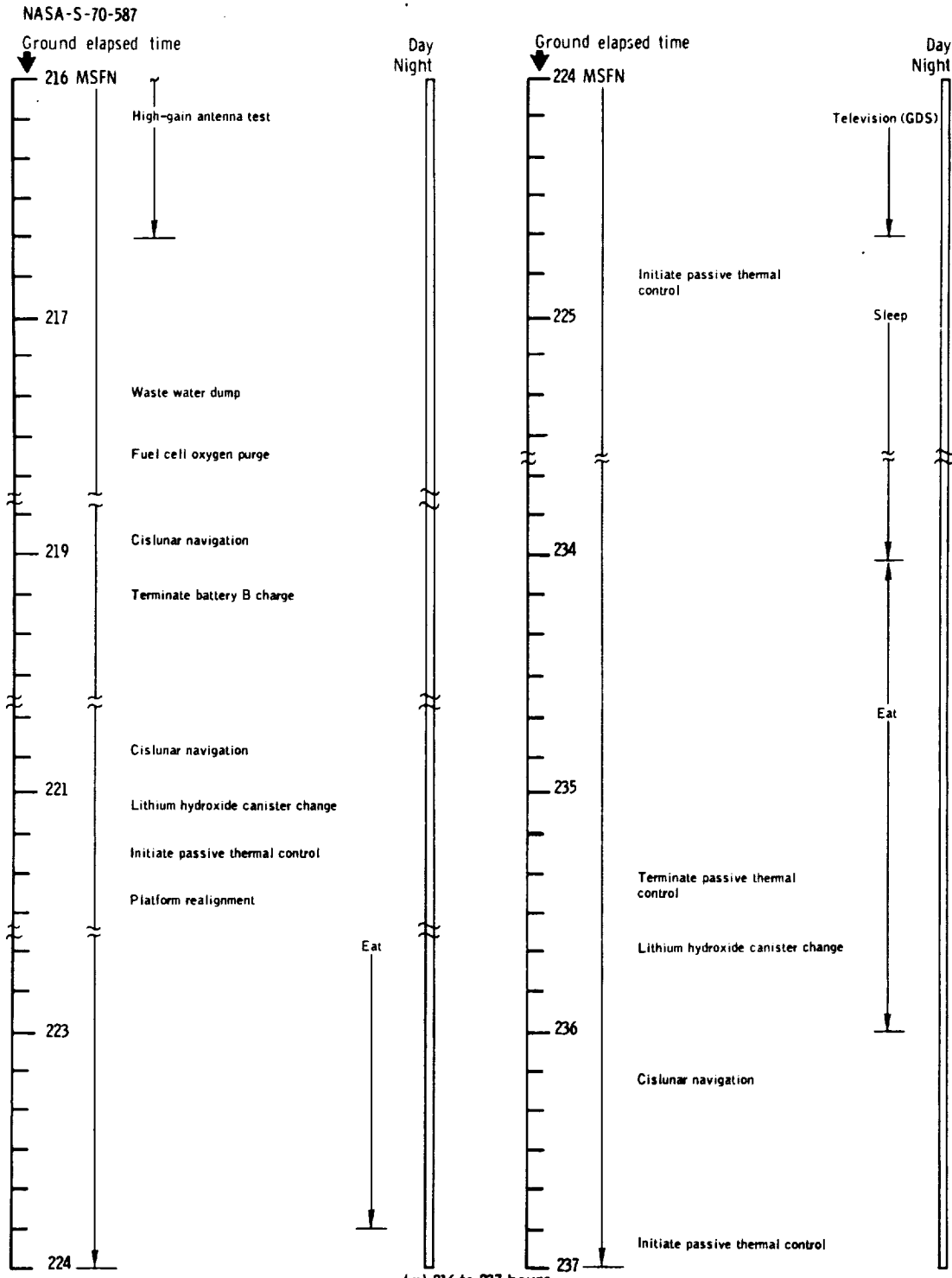


Figure 9-1. - Continued.



























with air bubbles in the middle ear cavity, but this symptom disappeared after 24 hours of decongestant therapy. Because the command module splashed down normal to the surface of the water, landing forces were greater than those experienced on previous Apollo flights. A camera came off the window bracket and struck the Lunar Module Pilot on the forehead. He lost consciousness for about 5 seconds and sustained a 2-centimeter laceration over the right eyebrow. The cut was sutured soon after retrieval and healed normally.

All crewmen suffered varying degrees of skin irritation at the biomedical sensor sites. The Command Module Pilot's skin condition was the worst of the three on recovery day. He had multiple pustules at the margins and in the center of the sensor sites. Healing lesions were noted on the Commander's skin at all sensor sites. He had removed his sensors 4 days prior to recovery and had cleansed the skin and applied cream to the affected areas daily. Red areas and small pustules were noted about all sensor sites on the Lunar Module Pilot.

The skin reaction to the sensors was the most severe seen in manned flight; therefore, a study was initiated to determine the cause of the skin irritation. The results disclosed that the Commander was allergic to some, as yet unidentified, substance in the flight electrode paste, while the other two crewmen developed no allergic reaction during these tests. Chemical analysis of the paste was inconclusive in determining the cause of the irritation. No bacteria were cultured from the electrode paste, which contains a substance to inhibit the growth of bacteria. There was a heavy concentration of *Staphylococcus aureus*, cultured from the skin of all three crewmen after the flight. This bacteria could account for the inflammation of the irritated skin area reported.

On the day after recovery, the Commander developed a left maxillary sinusitis which was treated successfully with decongestants and antibiotics.

Examinations were conducted daily in the Lunar Receiving Laboratory during the quarantine period, and the immuno-hematology and microbiology revealed no changes attributable to lunar material exposure.

#### 10.5 LUNAR CONTAMINATION AND QUARANTINE

The procedures for quarantine of the crew and the equipment exposed to lunar material and the measures for the prevention of back contamination are discussed in reference 9. The medical aspects of lunar dust contamination are briefly discussed in section 6.

U U U E E E L L L E E E H H H K K K I I



M M M M M E E L E E E K E H H E R L L L



## 11.0 MISSION SUPPORT PERFORMANCE

### 11.1 FLIGHT CONTROL

Flight control performance was satisfactory in providing operational support. Some spacecraft problems were encountered and evaluated, most of which are discussed elsewhere in this report. Only those problems which particularly influenced flight control operations or resulted in significant changes to the flight plan are discussed.

As a result of the lightning incidents which caused a power switch-over and loss of platform reference during launch, several additional systems checks were conducted during earth orbit to verify systems operation prior to translunar injection. Also, an early checkout of lunar module systems was made after ejection. Lunar module power remained on for approximately 24 minutes, and no problems were discovered during this inspection. The earth orbit operations recommended specifically because of the power switchover and platform loss were as follows:

- a. At insertion, the two inertial platform circuit breakers were pulled to remove power from the platform gyros and allow the gyros to spin down, terminating the tumbling of the platform gyros. The breakers were reset after 3 minutes, and the platform was aligned using an appropriate computer program during the first night pass. A new reference matrix was uplinked to the computer from the Canary Islands station, which had to be reconfigured from S-IVB to command module support. A platform realignment was performed during the second night pass to check gyro drift and verify that the lightning which caused the platform loss had not resulted in permanent damage.
- b. An erasable memory dump was performed over the Carnarvon station to verify that the potential discharges had not altered the computer memory.
- c. A new state vector was uplinked because the spacecraft had lost its state vector when platform reference was lost.
- d. A computer self-test, a thrust vector control check, and a gimbal drive check were performed to verify spacecraft operation for a safe abort to earth, if required.
- e. A new battery charging plan was transmitted to compensate for the battery power usage while the fuel cells were off the line during launch.

Following completion of the lunar module inspection and return to the command module, the lunar module current was found to be 1 ampere higher than expected. The floodlight switch on the lunar module hatch was believed to have malfunctioned, causing the floodlights to remain on. A



TABLE 11-I.- RECOVERY SUPPORT

| Landing area          | Maximum retrieval time, hr             | Maximum access time, hr | Support |        | Remarks  |
|-----------------------|--|-------------------------|---------|--------|--|
|                       |  |                         | Number  | Unit   |  |
| Launch site           |  | 1/2                     | 1       | LCU    | Landing craft utility (landing craft with command module retrieval capability)   |
| Launch abort          | 24 in Sector A, no maximum in Sector B | 4                       | 1       | HH-3E  | Helicopter with para-rescue team   |
|                       |  |                         | 2       | HH-53C |  |
|                       |  |                         | 1       | ATF    | Helicopters capable of lifting the command module; each with para-rescue team  |
|                       |  |                         | 2       | SH-3D  |  |
|                       | 24 in Sector A, no maximum in Sector B | 4                       | 1       | DD     | USS Salinan  |
|                       |  |                         | 3       | HC-130 |  |
| Earth orbit secondary | 24                                     | 6                       | 2       | DD     | USS Hawkins  |
|                       |  |                         | 4       | HC-130 |  |
| Deep space secondary  | 24                                     | 14                      | 1       | LPH    | Fixed wing aircraft; one each staged from Kindley AFB, Bermuda; from Pease AFB, N. M.; and from Lajes AFB, Azores  |
|                       |  |                         | 1       | CVS    |  |
| Primary               | Crew: 16<br>CM: 24                     | 2                       | 4       | SH-3D  | USS Strauss<br>Two each at Kindley AFB and at Hickam AFB, Hawaii   |
|                       |  |                         | 2       | HC-130 |  |
| Contingency           |  | 18                      | 3       | E-1B   | USS Austin<br>USS Hornet<br>Helicopters, 2 with swimmers, 1 recovery, and 1 photographic platform<br>Two each staged from Hawaii, Samoa, and Ascension<br>1 Airboss, 1 relay, and 1 Airboss/relay combination aircraft |
|                       |  |                         | 6       | HC-130 |  |

Total ship support = 6

Total aircraft support = 26 (This total is based on the recovery requirement that two HC-130 aircraft be in support of the mission from Kindley AFB, Bermuda; Hickam AFB, Hawaii; Ascension; Mauritius Island and Howard AFB, Canal Zone; and one HC-130 aircraft from Andersen AFB, Guam and Lajes AFB, Azores.)







|   |                    |
|---|--------------------|
| Container 1, controlled temperature shipping container 1, and film flown to Samoa     | 0640               |
| Container 2 removed from mobile quarantine facility                                   | 0811               |
| Container 2, remainder of biological samples and film flown to Samoa                  | 1130               |
| Container 1, controlled temperature shipping container 1, and film arrived in Houston | 2045               |
| Command module hatch secured and decontaminated                                       | 2223               |
| Mobile quarantine facility secured after removal of transfer tunnel                   | 2330               |
|   | <u>November 26</u> |
| Container 2, remainder of biological samples, and film arrived in Houston             | 0448               |
|   | <u>November 29</u> |
| Mobile quarantine facility and command module offloaded in Hawaii                     | 0218               |
| Safing of command module pyrotechnics complete  | 0840               |
| Mobile quarantine facility arrived at Ellington AFB                                   | 1150               |
| Flight crew entered Lunar Receiving Laboratory  | 1350               |
|   | <u>December 1</u>  |
| Deactivation of the fuel and oxidizer completed                                       | 1415               |
|   | <u>December 2</u>  |
| Command module delivered to Lunar Receiving Laboratory                                | 1930               |

### 11.3.3 Postrecovery Inspection

All aspects of the command module, mobile quarantine facility, and lunar sample return containers were normal except for the following discrepancies:

- a. Condensation was found between the panes of the number 1 window (far left). The number 5 window (far right) had a frosty film on the outer pane and condensation on the inner pane (section 14.1.11).
- b. The environmental control system hose was broken at the bulkhead connection for the center couch. The connection bracket came off the panel (section 14.1.14).
- c. The camera had dislodged from its mount at landing.
- d. Two whiskers on the VHF antenna did not deploy (section 14.1.12).
- e. The shaped charge ring was broken but was held by the spring clips. One of these spring clips was missing.
- f. Oxygen pressure was depleted during the command module water sampling operation, and no waste water or drinking water samples were taken.













## 13.0 LAUNCH VEHICLE SUMMARY

The trajectory parameters of the AS-507 launch vehicle from launch to translunar injection were close to expected values. The vehicle was launched on an azimuth 90 degrees east of north. A roll maneuver was initiated at 12.8 seconds to place the vehicle on a flight azimuth of 72.029 degrees east of north.

Following lunar module ejection, the vehicle attempted a slingshot maneuver to achieve a heliocentric orbit. However, the vehicle's closest approach of 3082 miles above the lunar surface did not provide sufficient energy to escape the earth-moon system. Even though the slingshot maneuver was not achieved as planned, the fundamental objective of not impacting the spacecraft, the earth, or the moon was achieved. The vehicle did not achieve a heliocentric orbit because the computed time for auxiliary propulsion ullage firing was based on the telemetered state vector, which was within the 3-sigma limit but was in excess of the 13.1 ft/sec slingshot window velocity.

In the S-IVB stage, the oxygen/hydrogen burner satisfactorily achieved tank repressurization for restart. However, burner shutdown did not occur at the programmed time due to an intermittent electrical open circuit, and this resulted in a suspected burnthrough of the burner. Subsequent engine restart conditions were within specified limits, and the restart at full-open propellant utilization valve position was successful. The electrical systems performed satisfactorily throughout all phases of flight except during the S-IVB restart preparations. During this time, the S-IVB stage electrical systems did not respond properly to burner liquid oxygen shutdown valve "close" and telemetry calibrate "on" commands from the S-IVB switch selector. All hydraulic systems performed satisfactorily, and all parameters were within limits, although the return fluid temperature of one S-IC actuator rose unexpectedly at 100 seconds.

This Apollo/Saturn vehicle was the first to be launched in inclement weather, and two distinct lightning strikes occurred (reference 12). However, the structural loads and dynamic environments experienced by the vehicle were well within the structural capability.

Low-level oscillations, similar to those of previous flights, were evident during each stage firing but caused no problems. The S-II stage experienced four new periods of 16-hertz oscillations, which apparently result from the inherent characteristics of the present S-II stage configuration; however, engine performance was not affected.

U U



14.0 ANOMALY SUMMARY

This section contains a discussion of the significant problems or discrepancies noted during the Apollo 12 mission. Anomalies in the operation of experiment equipment after deployment will be published in a separate anomaly report.

14.1 COMMAND AND SERVICE MODULES

14.1.1 Intermittent Display and Keyboard Assembly

The crew reported several intermittent, all-"8's" displays on the main display and keyboard assembly approximately 1-1/2 hours before launch, but no display malfunction occurred in flight. The display segments are illuminated by applying 250 V ac through the contacts of miniature relays, as shown in figure 14-1. When a segment is off, it is grounded through a resistor and the normally closed contacts of a relay to avoid residual illumination. The normally closed contacts of all relays are tied together; consequently, a short across the contacts of any one relay will apply the voltage to all segments of each display. The effect of the short in conjunction with the common discharge path is shown in figure 14-1 for a typical character and one sign. A short across the relay contacts will affect only the display function of the unit.

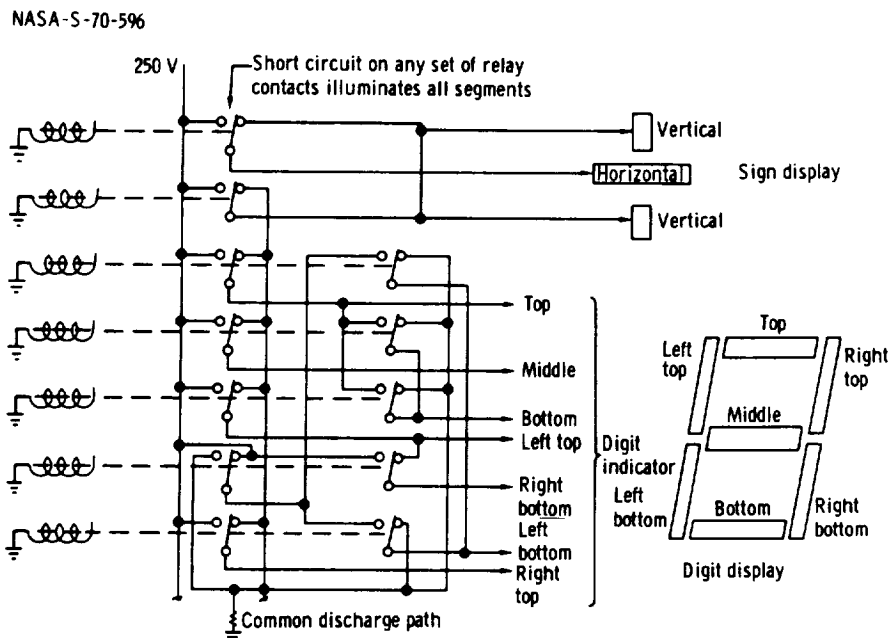
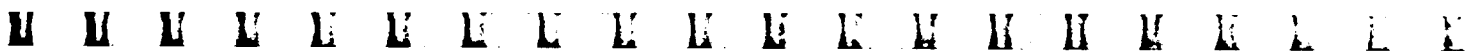


Figure 14-1. - Simplified schematic diagram of relay matrix.















Loss of inertial platform reference.- A loss in reference for the inertial platform at the second discharge was most likely caused by the setting of high-order bits in the coupling display unit by the discharge transients introduced between signal ground and structural ground. If this condition occurs and causes the Z-axis (yaw) coupling display unit (middle gimbal) readout to exceed 85 degrees, the computer will down-mode the platform to coarse align. When the coupling display unit is driving at high speed to null the noise-induced error and the coarse-align loop is energized, the servo loop from the coupling display unit to the platform becomes unstable and drives the platform in the manner observed. A change to the computer programming to inhibit the computer mode-switching logic during the launch phase has been implemented for Apollo 13.

Complete protection of the spacecraft from the effects of lightning is not considered practical at this stage of the program. The inherent temporary effects associated with solid state circuitry and the reasonable degree of safety in other circuits warrants the low risk of triggering lightning if potentially hazardous electric fields are avoided.

The following launch restrictions have been imposed for future missions to greatly minimize the possibility of triggering lightning.

a. No launch when flight will go through cumulonimbus (thunderstorm) cloud formation. In addition, no launch if flight will be within 5 miles of thunderstorm clouds or within 3 miles of an associated anvil.

b. Do not launch through cold-front or squall-line clouds which extend above 10 000 feet.

c. Do not launch through middle cloud layers 6000 feet or greater in depth where the freeze level is in the clouds.

d. Do not launch through cumulus clouds with tops at 10 000 feet or higher.

This report reflects the combined efforts of the investigating teams at the Manned Spacecraft Center, the Kennedy Spacecraft Center, and the Marshall Space Flight Center.

This anomaly is closed.

#### 14.1.4 Open Stabilization and Control System Circuit Breaker

During systems checks after earth orbit insertion, circuit breaker 23 for stabilization and control logic bus 3 and 4 on panel 8 was found in the open position (fig. 14-6). A crewman closed the circuit breaker and

U U U E E E L L E E E E H H H E E L L E













NASA-S-70-603

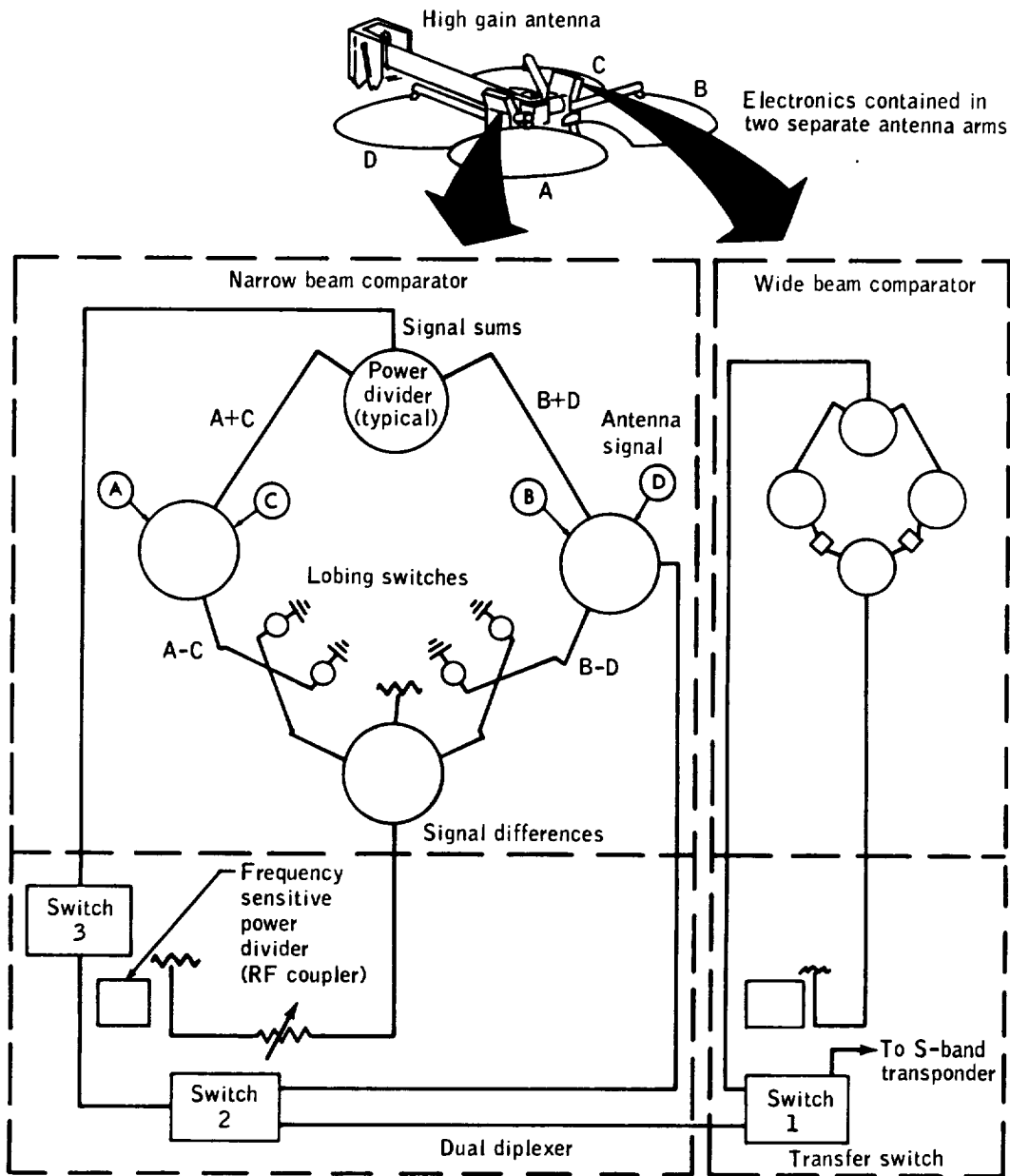
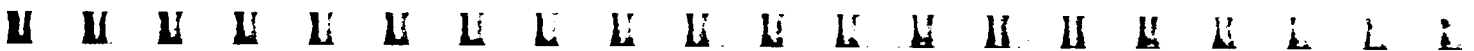


Figure 14-8.- S-band high gain antenna electronics.







NASA-S-70-605

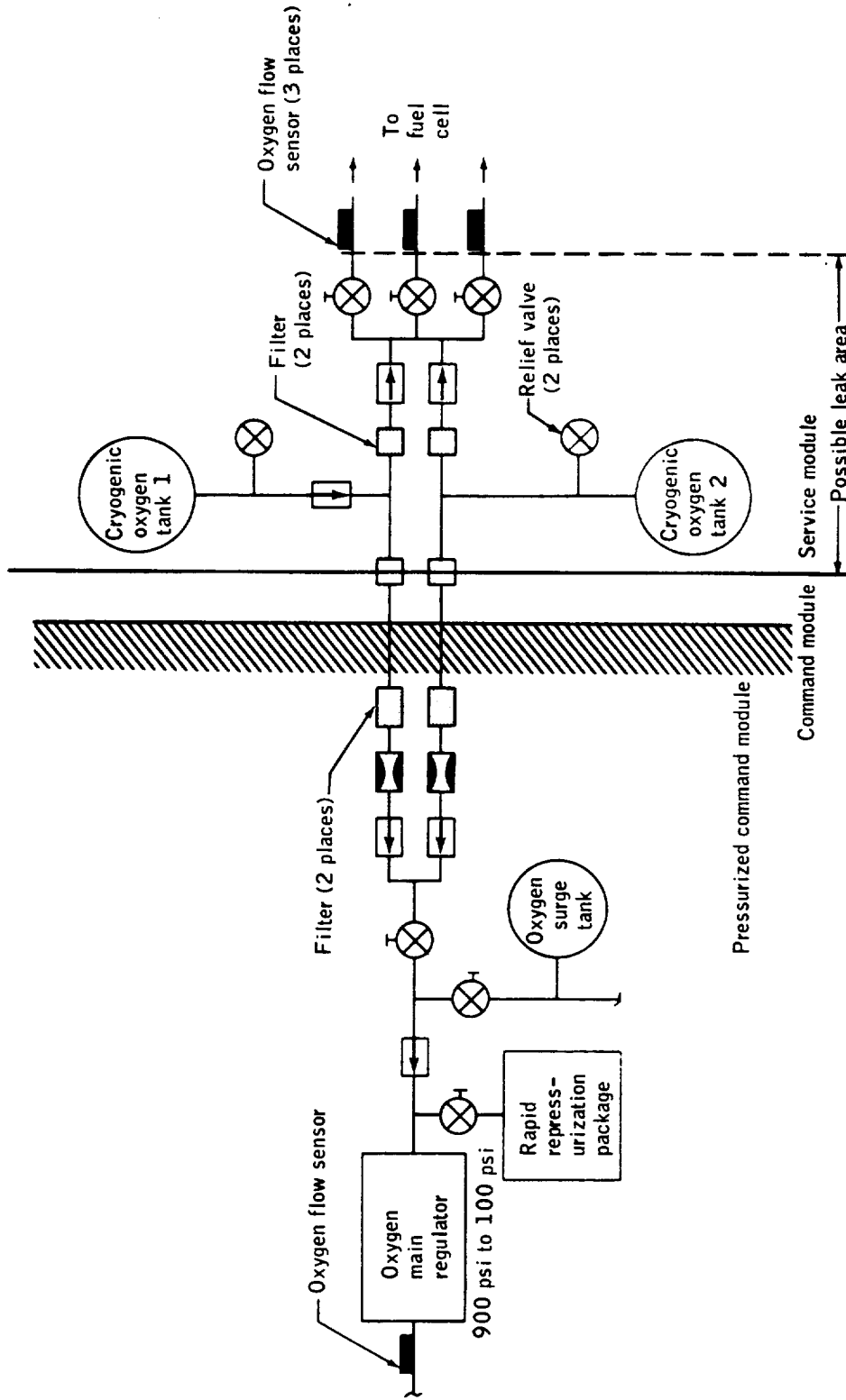


Figure 14-10.- Schematic of 900 psi oxygen system.













14.1.12 Improper Deployment of VHF Recovery Antenna

During the command module descent on the main parachutes, ground plane radials 1 and 3 of VHF recovery antenna 2 (fig. 14-15) did not properly deploy. However, voice communications with the recovery forces while using this antenna were not significantly affected. Postflight examination of the antenna revealed that the cloth flap which normally covers the radials to prevent entanglement with the parachutes could be made to stick to the gusset by an adhesive substance which was inadvertently present on both the flap and the gusset. The radials would not deploy when the flap had stuck to the gusset; however, radial 1 would not always deploy, even when the flap was not stuck. A slight binding at the spring end or at the retaining clip has been experienced on radial 1.

NASA-S-70-610

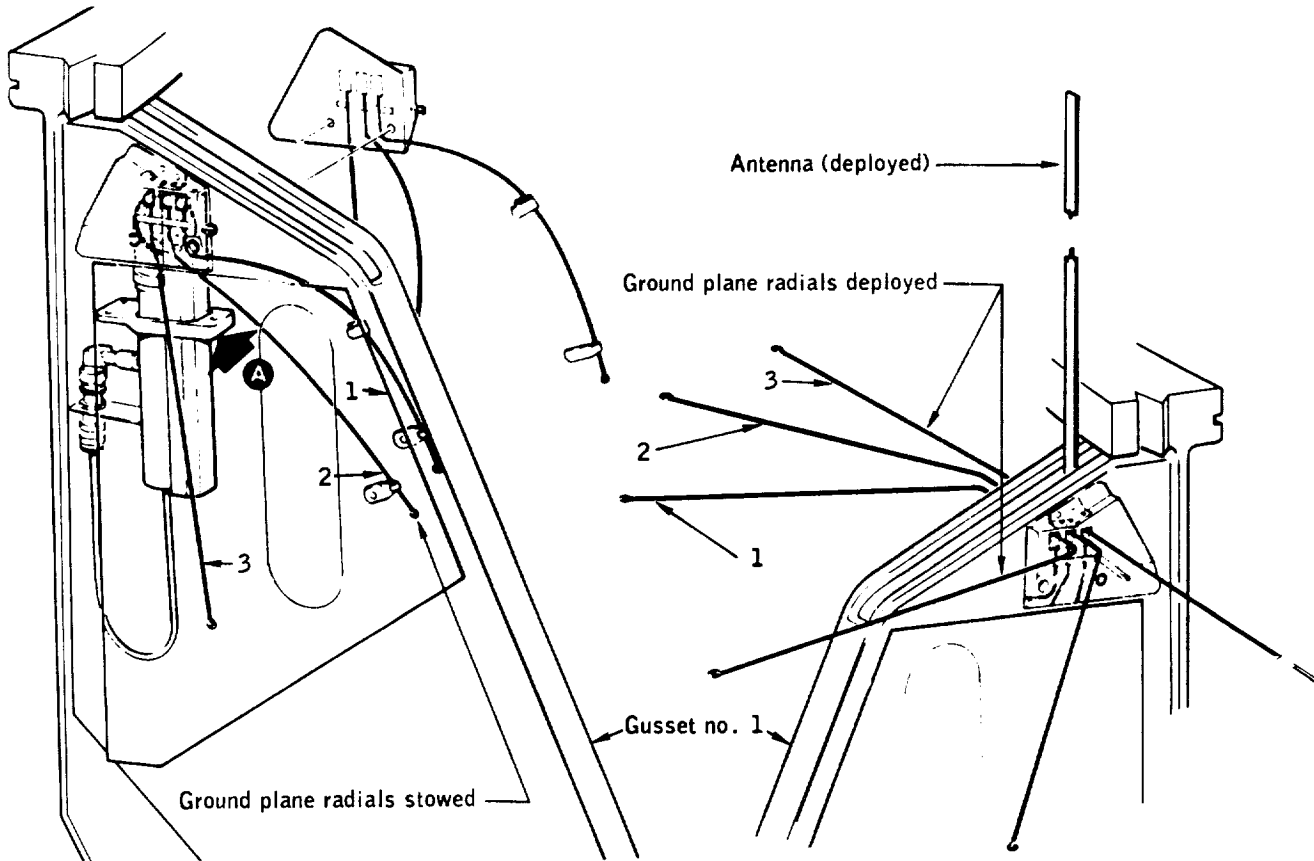


Figure 14-15.- VHF recovery antenna configuration.

For Apollo 13 and subsequent missions, recovery antenna 2 will be used for recovery beacon transmissions instead of voice. However, even















Examination and comparative laboratory tests on a similar type cord disclosed that the failure is nearly identical to those which occur in lanyard knots when loaded in tension. A small flake of yellow material was found embedded in the weave of the severed end of the lanyard. Comparison of the flake with yellow Mylar tape, which is used to wrap the steel drogue riser, showed a definite similarity. Foreign material removed from the lanyard and a piece of tape from a drogue riser contained significant amount of a grayish-black material (fig. 14-19), which is believed to be deposits of a dry-film lubricant used on the steel risers.

NASA-S-70-614



Figure 14-19.- Deposit on end of heat shield lanyard.









NASA-S-70-618

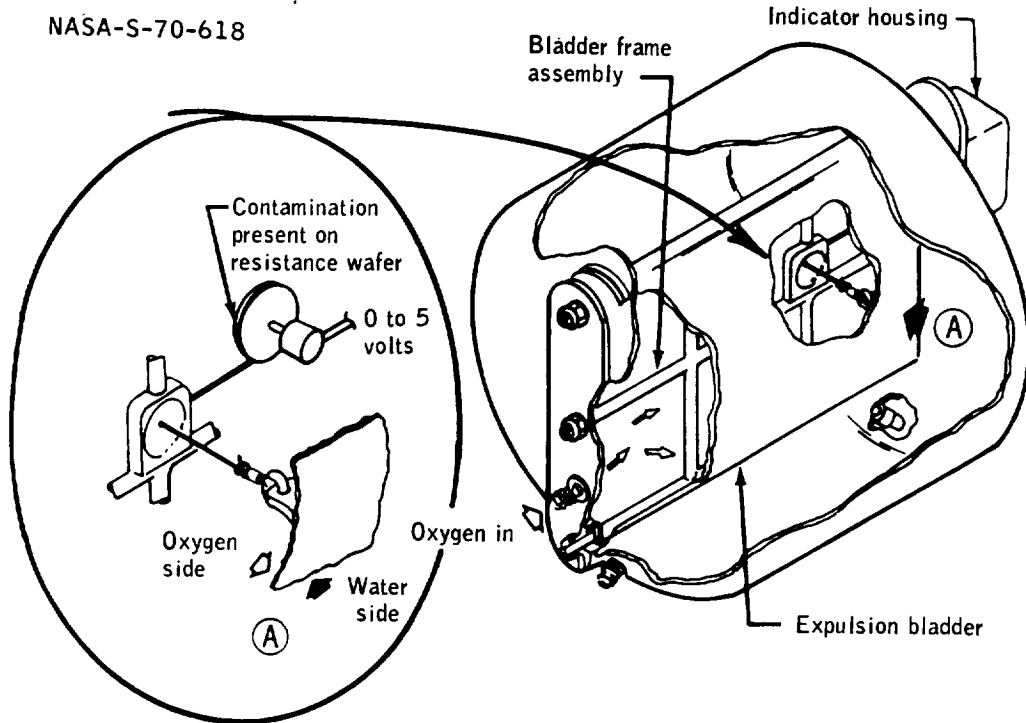


Figure 14-23.- Area of failure in erratic potable water transducer.

NASA-S-70-619

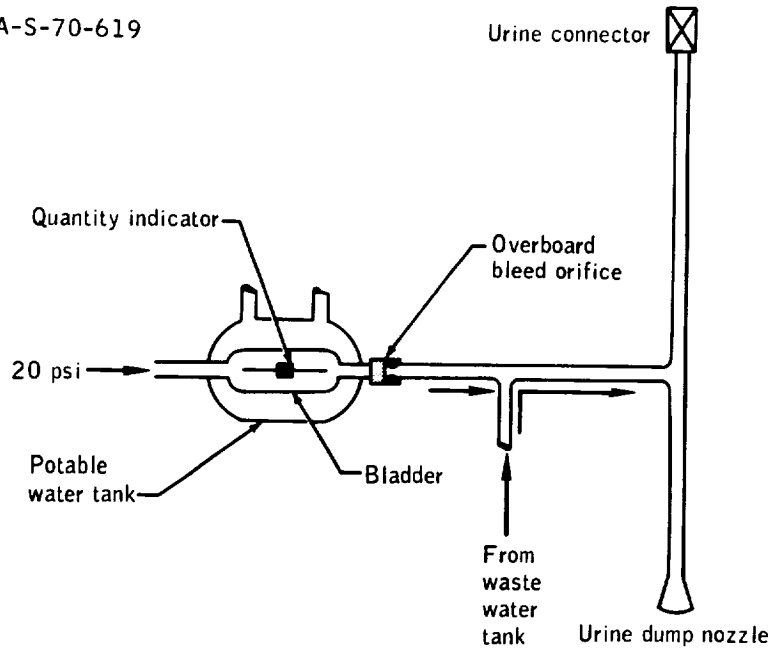


Figure 14-24.- Schematic of oxygen bleed flow and overboard urine dump line.





















NASA-S-70-1426

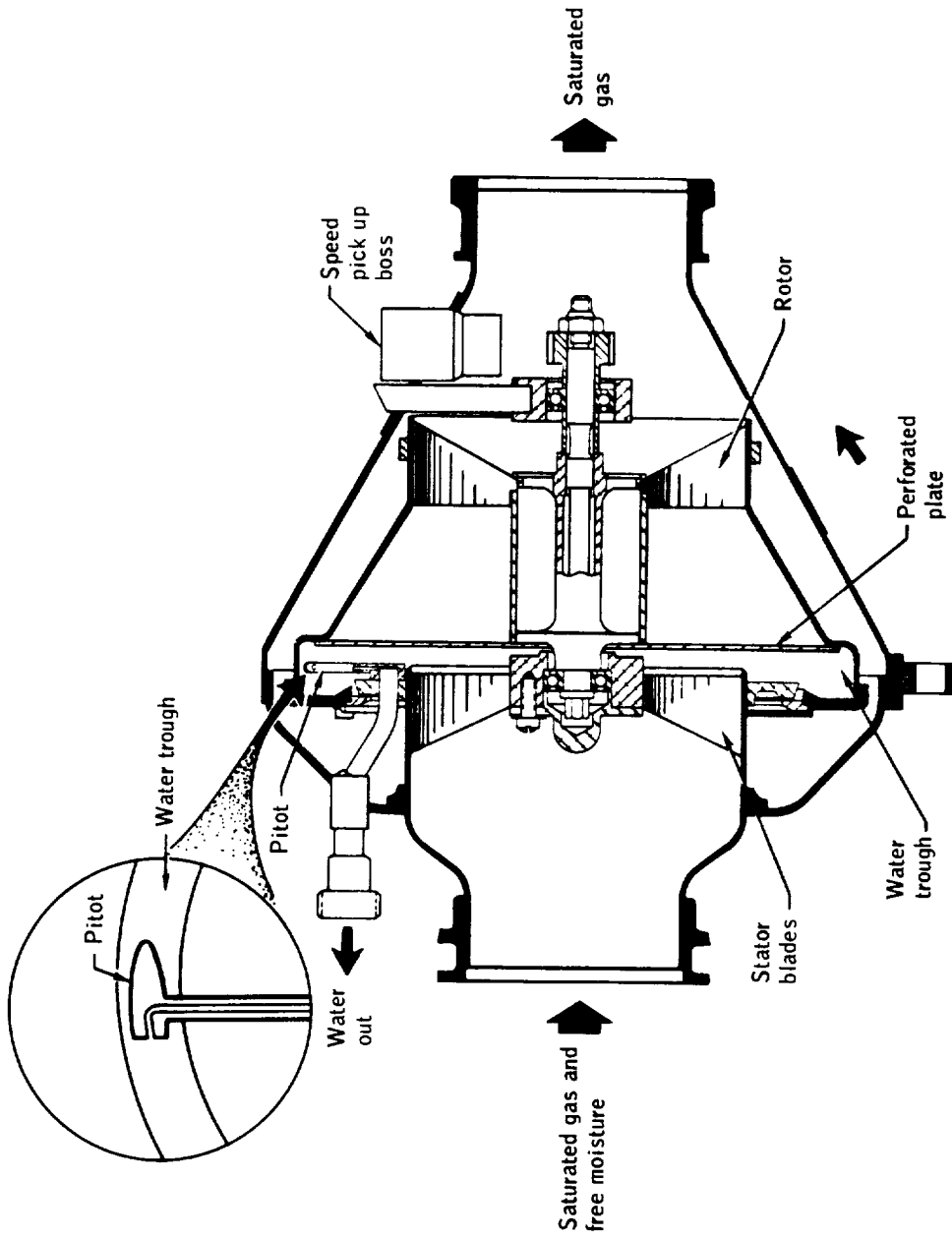
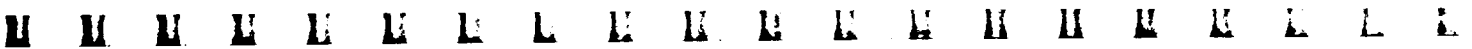


Figure 14-31. - Water separator and pitot configuration.







### 14.2.3 Carbon Dioxide Sensor Malfunction

Following lunar lift-off, the crew reported a master alarm at about the time of ascent-engine shutdown. Ground data show a short-duration spike in the indicated carbon dioxide partial pressure at that time. During the second pass behind the moon following lift-off, the crew reported that the indicated carbon dioxide partial pressure again tripped the carbon dioxide high partial pressure light and master alarm. The crew selected the secondary lithium hydroxide canister at this time. The primary canister was later reselected at the request of ground controllers. The crew later reported that erratic carbon dioxide indications occurred while using either the primary or secondary lithium hydroxide canisters.

The carbon dioxide sensor is sensitive to free water, and the malfunction was probably caused either by water from the water separator sump tank entering the sensor or by water bypassing the water separator and entering the sensor. The water separator sump tank vent line joins the carbon dioxide sensor inlet sense line (fig. 14-33). This vent line has been rerouted for Apollo 13 and subsequent vehicles.

This anomaly is closed.

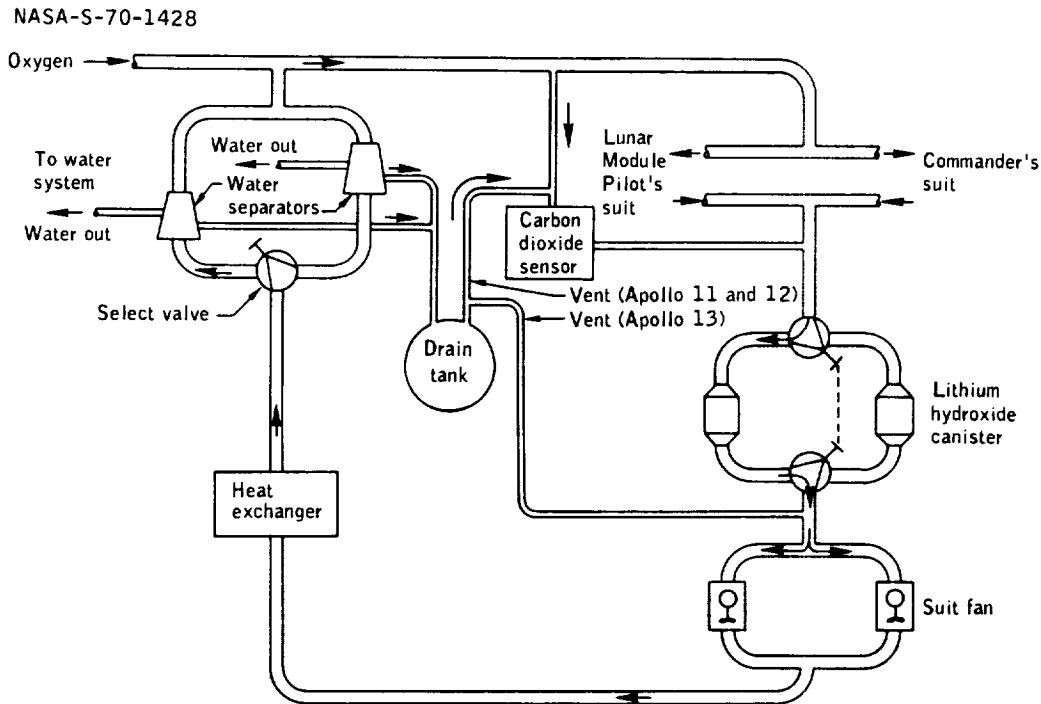


Figure 14-33.- Simplified suit loop schematic.

















NASA-S-70-1434

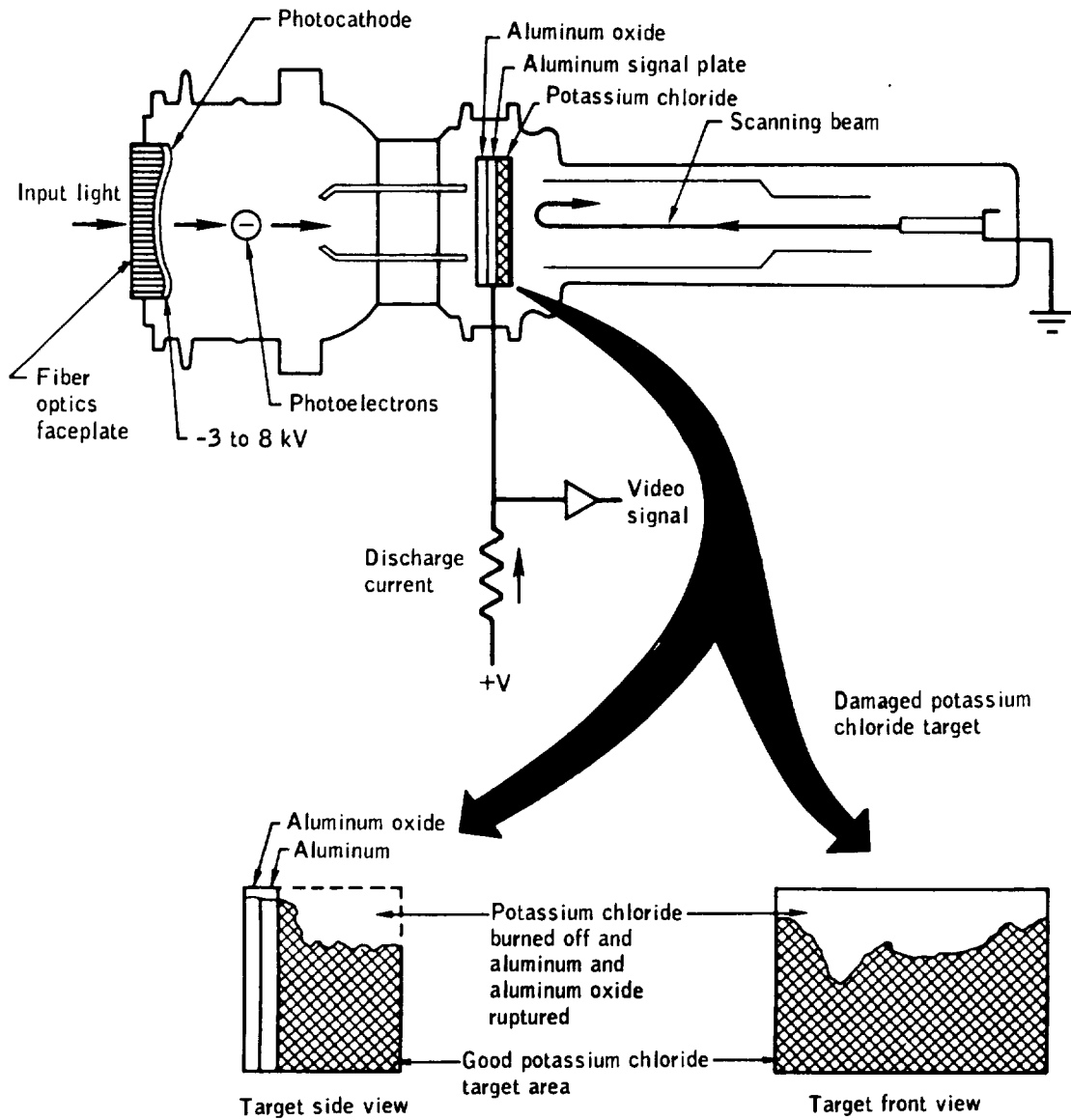


Figure 14-39.- Secondary electron conductivity tube in the color television.

U U U E E E L E E E K H H H H L L L





































U U





NASA-S-70-1443

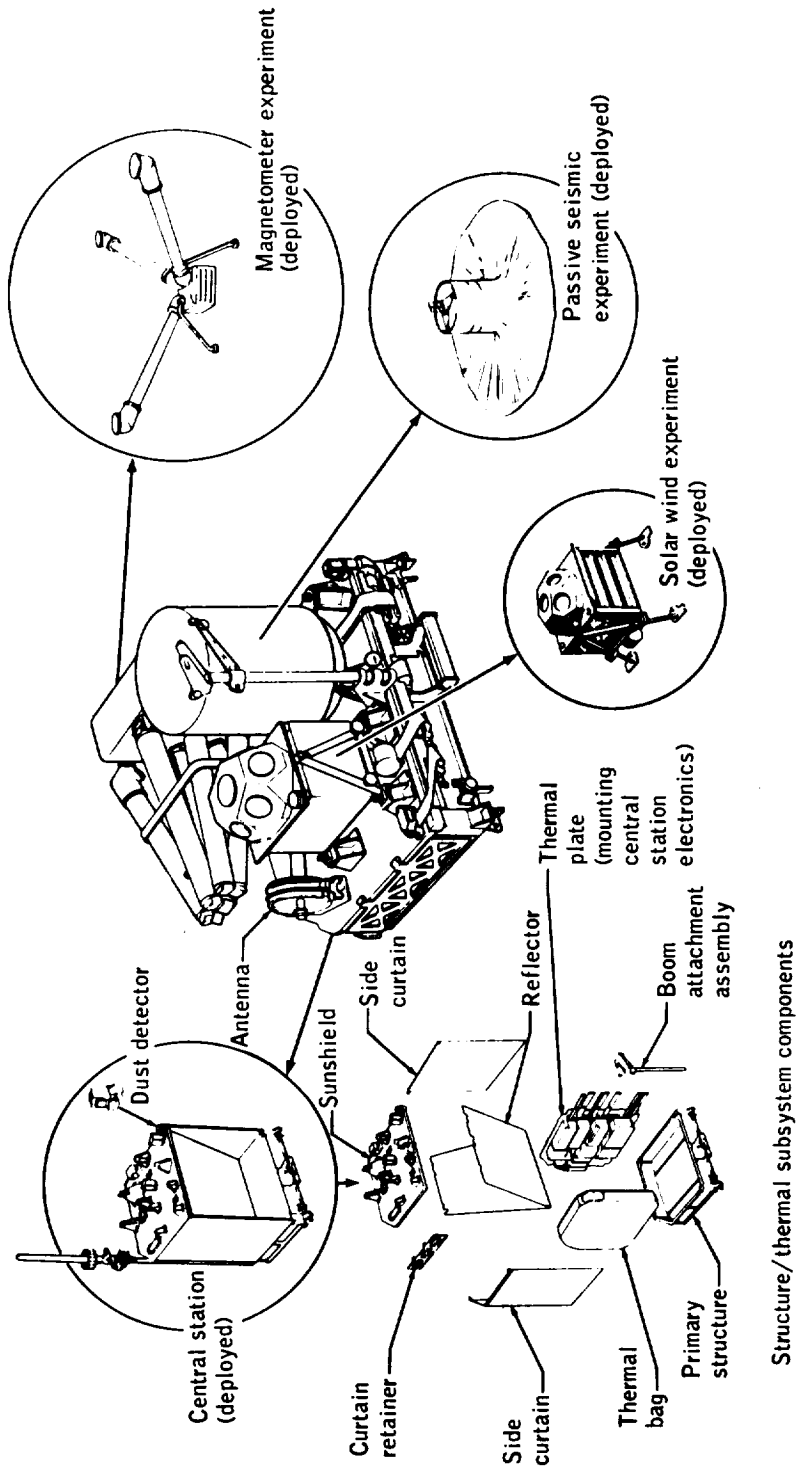


Figure A-1.- Experiment subpackage no. 1.

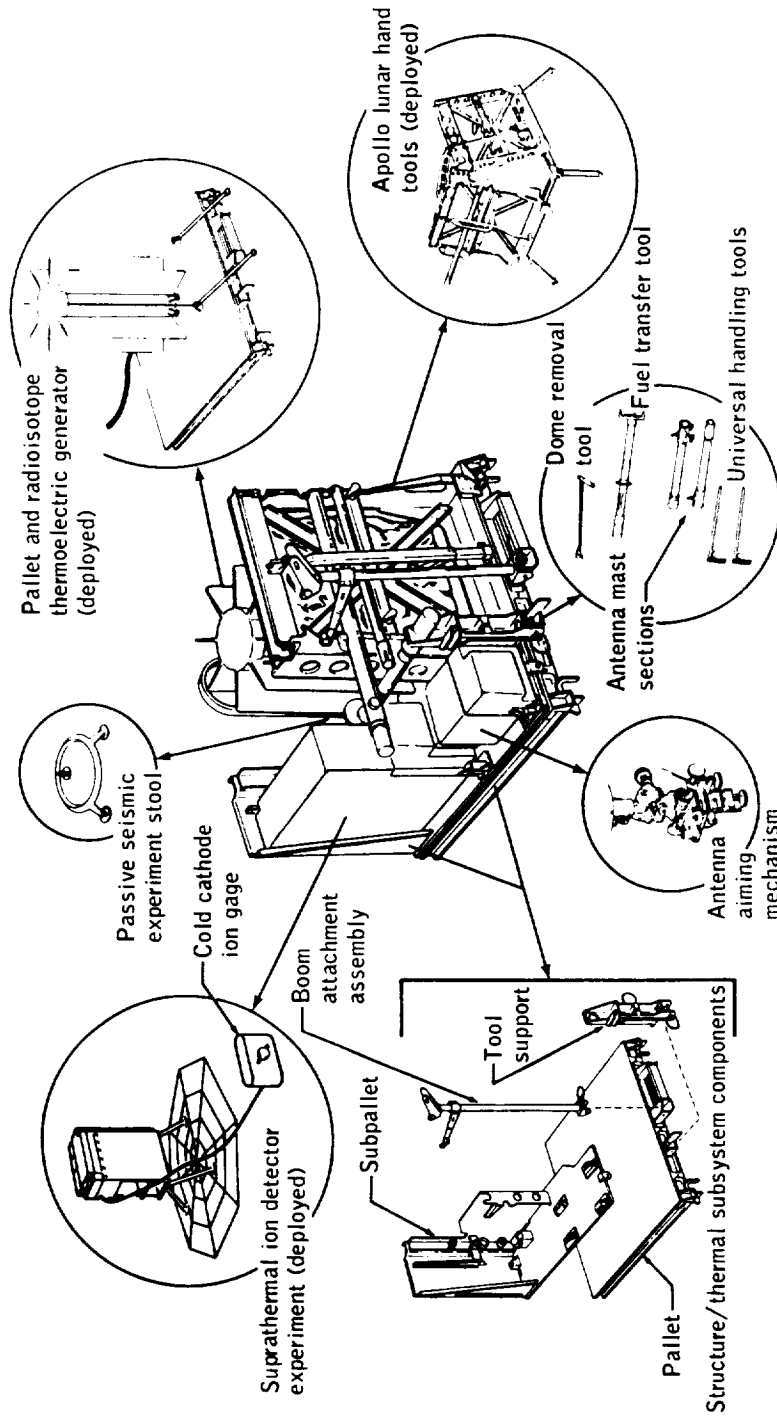


Figure A-2.- Experiment subpackage no. 2.





















NASA-S-70-1447

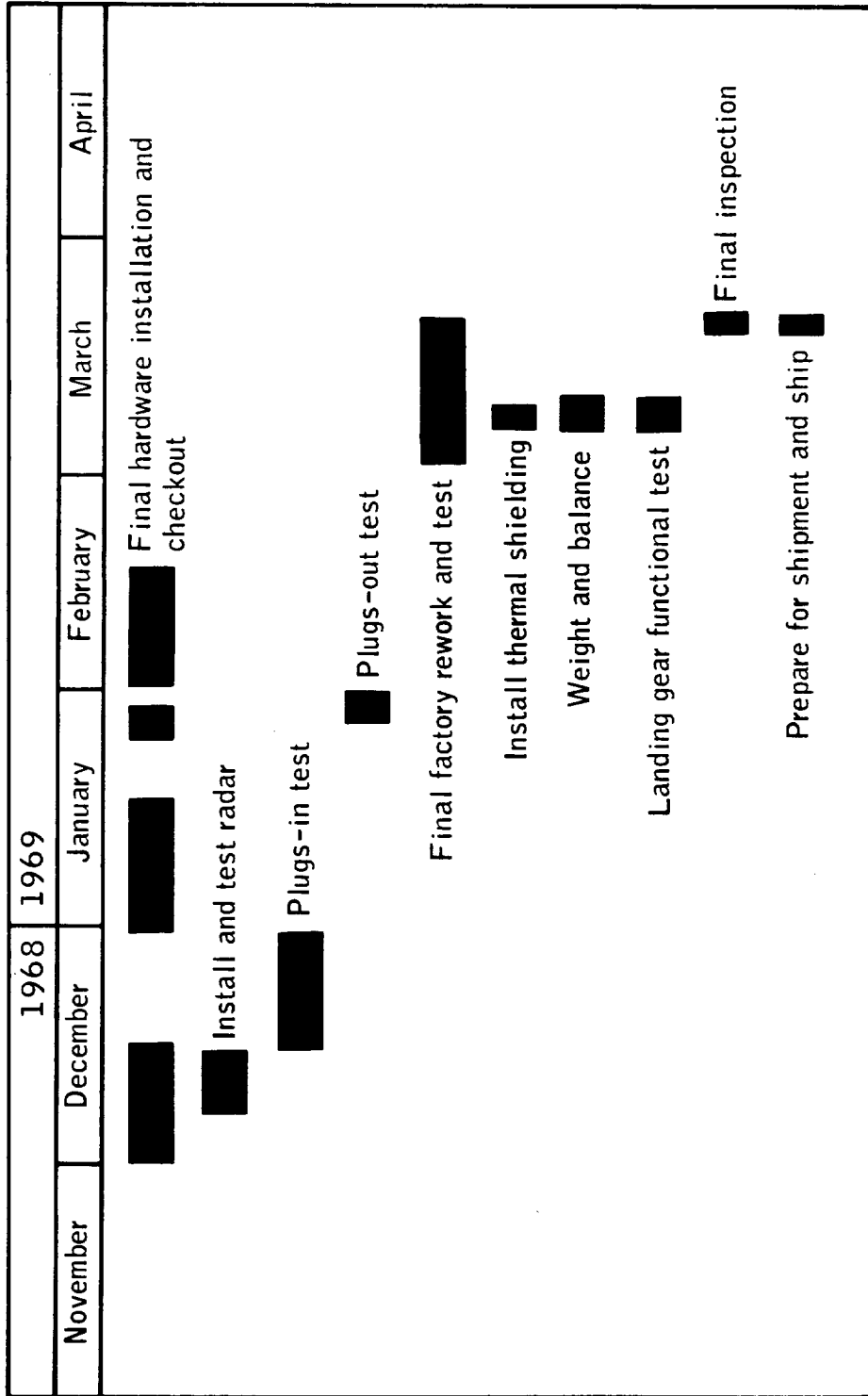


Figure B-3.- Factory checkout flow for the lunar module at Contractor's facility.





M M



TABLE C-1.- POSTFLIGHT TESTING SUMMARY

| ASHUR no.               | Purpose  | Tests performed   | Results   |
|-------------------------|--|---|---|
| Displays and Controls   |  |   |   |
| 108021                  | To determine the cause of the intermittent tuning fork display indication on the panel 2 mission clock.              | Determine solder joint integrity and wiring continuity. Perform failure analysis.   | Continuity check satisfactory. Unable to duplicate failure.   |
| Guidance and Navigation |  |   |   |
| 108008                  | To investigate the cause for optics coupling display unit indication of optics movement during the zero optics mode. | Perform operational test.   | Not complete.   |
| Electrical Power        |  |   |   |
| 108023                  | To determine why circuit breaker (CB23) was open during earth orbit checks.  | Perform pull test, mounting torque test, and calibration check.   | CB23 normal mechanically and electrically.  |
| Communications          |  |   |   |
| 108002                  | To determine the cause for the failure of the color television.  | Perform failure analysis.   | Potassium chloride burned off the target.   |
| 108019<br>108020        | To investigate the extravehicular activity tone problem.   | Perform functional test of communication carriers and bioinstrumentation.   | Tone was duplicated by lowering the voltage at the microphone.  |
| 108022<br>108035        | To determine the cause of the VHF garbled voice.   | Perform functional and systems tests of the VHF/AM transceiver, audio center, digital ranging generator, and lightweight headset. | VHF intelligibility dependent on range and squelch setting. Also dependent on lightweight headset microphone placement. |
| 108054                  | To investigate the failure of two VHF ground plane radials.  | Inspect and actuate the VHF ground plane radials.   | Ground plane radials deployment fouled by canvas flap.  |
| Environmental Control   |  |   |   |
| 108004                  | To investigate the unexplained high oxygen use rate.   | Determine the pressure integrity of the oxygen lines and tanks.   | No leakage in the command module portion of the system.   |
| 108005                  | To investigate the plugged urine filters.  | Determine water flow rate and pressure drop. Disassemble to determine quantity and source of contaminants.                        | Plugging caused by urine solids.  |
| 108006                  | To investigate the shift in the suit pressure transducer.  | Calibrate the transducer. Perform failure analysis.   | Calibration verified shift. Analysis not complete.  |

TABLE C-I.- POSTFLIGHT TESTING SUMMARY - Concluded

| AHSUR no.                            | Purpose  | Tests performed   | Results  |
|--------------------------------------|--|---|--|
| Environmental Control - concluded    |  |   |  |
| 108029                               | To investigate the leak at the food preparation water port.                              | Measure the water leak. Perform teardown and analysis.  | Unit did not leak with unheated water. Leak duplicated with heated water. Analysis not complete.   |
| 108039<br>108049<br>108050<br>108058 | To investigate the excessive quantity of particulate matter in the command module cabin. | Perform material analysis of particles in the lithium hydroxide cartridge, oxygen umbilicals, environmental control system ducts and filters. | Not complete.  |
| 108053                               | To determine the cause for erratic operation of the potable water transducer.            | Perform failure analysis.   | Not complete.  |
| Crew Equipment                       |  |   |  |
| 108026                               | To investigate reported fraying of the exercise rope.                                    | Perform visual inspection.  | Rope showed normal wear.   |
| 108028                               | To investigate reported difficulties with the tape cassettes and voice recorder.         | Perform operational tests, disassembly, and inspection.   | Recorder performance satisfactory.   |
| 108034                               | To investigate intermittent operation of 16-mm camera.                                   | Perform inspection and performance checks.  | Camera performed satisfactorily. Film perforations did not line up with index line on front of two magazines.  |
| 108051                               | To investigate possible failure of 70-mm camera.   | Perform visual inspection and operational tests.  | One magazine performed satisfactorily. One magazine of infrared film showed lines caused by normal heat from film rollers (lines were between frames). |









TABLE D-I.- COMMAND AND SERVICE MODULE DATA AVAILABILITY - Continued

| Time, hr:min |        | Range station                   | Bandpass plots or tabs | Bilevels | Computer words | O'graph records | Brush records | Special plots or tabs | Special programs |
|--------------|--------|---------------------------------|------------------------|----------|----------------|-----------------|---------------|-----------------------|------------------|
| From         | To     |                                 |                        |          |                |                 |               |                       |                  |
| 91:11        | 91:58  | HSK <sup>a</sup>                | X                      |          |                |                 |               |                       |                  |
| 93:09        | 93:56  | HSK <sup>a</sup>                | X                      |          |                |                 |               | X                     |                  |
| 95:07        | 95:54  | MAD <sup>a</sup>                | X                      |          |                |                 |               | X                     |                  |
| 95:07        | 98:35  | MSFN <sup>a</sup>               | X                      |          | X              |                 |               | X                     |                  |
| 97:05        | 97:53  | MAD <sup>a</sup>                | X                      |          |                |                 |               |                       |                  |
| 97:50        | 98:40  | MAD                             |                        |          |                |                 |               | X                     |                  |
| 98:35        | 102:53 | MSFN                            | X                      |          | X              |                 |               |                       | X                |
| 99:04        | 99:52  | MAD <sup>a</sup>                | X                      |          |                |                 |               |                       |                  |
| 99:57        | 100:57 | MAD                             |                        |          |                | X               |               | X                     |                  |
| 100:40       | 101:10 | MAD                             |                        |          |                |                 |               |                       | X                |
| 100:58       | 101:50 | MAD <sup>a</sup>                | X                      |          |                |                 |               |                       | X                |
| 102:53       | 106:40 | MSFN                            | X                      |          | X              |                 |               | X                     |                  |
| 103:00       | 103:48 | GDS <sup>a</sup>                | X                      |          |                |                 |               |                       |                  |
| 103:51       | 104:01 | GDS                             |                        |          |                |                 |               | X                     |                  |
| 104:59       | 105:48 | GDS <sup>a</sup>                | X                      |          |                |                 |               | X                     | X                |
| 106:12       | 106:48 | GDS                             |                        |          | X              |                 |               |                       |                  |
| 106:40       | 111:20 | MSFN                            | X                      |          | X              |                 |               |                       |                  |
| 107:46       | 108:57 | GDS                             |                        | X        | X              |                 |               |                       | X                |
| 107:50       | 108:00 | GDS                             |                        | X        | X              | X               |               |                       |                  |
| 108:20       | 108:30 | GDS                             |                        | X        | X              |                 |               |                       |                  |
| 108:23       | 108:26 | GDS                             |                        |          |                | X               |               |                       |                  |
| 108:55       | 109:44 | GDS <sup>a</sup>                | X                      |          | X              |                 |               |                       |                  |
| 109:41       | 110:20 | GDS                             |                        |          | X              |                 |               | X                     |                  |
| 110:40       | 110:55 | HSK                             |                        |          | X              |                 |               |                       |                  |
| 110:54       | 111:54 | GDS <sup>a</sup>                | X                      |          |                |                 |               |                       | X                |
| 111:20       | 115:39 | MSFN                            | X                      |          | X              |                 |               | X                     |                  |
| 111:50       | 112:00 | HSK                             |                        |          |                |                 |               |                       | X                |
| 112:03       | 112:30 | GDS                             |                        |          | X              |                 |               |                       |                  |
| 114:10       | 114:30 | HSK                             |                        |          | X              |                 |               |                       |                  |
| 114:50       | 115:38 | HSK                             | X                      |          |                |                 |               | X                     |                  |
| 115:41       | 118:57 | MSFN                            | X                      |          | X              |                 |               |                       |                  |
| 115:45       | 116:05 | HSK                             |                        |          |                |                 |               |                       | X                |
| 116:00       | 116:36 | HSK                             |                        |          | X              |                 |               |                       |                  |
| 116:49       | 117:30 | HSK <sup>a</sup>                | X                      |          |                |                 |               |                       |                  |
| 118:46       | 119:35 | MAD <sup>a</sup>                | X                      |          |                |                 |               | X                     |                  |
| 119:17       | 123:06 | MSFN                            | X                      |          |                |                 |               | X                     |                  |
| 119:39       | 119:56 | MAD                             |                        |          | X              |                 |               |                       |                  |
| 119:43       | 119:58 | MAD                             |                        | X        |                |                 |               |                       |                  |
| 120:00       | 120:30 | MAD                             |                        |          |                | X               |               | X                     |                  |
| 120:30       | 120:36 | MAD                             |                        |          |                |                 |               |                       | X                |
| 120:53       | 121:33 | GDS <sup>a</sup> X <sup>b</sup> | X                      |          |                |                 | X             |                       |                  |
| 123:06       | 127:40 | MSFN                            | X                      |          | X              |                 |               | X                     |                  |
| 125:03       | 125:31 | GDS <sup>a</sup>                | X                      |          |                |                 |               | X                     |                  |
| 126:43       | 127:29 | GDS <sup>a</sup> X <sup>b</sup> | X                      |          |                |                 |               | X                     |                  |
| 127:41       | 131:44 | MSFN                            | X                      |          | X              |                 |               | X                     |                  |
| 128:39       | 129:29 | GDS <sup>a</sup> X <sup>b</sup> | X                      |          |                |                 |               | X                     |                  |
| 130:35       | 131:26 | GDS <sup>a</sup>                | X                      |          |                |                 |               | X                     |                  |
| 131:44       | 135:39 | MSFN                            | X                      |          | X              |                 |               | X                     |                  |
| 132:37       | 133:26 | GDS <sup>a</sup>                | X                      |          |                |                 |               |                       |                  |
| 133:24       | 134:26 | GDS                             |                        |          |                |                 |               | X                     |                  |
| 134:00       | 134:35 | GDS                             |                        |          | X              |                 |               |                       | X                |
| 134:35       | 135:22 | HSK <sup>a</sup>                | X                      |          |                |                 |               |                       |                  |
| 135:39       | 139:20 | MSFN                            | X                      |          | X              |                 |               | X                     |                  |
| 135:50       | 136:10 | GDS                             |                        |          |                |                 |               |                       |                  |
| 136:33       | 137:21 | HSK <sup>a</sup>                | X                      |          |                |                 |               | X                     | X                |

<sup>a</sup>Data dump

<sup>b</sup>Indicates wing site.

U U E L L E L L E L E R K M H H E E L L E



















orthoclase a type of feldspar

pegmatitic pertaining to a natural igneous rock formation consisting of a variety of granite that occurs in dikes or veins and usually characterized by extremely coarse structure

pigeonite mineral consisting of pyroxene and rather low calcium, little or no aluminum or ferric iron, and less ferrous iron than magnesium

plagioclase a type of feldspar

polymorph rock crystallizing with two or more different structures

pyroxene a family of important rock-forming silicates

ray any of the bright, whitish lines seen on the moon as extending radially from impact craters

regolith fine grained material on the lunar surface

sanidine a variety of orthoclase in often transparent crystals in eruptive rock, sometimes called glassy feldspar

scoria rough, vesicular, cindery, usually dark lava developed by the expansion of the enclosed gases in basaltic magma

trachyte a usually light-colored volcanic rock, consisting primarily of potash feldspar

